Impaired fluoxetine-induced post-stroke depression recovery in a protocadherin αc2 deficient mouse model

Mylène Therrien

A thesis submitted in partial fulfillment of the requirements for the

Master's degree in Neuroscience

Department of Cellular and Molecular Medicine

Faculty of Medicine

University of Ottawa

Table of Contents

Abstract

Post-stroke depression (PSD) occurs in 30-50% of stroke patients and is associated with poor recovery, stroke recurrence, and increased death rate. Chronic SSRI treatment can recover the PSD phenotype in mice, but the mechanism of regrowth remains largely unknown. This study aimed to uncover the importance of protocadherin-alphaC2 (pcdhαC2), the main protocadherin isoform found in serotonin neurons, in PSD recovery. Previous studies have shown that knocking out pcdhα in serotonin neurons caused brain-wide tangling of serotonin axons and a depression-like phenotype. Pcdhαc2 knockout mice were used to assess baseline innervation differences, and then stroke recovery with or without fluoxetine (FLX) treatment.

Naïve pcdhαc2 knockout mice showed significantly impaired 5-HT innervation in the medial prefrontal cortex and hippocampus, with heterozygous knockout mice showing intermediate impairment. Stroke mice all exhibited significant anxiety and depression-like phenotypes post-stroke. Only wildtype mice properly recovered their depressive-like phenotype following FLX treatment, with only moderate recovery by heterozygous pcdhαc2 knockout mice. Stroke mice also had decreased 5-HT innervation in the medial prefrontal cortex and basolateral amygdala, with complete FLX-induced recovery only in the wildtype mice.

Taken together, these results indicate that in PSD mice depleted of pcdhαc2, chronic FLX fails to reverse the PSD behavioural phenotype and recover 5-HT innervation in key brain regions. This implicates pcdhαc2 in PSD recovery and could elucidate new targets to enhance neuroplasticity for recovery post-stroke.

List of Figures

List of Abbreviations

5-HT - 5-hydroxytryptamine; serotonin

ANOVA - Analysis of variance

AC2 – Protocadherin alpha c2

BLA – basolateral amygdala

CG – cingulate cortex

DDR - Dorsal dorsal raphe

DG – dentate gyrus

DR - Dorsal raphe

EPM - Elevated plus maze

ET-1 - Endothelin-1

FLX - Fluoxetine

FST - Forced swim test

HET – Heterozygous pcdhαc2 knockout

IL – infralimbic cortex

KO – Pcdhαc2 complete knockout

MDD - Major Depressive Disorder

mPFC – medial prefrontal cortex

Pcdh – Protocadherin

PL – prelimbic cortex

PSD - Post-stroke depression

SR – stratum radiatum

SLM – stratum lacunosum moleculare

SERT - Serotonin transporter

SSRI - Selective serotonin reuptake inhibitor

WT - Wild type

Acknowledgements

I would like to express my deepest gratitude to my supervisor, Dr. Paul Albert, for giving me the opportunity to complete my master's degree in his laboratory, and for guiding me through each step of my project. My time in his lab has deeply broadened my view of neuroscience and taught me to always remain curious.

I would also like to thank all the members of the Albert lab, both past and present, that I have had the pleasure of working alongside. Thank you all for your insightful collaboration, thoughtful discussions, and support. I would like to extend a special thanks to Dr. Faranak Vahid-Ansari for her assistance with imaging, her wealth of knowledge, and her willingness to work through all steps of the project with me. Special thank you as well to Mireille Daigle for completing the breeding and genotyping for my experiment, and overall, for keeping the lab in working order.

I would also like to thank my TAC members, Dr. Greg Silasi and Dr. Simon Chen, for their guidance throughout my project.

Thank you to Dr. Tom Maniatis and his lab members for providing us with the mice for my project, and to NSERC for funding a portion of my graduate studies.

I would also like to thank Alberto and Sara, without whom I never would have stayed sane for these last few years. Thank you for your constant willingness to go the extra mile for me and for reminding me to eat lunch when the days got long. I couldn't have done it without you.

Last but certainly not least, I'd like to thank my wonderful friends and family for their unwavering support. Thank you all so much.

1. Introduction:

1.1 Major Depressive Disorder

1.1.1 General overview

Major Depressive Disorder (MDD) is a pervasive mental health disorder, affecting an estimated 4.36%, or around 350 million people worldwide (GBD, 2021). Lifetime prevalence of the disease varies, with up to 21% of some populations experiencing MDD in their lifetime (Gutiérrez-Rojas et al. 2020). Certain subpopulations are particularly vulnerable to depressive disorders, such as women, younger adults, those with a family history of mental health disorders, and those living in poverty. (Meng et al., 2017).

MDD is diagnosed according to the Diagnostic and Statistical Manual of Mental Disorders, 5th Edition (DSM-5). Diagnosis requires a patient to be experiencing five or more persistent symptoms (present for more than 2 weeks) including depressed mood and/or anhedonia, as well as weight changes, sleep disturbances, psychomotor agitation/retardation, fatigue, feelings of worthlessness, poor concentration, and suicidal ideation (American Psychiatric Association, 2013).

A diagnosis of MDD not only entails low mood, anhedonia and other related symptoms, it also puts patients at elevated risk for comorbid diseases (Berk et al., 2023; Thaipisuttikul et al., 2014). Perhaps the most severe of these comorbidities is suicide; globally, over 700,000 people die by suicide annually (World Health Organization, 2021). Women have elevated levels of suicidal ideation compared to men, though men have higher rates of death by suicide, likely due to their

use of more lethal methods (Varin et al., 2021). Marginalized communities, such as Indigenous Canadians (Kumar & Tjepkema, 2019) and LGBTQ+ youth are also at elevated suicide risk (Williams et al., 2021).

In addition to increased suicidality, MDD is comorbid with a variety of conditions including anxiety disorders and other mental health disorders, type 2 diabetes, sleep disorders, and cardiovascular disorders, including stroke (Berk et al., 2023; Thaipisuttikul et al., 2014).

1.1.2 Treatment of MDD

MDD is most commonly treated with a combinational approach and is highly specific to the individual. Due to the heterogeneity of the depressed population, different approaches are taken for different people. A classical treatment strategy will often involve psychotherapy delivered concurrently with an antidepressant medication, most often targeting the monoamine system. Several psychotherapy modules and medication types exist, all with unique benefits and applications (Simon et al., 2024).

1.1.2.1 Monoaminergic antidepressant medications

Being the first line of treatment for such a pervasive disorder, many antidepressants have been studied, most of which target monoamines. The most pervasive class of antidepressants used are selective serotonin reuptake inhibitors (SSRIs). Unfortunately, this class of drugs rarely works on first attempt, with many patients trying various SSRIs in their lifetime. On top of this, SSRIs are only effective in around 50% of patients, with only 30% of those achieving remission (Rush et al., 2006). Nonetheless, they are generally well tolerated drugs with few adverse side effects, and

as such are typically the first antidepressants prescribed (Cipriani et al., 2018). As their name suggests, they inhibit the reuptake of post-synaptic serotonin by blocking the serotonin transporter (SERT). This increases synaptic serotonin allowing for enhanced neurotransmission (Hillhouse & Porter, 2015). SSRIs generally take 3-4 weeks of chronic treatment to achieve antidepressant effects in patients, and this is hypothesized to be due to 5-HT1A auto receptor activity (Vahid-Ansari et al., 2019; Mead et al., 2012). Increased extracellular serotonin activates post-synaptic 5-HT receptors, but also 5-HT1A autoreceptors. Autoreceptor activation triggers negative feedback by inhibiting neuronal firing, dampening the SSRIs effect. This process is hypothesized to be desensitized by chronic treatment, disinhibiting serotonin neurons and enabling the desired enhanced post-synaptic serotonin accumulation (Albert & Lemonde, 2004).

Monoamine oxidase inhibitors (MAOI) were discovered serendipitously in 1954 when researchers developed isoniazid, and then iproniazid, as a tuberculosis treatment. While effective for their original condition, researchers also noted the elevated mood of patients taking iproniazid (Hillhouse & Porter, 2015). Later marketed as Marsilid, this MAOI was the earliest antidepressant to warrant clinical research. MOAIs inhibit the breakdown of the body's amines, notably serotonin, dopamine, epinephrine, and norepinephrine. As a result of this inhibition, synaptic monoamine concentrations are increased, allowing for more neurotransmission (Meyer et al., 2022). MAOIs like iproniazid are now rarely used clinically, in part due to their undesirable hypertensive side effects, and are reserved for patients who have not responded to other treatments (Meyer et al., 2022; Karrouri et al., 2021).

Tricyclic antidepressants (TCA) were also discovered as a result of targeting another disorder. In this case, following the discovery of chlorpromazine for the treatment of schizophrenia, promethazine, another antipsychotic, was developed and later altered into imipramine, the earliest derived TCA (Laux, 2022). TCAs consist of three benzene rings, and their antidepressant action is thought to be a result of the inhibition of serotonin and norepinephrine reuptake transporters; this results in elevated synaptic serotonin and norepinephrine (Hillhouse & Porter, 2015). These drugs are typically prescribed to patients with severe depression who have not responded to first line treatments, as they have more adverse side effects than SSRIs (Cipriani et al., 2016).

Another class of antidepressant that enhances monoamine levels is serotonin-norepinephrine reuptake inhibitors (SNRI). These were first introduced in the 1990s, with the drug venlafaxine. SNRIs inhibit the reuptake of serotonin and norepinephrine via inhibition of their transporters, but unlike TCAs they don't act upon adrenergic, histamine, muscarinic, dopamine, or postsynaptic serotonin receptors (Hillhouse & Porter, 2015). SNRIs are typically well tolerated and prescribed to patients who do not respond to SSRIs (Karrouri et al., 2021).

1.1.2.2 Psychotherapies

Psychotherapy plays a crucial role in MDD treatment and is often delivered in conjunction with pharmacotherapy. A variety of psychotherapy options exist for the treatment of MDD, each with their individual benefits and drawbacks. When administered alone, or in conjunction with antidepressant medications, psychotherapy is an effective tool in the treatment of MDD (Munder et al., 2018; Cuijpers et al., 2020, 2021)

A widely studied and praised psychotherapy modality is cognitive behavioural therapy (CBT). CBT aids patients in identifying and modifying their thoughts and behaviours. CBT has shown long-term efficacy and relapse prevention in MDD treatment (Health Quality Ontario, 2017).

Offshoots of CBT, acceptance and commitment therapy (ACT) and mindfulness-based cognitive therapy (MBCT) are also used in the treatment of mood disorders like MDD. These therapies share CBT's emphasis on mindfulness while focussing more on developing flexible thoughts and emotions, as opposed to changing behaviours. ACT and MBCT have shown effective treatment and relapse prevention in MDD patients (Tickell et al., 2020; Dindo et al., 2017).

Another psychotherapy technique is interpersonal therapy (IPT), which focusses on addressing and resolving interpersonal conflicts. IPT has also been shown to reduce major depressive scores and relapse in MDD patients (Health Quality Ontario, 2017).

Supportive therapy, though not classified as a psychotherapy technique, was also effective at reducing depressive scores and improving recovery in MDD patients (Health Quality Ontario, 2017). Supportive therapy is an unstructured talk therapy that focusses on current problems and relies on the support of the therapist (Cuijpers et al., 2012).

1.1.2.3 Other treatments

Beyond the first line treatments, alternative treatments exist for patients who show resistance to classical monoamine-acting antidepressants. These treatments include novel drugs, like esketamine and psilocybin, and non-invasive brain stimulation techniques like transcranial direct current stimulation (tDCS), repetitive transcranial magnetic stimulation (rTMS), deep brain stimulation (DBS) and electroconvulsive therapy (ECT).

Esketamine, the more potent ketamine S-enantiomer, modulates the glutamatergic system as a non-selective, non-competitive NMDA receptor antagonist (Vasiliu, 2023). This antagonism leads to a rapid increase in glutamate release and stimulation of α-amino-3-hydroxy-5-methyl-4-isoxazolepropionic acid (AMPA) receptors and enhanced synaptogenesis. Esketamine can also inhibit dopamine transport, elevating extracellular dopamine, and reducing anhedonia. While fast-acting and effective in clinical trials, esketamine is only prescribed after other avenues have been exhausted due to its neurocognitive side effects and potential for dependence (Kawczak et al., 2024).

Another novel class of drugs gaining recent interest for their antidepressant action are psychedelics, mainly psilocybin but also Lysergic Acid Diethylamide (LSD) and Dimethyltryptamine (DMT). Psilocybin, used recreationally as “magic mushrooms”, is a 5-HT2A receptor agonist that has shown rapid antidepressant action (Nutt et al., 2023). Just a single dose of psilocybin has been shown to significantly improve depression scores clinically but was also accompanied by adverse side effects in 77% of patients (Goodwin et al., 2022). This

class of drugs shows promise for patients who do not respond to first line treatments but will require dose optimization and more expansive clinical trials.

Many non-invasive brain stimulation techniques also exist for patients who do not respond to classical pharmacological treatments. tDCS utilizes electrodes to deliver electric current to distinct scalp areas. This stimulation can modulate neuronal activity via depolarizing or hyperpolarizing stimuli. (Liu et al., 2017). When delivered to the left dorsolateral prefrontal cortex this technique induces neurostructural changes. (Jog et al., 2023).

rTMS is another non-invasive brain stimulation technique that uses electromagnetic current to modulate cortical excitability (Liu et al., 2017). rTMS primarily targets the left dorsolateral prefrontal cortex to improve MDD symptoms, at times in combination with antidepressant drugs (Wang et al., 2017, Liu et al., 2017).

Lastly, electroconvulsive therapy is a potent treatment modality in a variety of psychiatric disorders. By inducing a seizure via electrical current to the scull, patients achieve rapid relief in MDD symptoms. The exact mechanism of action is still inconclusive; however, research reports changes in neuroplasticity markers such as increased BDNF levels (Brunoni et al., 2014; Pelosof et al., 2023), alterations in neurotransmission and HPA axis dysregulation (Salik & Marwaha, 2025).

Taken together, MDD is a highly prevalent mental disorder with serious comorbidities, and a high death rate. Not only that, but treatments often lack efficacy and remittance. This highlights the need for continued research of the disease and its many facets.

1.2 Stroke

Stroke, much like MDD, is a serious health condition with significant risk of disability and mortality. As of 2021, the World Health Organization (WHO) ranked stroke as the third leading cause of both death and disability, following COVID-19 and ischemic heart disease. In fact, for the past two decades, stroke has been in the top 10 leading causes of death worldwide, often ranking around 2nd or 3rd (World Health Organization, 2021; He et al., 2024). Of these strokes, the vast majority are ischemic, accounting for around two thirds of all stroke cases (Feigin et al., 2022). An ischemic stroke occurs when there is a blockage of a blood vessel, most commonly an artery, but in some rare cases a vein, leading to reduced blood flow to the brain (Majumder, 2024). The less common hemorrhagic stroke occurs when there is a tear in a blood vessel of the brain, leading to blood leakage and excessive pressure on surrounding brain cells (Unnithan et al., 2025). Within these classifications, there are subclasses defined by the source or location of the stroke, such as a large artery atherosclerosis, or intracerebral hemorrhage. Despite ischemic strokes being more common, hemorrhagic strokes are often more severe, and more deadly (Andersen et al., 2009; Chiu et al., 2010).

Many risk factors are shared between all strokes, such as hypertension, age, and smoking (Boehme et al., 2017). Ischemic strokes have a strong link to atherosclerosis, the buildup of fatty deposits on artery walls. This atherosclerosis can be developed through a variety of subsequent

risk factors, such as hypertension, cardiac disease, diabetes, obesity, and so on. Atrial fibrillation is also a specific risk factor for a subtype of ischemic stroke, cardioembolic stroke. (Boehme et al., 2017). Unique to hemorrhagic stroke, a low glomerular filtration puts patients at risk (Bos et al., 2007).

Treatments for stroke vary depending on several factors like stroke type, time since event, age, and severity of stroke. For hemorrhagic stroke, the primary priority is to stop the bleeding. This is often done through beta blocker administration to reduce blood pressure, and a clotting agent to assist the body in stopping the bleed. For severe cases, surgery is also used to relieve the buildup of blood in or around the brain (Unnithan et al., 2025). For ischemic stroke, treatment with tissue plasminogen activator (tPA) can break up the blood clot but must be administered within 4.5 hours of symptom onset, leaving a small treatment window (Hatcher & Starr, 2011). Surgical thrombectomy can also be performed to remove the responsible clot, though rapid treatment remains imperative, with outcomes worsening with every hour delayed (Saver et al., 2016).

Chronic treatments depend on the location of the stroke, and the subsequent presenting symptoms. Common treatments include speech, physical, occupational, and cognitive therapies. For patients experiencing a common side effect of stroke – post stroke depression, these treatments will often be given in tandem with antidepressant medication and psychotherapy. Antidepressants have also been tested more broadly for stroke recovery. The FLAME study found a benefit of SSRI treatment for motor recovery, but subsequent studies have found variable results (Chollet et al., 2011; Mead et al., 2012; Legg et al., 2019).

1.3 Post Stroke Depression

1.3.1 General overview

Post-stroke depression (PSD) is a common co-morbidity of stroke, experienced by approximately one third of all stroke patients, with some studies citing up to 80% of patients experiencing a milder depressive episode following their stroke (Ayerbe et al., 2013; Paolucci et al., 2006; Hackett & Pickles, 2014; Medeiros et al., 2020). This high incidence leads to extensive burden on the patients, their family and the healthcare system. PSD patients have lower treatment compliance, worse rehabilitation results, elevated risk of a subsequent stroke, poor functional outcomes, as well as higher disability and mortality rates (Zhou et al., 2024; Sibolt et al., 2013; Wijeratne & Sales, 2021).

The DSM-5 classifies PSD under "Depressive Disorder Due to Another Medical Condition". The diagnostic criteria are very similar to MDD, requiring a pervasive period of depressed mood or anhedonia, clinically significant impairment in social/occupational areas of function, the lack of a better explained mental disorder, and of course, the presence of diagnosed medical condition (in the case of PSD, stroke). A large variety of diagnostic tools exist for the diagnosis of MDD and PSD. These include the Center for Epidemiological Studies Depression Scale (CESD) the Hamilton Depression Scale (HDS), the Hospital Anxiety and Depression Scale (HADS), the Beck Depression Inventory-II (BDI-II), the Distress Thermometer (DT), and the Kessler-10 (K-10) the Patient Health Questionnaire-2 (PHQ-2), and the Patient Health Questionnaire-9 (PHQ-9), among others. Studies recommend the use of the yes/no version of PHQ-2 and the longer PHQ-9 for assessment of a PSD population (Lavu et al., 2022; Meader et al., 2014).

1.3.2 PSD causes

PSD is a complex disorder with many potential causes. No two strokes are the same, and they impact individuals differently based on a variety of factors such as age, gender, stroke severity, initial treatment response, etc. (Wijeratne & Sales, 2021). This heterogeneity in the patient population makes it difficult to establish an exact cause of the disorder; however, studies have shown various associations. While no one underlying cause of PSD has been identified, several possible mechanisms have been elucidated. While these mechanisms are presented as distinct hypotheses, they are all interconnected and likely all contribute, to varying extents, to the development of post-stroke depression.

The physical and psychological effects of a stroke can greatly impact a patient's quality of life and mental wellbeing. Strokes can affect a variety of functions depending on their size and location, but common effects include motor, cognitive, and speech impairment (Mane et al., 2022). These impairments may lead to a lack of ability to complete daily tasks unassisted, known as activities of daily living (ADL), which is correlated with PSD (Li et al., 2022). Additionally, stroke survivors report fear of future stroke, a loss of self, and a sense of loneliness/isolation (Crowe et al., 2016). Studies show that a lack of social support is associated with post stroke depression (Teoh et al., 2009, Northcott et al., 2016; Saadi et al., 2018; Babkair et al., 2022) and has predictive value (Volz et al., 2016). A study of Egyptian stroke patients also found PSD to be associated with the severity of post-stroke impairment, finding higher rates among those with greater impairment (Khedr et al., 2020). These factors all suggest a psychosocial component to the development of PSD, with strong ties to social support.

Beyond the psychosocial factors at play, the size and location of the stroke have associations with PSD incidence. A 2021 review by Wijeratne & Sales identified 15 studies linking lesion volume and PSD. Four found no effect, but seven found a relationship between larger stroke volumes, and PSD incidence. Two of these studies found that this association is only evident 3 months post-stroke, which could potentially account for the studies that found no association (Wijeratne & Sales, 2021).

In addition to lesion volume, the location of the lesion has shown correlations with PSD incidence, although results vary by study. Many studies have found that PSD is more frequently associated with left hemispheric lesions (Robinson et al., 1984; Aström et al., 1993; Narushima et al., 2003; Barker-Collo, 2007; Grajny et al., 2016; Thomas, 2023), though some studies have also found a significant correlation with right-hemispheric lesions (Wei et al., 2015; Weaver et al., 2023). Additional studies cite that damage to the cortico-limbic pathways are associated with PSD (Weaver et al., 2023; Klein et al., 2010). There is also evidence that damage to the prefrontal cortex, basal ganglia, and amygdala is associated with PSD (Grajny et al., 2016; Klingbeil et al., 2022; Terroni et al., 2011; Weaver et al., 2023; Douven et al., 2017).

Another physiological factor involved in PSD onset after stroke is the immediate inflammatory response. Immediately after vessel occlusion, the inflammatory cascade is activated (Anrather & Iadecola, 2016). This activation aims to clear dead cells and prepare for repair, but the influx of inflammatory mediators, such as cytokines, chemokines, and reactive oxygen species (ROS) can exacerbate the initial damage (Feng et al., 2024). These mediators attract white blood cells which leads to overexpression of pro-inflammatory genes, further exacerbating the injury. Recruited

astrocytes contribute to blood brain barrier (BBB) permeability, allowing for an influx of peripheral immune cells and inflammatory agents, and an efflux of cytokines, triggering a systemic immune response (Feng et al., 2024).

Neuroinflammatory processes have been suggested to underlie depression, with studies showing links between inflammatory markers and MDD (Mechawar & Savitz, 2016; Miller et al., 2016). Studies have shown increased pro-inflammatory cytokines in patients with depression (Wohleb et al., 2016). Studies also link depression, and death by suicide, with elevated IL-6 and TNF-a levels in the brain and periphery (Hayley et al., 2020). A 2017 study also reported elevated TNF-a and IL-1B levels in post-stroke depression patients (Kim et al., 2017). IL-1B plays key roles in modulating synaptic plasticity and inducing depressive-like behaviour in stress exposed mice (Koo & Duman, 2008; Abelaira et al., 2014). Notably, proinflammatory cytokines can stimulate indoleamine-pyrrole 2,3-dioxygenase (IDO), a metabolizer of tryptophan, and reduce brain serotonin (Hayley et al., 2020). This links inflammation to the monoamine hypothesis of depression, proposing a potential mechanism to explain these correlations.

1.3.3 Treatment of PSD

There exists little consensus regarding the ideal course of treatment for PSD. Treatments tend to mirror that of MDD, though they must take into consideration the limitations faced by stroke patients, as well as the clinical variability of the disorder. While routinely used in the treatment of MDD, psychotherapy treatments in the specific context of PSD have not been extensively studied. Early studies of CBT for PSD recovery found varying results, with the therapy having some positive effect, but not in all patients (Lincoln et al., 1997; Lincoln & Flannaghan, 2003;

Rasquin et al., 2009). Broomfield, 2011 argues that the variable or null results in these studies may be due to the short-term treatment and lack of modification to account for the physical comorbidity of stroke, proposing that an augmented, individually tailored CBT intervention approach be used.

A 2018 meta-analysis of 23 studies found that CBT alone, and in conjunction with antidepressant treatment, significantly improved depressive symptoms in PSD patients (Wang et al., 2018). This recovery included significantly higher remission and response rates, though individual trials still show high degrees of variability.

There is also promising evidence of psychotherapy for the prevention of PSD. In a group of 104 ischemic stroke patients, those given group acceptance and commitment therapy (G-ACT) had significantly lower scores on the Hamilton depression scale at 1 and 3 months compared to the control group receiving only routine stroke treatment (Niu et al., 2022).

Pharmacotherapy treatment research for PSD has shown variability between cohorts, but meta-analyses find that SSRIs, SNRIs and TCAs can significantly improve PSD symptoms (Deng et al., 2017; Allida et al., 2023; Xu et al., 2016; Qin et al., 2018). However, due to a limited number of RCTs, it is difficult to identify a singular superior antidepressant (Towfighi et al., 2017).

In animal models, the benefit of antidepressants is clearer. A 2014 meta-analysis found that antidepressants, and specifically SSRIs, could significantly improve neurobehavioral outcomes in animal stroke models (McCann et al., 2014). In a photothrombotic PSD model, fluoxetine was

able to significantly improve depressive-like behaviour and upregulate hippocampal BDNF expression (Jin et al., 2017). Our lab's past research also showed that fluoxetine, but not exercise via running wheel, was able to recover the behavioural phenotype and serotonergic innervation of PSD mice (Vahid-Ansari & Albert, 2018).

While antidepressants remain the primary line of treatment for PSD, emerging evidence suggests positive results from neuro-modulatory treatments, namely transcranial direct current stimulation (tDCS) and repetitive transcranial magnetic stimulation (rTMS). In a small randomized double-blind trial, tDCS had significantly higher response and remission rates compared to sham control (Valiengo et al., 2017). rTMS has been more thoroughly studied and two meta-analyses concluded an improved PSD recovery in the rTMS treated group compared to control (Shen et al., 2017; Shao et al., 2021), noting large heterogeneity in the samples and a need for future research.

1.4 Serotonin

1.4.1 General overview

Serotonin is a monoamine neurotransmitter whose cells originate in the raphe nuclei of the midbrain and extend widely to innervate a variety of target regions in the brain. Despite only originating from this small and localized brain region, 5-HT modulates nearly all neural circuits of the brain (Donovan et al., 2019). First identified in 1964, serotonin cells have been classically organized into 9 groups, B1-9 (Dahlström & Fuxe, 1964). Further studies have shown the caudal groups (B1-3), extend down to the spine and cerebellum, while the more rostral groups (B4-9)

extend rostrally to the rest of the brain. Of these cell groups, the dorsal raphe nucleus is comprised of B6 and B7, and the median raphe groups B8 and B9 (Deneris & Gaspar, 2018).

Once released, serotonin acts both pre- and post-synaptically on serotonin receptors, of which there are 7 classes (5-HT1-7 receptors) made up of 14 receptors (Vahid-Ansari & Albert, 2021; Barnes et al., 2021). Most serotonin receptors are post-synaptic receptors; however, two members of the 5-HT1 receptor class, 5-HT1A and 5-HT1B receptors, are expressed on serotonin cells as auto receptors (Vahid-Ansari & Albert, 2021; Sari, 2004). Implicated in MDD pathology, 5-HT1A autoreceptors bind exogenous 5-HT and attenuate neurotransmission via coupling to Gi/Go proteins. One main hypothesis of SSRI action involves the desensitization of this autoreceptor over time, leading to upregulated 5-HT neurotransmission (Albert & Lemonde, 2004).

1.4.2 Development of the serotonin system

In early development, around week 5-7 gestation in humans and E9.5-13 in rodents (Deneris & Gaspar, 2018), the serotonin system begins to differentiate. With its cells located in the brainstem, the early development of this neurotransmitter system is unsurprising. As such, serotonin has been linked to many early developmental processes throughout the brain. Some examples include neurogenesis and neuronal survival, dendritogenesis, axonal projection, and synapse formation (Shiga et al., 2006).

Regarding 5-HT development, serotonin neurons begin to project out of the raphe in two distinct bundles: one projecting caudally down to the spinal cord and cerebellum, and the other

projecting rostrally up through the medial forebrain bundle. This rostral bundle houses the median and dorsal raphe nuclei (Deneris & Gaspar, 2018).

Serotonin cell bodies emerge around the 12th day of gestation in rats (E12), beginning with the bilateral rostral group, and closely followed by the bilateral caudal group at E14-16 (Aitken & Törk, 1988). By E16, the rostral group ascends through the mesencephalon, forming the medial forebrain bundle. This rostral bundle then splits, to send projections both dorsally and ventrally. The ascending fibers reach the frontal pole by E17, and by E19 all major divisions and pathways have been established (Aitken & Törk, 1988; Lidov & Molliver, 1982). Serotonin fibers were not observed to branch along these main ascending fibers, or in early cerebral cortex areas – suggesting that this branching occurs at a later stage of development, or postnatally (>E21), closer to final target regions (Aitken & Törk, 1988).

This early outgrowth of serotonin axons is guided by key axon guidance cues, of which several have been elucidated. These include broadly expressed growth factors like brain-derived neurotrophic factor (BDNF), S100B, growth associated protein 43 (GAP43) and stable tubule only polypeptide (STOP), as well as more specific guidance cues like WNTs, Slit 1/2, Robo 1/2, Lmx1b, Pet-1, ephrins, pcdhα, and even serotonin itself (Vahid-Ansari & Albert, 2021; Deneris & Gaspar, 2018).

S100B has been found to increase neurite length, as well as neurite number and total field area in cultures of embryonic rat serotonin neurons (Azmitia et al., 1990; Liu & Lauder, 1992). BDNF, a key regulator of neuronal plasticity, has also been shown to enhance 5-HT cell differentiation,

axon outgrowth, length and total arborization (Rumajogee et al., 2002; Leschik et al., 2022), and even enhanced sprouting of 5-HT axons post-PCA-induced injury (Mamounas et al., 2000).

Further, the cytoskeleton associated protein growth-associated protein 43 (GAP-43), and the microtubule-associated protein stable tubule only polypeptide (STOP) play roles in 5-HT axonal outgrowth as well, with knockout mice showing deficient target innervation (Donovan et al., 2002; Fournet et al., 2010).

The anterio-posterior (A-P) guidance cue family of Wnt proteins provide directional cues for ascending and descending fibers. Wnt signalling has been shown to be required for proper 5-HT cell orientation (Fenstermaker et al., 2010). Specific planar cell polarity genes expressed by raphe neurons were also implicated, with Fzd3, Celsr3, and Vang12 knockout mice showing A-P orientation abnormalities (Fenstermaker et al., 2010). A 2002 study summarized the importance of Slit1 and 2 in midline axonal guidance for long range projections (Bagri et al., 2002), furthered in 2007 by the finding that Robo1 and 2, which meditate Slit proteins, are also crucial for proper axon guidance (López-Bendito et al., 2007).

Lmx1b and Pet-1, key transcription factors in the differentiation of 5-HT neurons, have also been identified as key outgrowth regulators using knockout mice. Lmx1b knockout mice showed impairment in all stages of 5-HT axon outgrowth, pointing to its intrinsic control of 5-HT system development (Donovan et al. 2019). Pet-1 knockout mice show depleted serotonergic innervation in the cortex and hippocampus, linked to a subset of 5-HT neurons (Kiyasova et al., 2011; Kiyasova & Gaspar, 2011).

Ephrin signalling has also recently been implicated in serotonergic guidance. Long known to act as guidance cues, ephrinA signalling has shown importance in 5-HT axon repulsion in a subset of raphe neurons. EphrinA5, the most abundantly expressed EphA receptor in the DR, is dynamically, and differentially expressed amongst raphe neurons during development. Ectopic expression of ephrinA inhibits axonal growth, whereas loss of function of ephrin 5A causes increased localized growth in the olfactory bulb, ventromedial hypothalamus and suprachiasmatic nucleus – regions with high ephrinA5 expression in WT mice (Teng et al., 2017).

Protocadherins are key cell adhesion molecules implicated in axonal arborization (Chen et al., 2017; Katori et al., 2009, 2017). In serotonin neurons, protocadherin alpha, and more specifically protocadherin alpha c2, have shown to be indispensable for proper serotonergic development. Knockout models display abnormal axonal tangling in target regions, implicating it as a key regulator of localized arborization. (Chen et al., 2017; Katori et al., 2009, 2017)

Interestingly, serotonin itself has also been shown to act as both an attractive and repulsive guidance cue for rat sensory neurons, in vitro (Vicenzi et al., 2020). Further, in Tph2 knockout mice, severe disruption to serotonergic circuitry was observed (Migliarini et al., 2013). A lack of Tph2, the rate limiting enzyme in serotonin production, led to reduced serotonergic innervation of the suprachiasmatic and thalamic paraventricular nuclei, and increased innervation in the nucleus accumbens. Additionally, these knockout mice displayed upregulation of hippocampal BDNF aligned with hyperinnervation of the hippocampus, pointing to a possible regulatory mechanism (Migliarini et al., 2013). Taken together, with the knowledge that 5-HT growth cones

possess high levels of 5-HT at the earliest stages of development (Migliarini et al., 2013), this suggests that serotonin may be a key factor directing the outgrowth of its own axons in development.

1.4.3 Role of 5-HT in MDD

Serotonin was first suggested to be implicated in the pathology of depression in the 1960's, and since then, a large body of research has examined the role of 5-HT in depressive disorders and sought to manipulate it for recovery.

The monoamine hypothesis of depression stipulates the involvement of monoamines, namely serotonin, norepinephrine and/or dopamine in MDD pathology. This hypothesis stemmed from research in the 1950's, starting with the findings of Edward D Freis, showing depressive symptoms after treatment with reserpine (Freis, 1954), which binds monoamine transporters and reduces 5-HT levels in the brain (Bremshey et al., 2024). In 1958, the tricyclic antidepressant (TCA) imipramine became the first commercially available antidepressant, introduced by Roland Kuhn (Bremshey et al., 2024). Imipramine acts by inhibiting serotonin and noradrenaline reuptake, leading to higher synaptic levels of these monoamines (Hillhouse & Porter, 2015).

Following these findings, the monoamine hypothesis of depression was first proposed in 1965 by Schildkraut and Bunney & Davis, and then broadened in 1967 by Coppen to emphasize the potential role of serotonin (Albert et al., 2012). In the 6 decades that have followed, supporting research has emerged showing effective depression treatment by SSRIs (Karrouri et al., 2021), the relapse of depression in tryptophan-depleted MDD patients in remission (Young & Leyton,

2002; Yatham et al., 2012), elevated 5-HT1A binding in antidepressant-naïve and not recently medicated MDD patients (Parsey et al., 2006, 2010) and reduction in 5-HT1A auto receptor binding with antidepressant treatment (Gray et al., 2013) and reduced 5-HT innervation in post-mortem tissue (Underwood et al., 2012, 2018; Rajkowska et al., 2017). This ever evolving and expanding area of research strongly suggests the involvement of serotonin in the complex disorder MDD.

1.4.4 Axonal regrowth

It has long been held that adult neurons cannot regenerate their damaged soma, and only a minority regenerate their damaged processes following injury. This is due to the intrinsic and extrinsic inhibitory mechanisms, resulting in little progress in this field (Fawcett, 2020). Despite this inhibitory environment, the serotonin system has been shown, in a variety of models, to be uniquely capable of regrowth following injury. Early evidence of this process came largely from chemical injury models. Some key examples include the monoaminergic neurotoxins 5,7-dihydroxytryptamine (5,7-DHT) and amphetamines like MDMA and para-chloroamphetamine (PCA).

5,6-DHT was first introduced in 1971 as a selective destructor of serotonin neurons and later optimized in 1972 to use isomer 5,7-DHT for fewer side-effects (Baumgarten & Lachenmayer). This chemical injury model is quite severe; ten days after intraventricular injection in female rats, endogenous 5-HT levels were reduced to 13% of the control level in the spinal cord, 81% in the medulla oblongata and 57% in the hypothalamus (Björklund et al., 1973). Interestingly, this dramatic reduction does gradually recover over 2-3 months, up to 108% in the medulla oblongata

and 123% in the hypothalamus. At 10-17 days, axonal sprouting could be observed from the damaged ends of serotonin axons in the MFB. (Björklund et al., 1973). In a later study, using this model in the dorsolateral hypothalamus of rats, degenerated serotonin axons were observed to sprout 12-19 days post lesion, and recover fully in the medial forebrain bundle, although deficiencies remained in medial and periventricular areas (Frankfurt & Azmitia,1984).

Similar effects were observed when using amphetamines to degenerate serotonin neurons. MDA, MDMA, PCA and fenfluramine all caused acute 5-HT depletion in the rat forebrain, and subsequent axonal degeneration within 48 hours. 2-8 months after treatment, gradual re-innervation was observed in the cortex (O'Hearn et al., 1988; Molliver et al., 1990). These compounds seem most toxic to fine fibers and axon terminals, while sparing preterminal axons and cell bodies (Wilson & Molliver. 1994). As previously mentioned, BDNF application also enhanced this post-degeneration sprouting of 5-HT axons in a PCA model (Mamounas et al., 2000).

These early chemical models laid the groundwork for future research in serotonergic re-innervation following injury. One such study was conducted in 2016 (Jin et al.) and examined serotonin axon regrowth following either stab injury to the somatosensory cortex or para-chloro-amphetamine-induced brain injury. This study used in-vivo imaging to follow the regrowth of specific serotonergic fibers. What they found was that stab-lesioned serotonin axons were able to regrow and cross the stab rift, with over 80% of the regrowth originating from the severed axons. With para-chloro-amphetamine-driven lesion, they also saw robust recovery of the damaged region; however, most of the re-innervation originated from axons beyond their field of view,

suggesting long-distance regrowth rather than local sprouting or true regrowth as observed in the injury model. This study demonstrates the plasticity of the serotonin system, showing spontaneous recovery in these injury models.

This regrowth research extends even further into alternative injury models, such as traumatic brain injury (TBI) and stroke. Following TBI, female mice had a reduction in serotonin axonal density posterior to the lesion site at 1-week post-surgery, most notably at cortical layer 1. By 1-month post-surgery, this axonal density was significantly recovered. This again speaks to the capacity of serotonin neurons to re-innervate damaged brain areas, in a variety of mouse models (Kajstura et al., 2018).

In our lab, we study post-stroke depression and as such, use a stroke model. In this stroke model (as described in methodology), a 1-mm^3 lesion to the left medial prefrontal cortex of adult mice resulted in a significant reduction in serotonin axons in the left cingulate cortex of the mPFC, and the left basolateral amygdala. 6 weeks post-stroke, when left untreated, serotonin innervation increased significantly compared to 1-week post-stroke, indicating a partial spontaneous recovery of these axons. This is consistent with the other previously described injury models of regrowth. This re-innervation was still incomplete compared to baseline, but treatment with fluoxetine fully recovered both the innervation and associated behavioural deficits, implicating this SSRI in serotonergic re-innervation following stroke (Zahrai et al., 2020).

Taken together, the serotonin system is highly plastic, and capable of regrowth following injury despite the inhibitory microenvironment.

1.5 Rodent models of PSD

PSD is a complex disorder, and as such, can be a challenge to model. Various animal models have been developed to replicate the behavioural, cognitive and innervation changes associated with the disorder, achieving varying levels of success.

1.5.1 MCAO model

The middle cerebral artery occlusion (MCAO) model has long been used to induce stroke in animal models. This technique involves temporary occlusion of the middle cerebral artery, restricting blood flow to the brain. The result is a large and variable stroke, particularly in mice, impacting a variety of brain regions (Carmichael, 2005). This model is mainly designed to test primary stroke outcomes but has also been adapted for modelling post stroke depression. Most studies find no consistent, long-term depression-like phenotype when using the MCAO model alone, so will commonly use a secondary stressor to achieve the desired phenotype (Zhang et al., 2015). Of these stressors, the MCAO is most commonly paired with a chronic mild stress paradigm (CMS), though restraint stress and social defeat have also shown success (Zhang et al., 2015; O'Keefe et al., 2014). These models are used to induce a PSD phenotype, while mimicking the stress, social isolation and/or immobility experienced by stroke patients. These combinational approaches may represent the complex nature of human PSD, but the lack of clear depression phenotype induced by the stroke itself makes it less obvious whether this is a true PSD model, or rather a stress model. The large and variable lesion also makes behavioural testing more difficult, limiting the applicability of this model.

1.5.2 Photothrombotic model

First introduced in 1985 (Watson et al.), the photothrombotic stroke model involves the injection of a photosensitive dye, such as Rose Bengal, and subsequent activation by light to initiate thrombosis. This creates a relatively consistent cortical lesion, though variability still exists primarily based on the location and angle of the light (Zhang et al., 2024). When used to assess PSD, researchers found a significant anxiety and depression-like phenotype that could be recovered by fluoxetine treatment (Jin et al., 2017). A study has also shown that neuronal activation of protein tyrosine phosphatase 1B (PTP1B) contributed to the PSD phenotype in a photothrombotic stroke to the peri-prefrontal cortex (Cruz et al., 2020). This stroke model produces a comparatively smaller and more consistent lesion than the MCAO model, with an intrinsic ability to induce PSD. Despite its advantages over the foundational MCAO model, photothrombotic lesions lack the ability to produce a very small and reproducible lesion to deeper cortical regions and lacks the peri infarct penumbra that is highly characteristic of human stroke (Labat-gest & Tomasi, 2013).

1.5.3 ET-1 model

To avoid motor impairment, the need for an additional stressor, and/or a large stroke impacting various brain regions, a novel PSD mouse model was developed by our lab (Vahid-Ansari et al., 2016), adapted from the methods described in Windle et al. (2006). In this model, adult mice are intracranially injected with 2 x 1 µl of endothelin-1 (ET-1) in the medial prefrontal cortex, inducing focal ischemia. Endothelin-1 is a potent vasoconstrictor peptide produced by endothelial cells (Titus & Marappa-Ganeshan, 2025). First demonstrated in 1989 to successfully induce focal ischemia in rats, ET-1 has become a useful tool in animal models of stroke (Fuxe et

al., 1989). Injection of ET-1 at coordinates AP +2, ML +0.5 DV -2.4 and AP +1.5, ML +0.5, DV -2.6 induces a highly specific and reproducible stroke in the prelimbic and cingulate cortices, averaging 1mm^3. This stroke model also induces anxiety-like, depression-like and cognitive impairment phenotype that persists for 6 weeks, with no need for additional stressors. By targeting only the mPFC, this model does not induce motor deficits, allowing for extensive behavioural testing. By 6 weeks the stroke site is refilled with NeuN+ and FosB+ cells, however only minorly reinnervated by SERT+ fibers (Vahid-Ansari et al., 2016; Zahrai et al., 2020). This model is also sensitive to SSRI treatment, with fluoxetine treated mice displaying complete behavioural recovery and reinnervation of damaged regions (Vahid-Ansari & Albert, 2018; Zahrai et al., 2020).

1.6 Protocadherins

1.6.1 General overview

Protocadherins (pcdh), the largest subfamily of the cadherin superfamily, are homophilic cell-adhesion proteins that play a role in the development and maintenance of the brain's neural networks (Chen & Maniatis, 2013). Protocadherins exist in both a non-clustered form, spread throughout the genome, and clustered form organized into the three closely linked gene clusters, alpha, beta, and gamma. Located on mouse chromosome 18/human chromosome 5q31, the clustered protocadherins encode over 50 protein isoforms (Wu & Maniatis, 1999). Thought of as the vertebrate functional counterpart of the invertebrate Dscam1, these proteins are largely involved in neuronal recognition and repulsion, which is required for proper arborization and innervation (Chen & Maniatis, 2013; Zipursky & Sanes, 2010).

1.6.2 Tiling and self-avoidance

Protocadherins play a key role in neuronal arborization, through processes known as self-avoidance and tiling. Self-avoidance is the process by which neuronal processes on the same cell repel each other. Tiling is the process by which neuronal processes on different neurons of the same cell type (eg. the axons of two different serotonin cells) repel each other. Self-avoidance and tiling are both essential for proper coverage of target brain regions, to prevent crossover and redundancy in innervation (Grueber & Sagasti, 2010).

Most cell types stochastically express a variety of protocadherin isoforms. This diverse expression pattern allows for highly controlled repulsion. This repulsion is achieved by contact-mediated homophilic interaction (Chen & Maniatis, 2013; Mancini et al., 2020). This process has been shown in a variety of models and cell types. In retinal starburst amacrine cells and cerebellar Purkinje cells, pcdhg isoform deletion results in dysfunctional self-avoidance, and dendritic tangling (Lefebvre et al., 2012). In serotonin cells, mediation of tiling is the responsibility of a specific protocadherin isoform, protocadherin alpha c2 (pcdhαc2), which when knocked out also results in dysfunctional arborization and tangling (Chen et al., 2017; Katori et al., 2017).

1.6.3 Protocadherin alpha C2

A 2017 study by Chen et al. revealed via single-cell RNA sequencing that protocadherin alpha c2 (pcdhαc2) is the only alpha isoform expressed at a significant level in serotonin cells. Other isoforms, including pcdhαc1 were either not expressed at all, or barely detectable by their assay. Lower expression levels of pcdh gamma c3 and 4 was detectable, but a further conditional

knockout of all pcdh gamma isoforms from serotonin cells showed that the entire gamma cluster, including these isoforms, is dispensable for proper wiring. By contrast, both conditional and constitutive knockouts of pcdhα and pcdhαc2 show that this gene cluster, and specific isoform, are indispensable for proper serotonergic wiring (Chen et al., 2017). These findings are supported by a similar study from the same year, showing once again that protocadherin alpha c2 is indispensable for serotonergic neurons, using knockout mice (Katori et al., 2017).

In both studies, pcdhα/pchdαc2 knockout mice exhibit abnormal serotonergic wiring compared to control. Knockout mice exhibit axonal clumping and improper distribution in the target region. This was qualitatively reported in the prelimbic cortex, cingulate cortex, entorhinal cortex, basolateral amygdala, nucleus accumbens, ventral pallidum, anterior hypothalamus and hippocampus (Chen et al., 2017). This clumping was most prominent in the hippocampus, with a significantly increased serotonergic innervation of the SLM and significantly decreased serotonergic innervation of the DG, as quantified by Katori et al. (2017). This is further supported by the finding that Lmx1b and Pet1 temporally regulate post-natal pcdhαc2 expression, and that their knockout leads to similarly dysregulated 5-HT innervation (Donovan et al., 2019).

Pcdhα knockout mice also show modest behavioural differences, with poorer performance on the accelerating rotarod and spontaneous alternation test, suggesting deficits in motor coordination and working memory, respectively. They also showed anxiety-related behaviour in the open field test, marble burying test and light-dark exploration test, as well as depression-related behaviours in the tail suspension, forced swim, and contextual fear conditioning tests (Chen et al., 2017).

1.6.4 Associated Pathologies

Various protocadherin isoform changes are associated with human pathologies. Non-clustered protocadherin abnormalities have been linked to a variety of human diseases. Some examples include the role of protocadherin-1 in respiratory infection (Koning et al., 2012; Modak & Sotomayor, 2019), and the many protocadherins associated with cancers (Hirabayashi & Yagi, 2014).

Non clustered protocadherins have also shown implications in cognitive dysfunction. Deletions proximal to Pcdh10 and recurrent copy number variations in pcdh9 are associated with autism, and pcd17 is involved in schizophrenia pathogenesis (Kim et al., 2011). A meta-analysis also uncovered a previously unidentified single-nucleotide polymorphism (SNP) in pcdh9 gene to be significantly associated with MDD (Xiao et al., 2018). A meta-analysis also linked SNPs spanning pcdh17 with mood disorders like MDD (Chang et al., 2018).

Amongst the clustered protocadherins, fewer pathologies are known, and they are mainly neurodevelopmental in nature. In 2013, an examination of SNPs on the pcdhα gene cluster revealed significant association with autism spectrum disorder (Anitha et al., 2013). A study of SSRI resistant MDD patients also revealed significantly lower expression of pcdhα6 and pcdhα8, and abnormal axonal projections, in iPSC-generated serotonin neurons of non-remitting patients (Vadodaria et al., 2019). Further, a recent epigenome-wide analysis of early-onset major depression also identified differential methylations in the human protocadherin alpha gene cluster (Roberson-Nay et al., 2020). Additional genetic and epigenetic dysregulations of clustered protocadherins are outlined in 2020 reviews by Wu & Jia, and Flaherty & Maniatis.

2. Rationale

This research project aimed to uncover the importance of pcdhαc2 in recovery from post-stroke depression.

Past research has shown that lesioning the left mPFC led to a significant PSD phenotype in mice (Vahid-Ansari et al., 2016). When treated with fluoxetine the behavioural phenotype was recovered, as was the serotonergic innervation (Zahrai et al., 2020). These findings, along with results from previous injury models, point to the plasticity of the serotonin system in injury recovery (Jin et al., 2016, Kajstura et al., 2018). While the exact process of this re-innervation remains unknown, it could be in part due to guidance cues like pcdhαc2.

Pcdhαc2 was previously discovered to be the predominant clustered protocadherin in serotonin neurons (Chen et al., 2017). When knocked out, mice lacking pcdhαc2 exhibited unusual serotonergic wiring patterns. Serotonin fibers clumped and tangled throughout the brain, predominantly in the hippocampus, but also in the prefrontal cortex, amygdala, and other areas (Chen et al., 2017; Katori et al., 2017). This abnormal 5-HT innervation profile was also coupled with cognitive and behavioural deficits (Chen et al., 2017).

Due to its evident role in the development of the serotonin system, I sought to investigate the role of pcdhαc2 in re-innervation post stroke. Based on the incomplete re-innervation previously observed in the absence of fluoxetine treatment, I also sought to analyze the effect of fluoxetine on this process (Zahrai et al., 2020). This was completed using pcdhαc2 knockout mice, and the previously described surgically induced PSD phenotype.

3. Hypothesis & Aims

I hypothesize that mice partially deficient in pcdhαc2 will display incomplete PSD behavioural recovery in response to fluoxetine treatment compared to wildtype mice. I also hypothesize that pcdhαc2 knockout mice will exhibit abnormal serotonergic wiring at baseline and deficits in serotonergic innervation post stroke, that will not be recovered with fluoxetine treatment, compared to wildtype mice.

Aim 1: Quantify the serotonergic innervation profile of naïve wild type, heterozygous and homozygous knockout mice

Aim 2: Assess the behavioural phenotype and post-stroke recovery in protocadherin alpha C2 (pcdhαc2/AC2) heterozygous knockout mice

Aim 3: Quantify the serotonergic re-innervation of PSD AC2 heterozygous mice with/without FLX treatment

4. Materials and Methods

4.1 Animals

All animal procedures were approved by The University of Ottawa Animal Care Committee and were performed in accordance with guidelines established by the Canadian Council of Animal Care. Mice were housed on a 12/12h light/dark cycle with ad libitum access to food and water. Animals were group housed up to 1-week prior to behavioural testing and single-housed thereafter to maintain consistency for behavioural testing and monitor individual FLX consumption post-stroke.

Mice were provided by the Tom Maniatis lab and bred in house thereafter. AC2 knockout mice were generated by CRISPR-Cas9 genome editing as described in Chen et al. (2017) and subsequently crossed into C57BL/6J mice. Single guide RNAs were designed using the CRISPR Design Portal (crispr.mit.edu) to target the following regions:

>aC2-up-gRNA1 TGAGACGCGTTAAGCCTGCT

>aC2-up-gRNA2 AGTCACTTTGCACTTTGACC

>aC2-dwn-gRNA1 TGAGAAGTGAGGATTAGTCC

>aC2-dwn-gRNA2 GGAATAAGAGTTCTATTACT

4.2 Genotyping

At 3 weeks of age, ear punches were obtained from all mice, and DNA was extracted using the REDExtract-N-Amp Tissue PCR kit (Millipore Sigma). PCR was performed using the following primers and conditions:

Wildtype: ac2F_wt_408bp: 5′-TTG TAG TGC GTG AGA GGT GAA G-3′ and ac2R_wt_408bp: 5′-CAT TGG TCA AGT CCA GTT CCA G-3′. The PCR conditions were as follows: 94°C, 3 min; 34 cycles at 94°C, 15 s, 64.4°C, 30 s, and 68°C, 30 s; 68°C, 5 min; and 12°C. This protocol results in a 408 bp (WT) product detected using a green dye master mix (New England Biolabs).

Knockout: ac2_deletion_F1: 5′-CTG GGC AGA CCG AGA GTA AC -3′ and ac2_deletion_R5: 5′-AGG CTA TCA CAT TAG CCC TG-3′. The PCR conditions were as follows: 94°C, 3 min; 10 cycles at 94°C, 30 s; 64°C, 30 s -0.5°C per cycle and 68°C, 1 min; 24 cycles at 94°C, 30 s; 59°C, 30 s, and 68°C, 1 min °C; 68°C, 5 min; and 12°C. This protocol results in > 1kb (mutant)

product detected using a ONE-Taq Hot start master mix with standard buffer (New England Biolabs).

4.3 Experimental Groups

This study consisted of two main cohorts of mice, stroke mice and naïve mice. The stroke mice were behaviourally tested, given a stroke, and received either vehicle or fluoxetine treatment post-stroke. Wildtype mice were used as a control group (n= 42 for behavioural testing, n= 5/group for histology), and heterozygous mice were used as the experimental group (n=34 for behavioural testing, n= 5/group for histology).

The naïve mice did not undergo behavioural testing, were not given a stroke, and were kept in the same single housing condition for the duration of the experimental timeline. For histology, naïve mice consisted of WT (n=5-6), heterozygous knockout mice (n=5-6) and full knockout mice (n=5).

4.4 Behavioural Testing

Mice were single housed one week prior to behavioural testing to allow for acclimatization to housing conditions. Mice needed to be single housed for proper assessment of fluoxetine/vehicle intake via drinking water.

4.4.1 EPM

An elevated plus maze (EPM) was conducted to assess anxiety-like behaviour. Mice were habituated for a minimum of 30 minutes prior to testing in the same light condition as their housing room (bright white light). Mice were placed in the center of an elevated plus maze with 75cm x 6cm arms, sitting 74cm off the ground. The test was performed at 100 lux for 10 minutes. The closed arms have 20 cm high black walls, which provide a shaded enclosed space, while the open arms possess no walls. Mice were filmed and tracked by their centre point, and videos were analyzed using Ethovision software (Noldus).

4.4.2 FST

A forced swim test (FST) was conducted to assess depression-like behaviour. Mice were habituated for a minimum of 30 minutes prior to testing in the same light condition as their housing room (bright white light). A maximum of two mice at a time (same sex, all males first) were each placed into an inescapable clear plastic cylinder (22cm diameter, 37cm height) filled with 24ºC water for 6 minutes under red light. Mice were filmed and videos were analyzed using Ethovision software (Noldus) for activity duration and inactivity duration. Activity duration assesses what percentage of the field of view is changing. Activity duration was chosen over mobility duration to mitigate any detection setting inconsistencies or tracking errors.

4.5 Stroke Surgery

10–12-week-old male and female mice were intracranially injected with the vasoconstrictor endothelin-1 (ET-1) to surgically induce a stroke. Mice were anesthetized by inhalation of 4%

isoflurane with 1.5 mL/min oxygen. Once anesthetized, mice were subcutaneously injected with a sterile saline solution (1mL), and buprenorphine (0.03mg/kg) for pain control. The heads were shaved, eye lubricant was applied, and 2% lidocaine hydrochloride jelly was inserted in the ears prior to mounting. Mice were then mounted on a stereotaxic frame and maintained at 2% isoflurane and 1.5 mL/min oxygen, with breathing monitored and a heating pad set to 37ºC. Using forceps and small scissors, a small incision was made along the scalp, and measurements were taken using the stereotaxic frame. Two small holes were drilled at AP +2mm, ML +0.5mm, DV -2.4mm, and AP +1.5mm, ML +0.5mm, DV -2.6mm. Two injections of ET-1 (2 μg/μL = 800 pmol/μL), 1 μl each, were delivered at the mPFC coordinates at a rate of 0.1 μl/minute for a total of 10 minutes. After each injection the needle was left inside the brain for 5 minutes and the removed slowly, to prevent backflow of the ET-1. The incision was glued shut and 2% transdermal bupivacaine was applied. Mice were placed in an incubator set to 37ºC to recover from anesthesia. Post-op buprenorphine was injected again 4-6 hours later for pain management.

4.6 MRI

At 4 days post-stroke, a small subset of mice underwent magnetic resonance imaging (MRI) via 7T GE/Agilent MRI (Milwaukie, WI, USA) at the University of Ottawa Preclinical Imaging Core to verify the presence of a lesion (Figure 1). Animals were anesthetized with 3% isoflurane in O2 and maintained at 1.5%. 300 μm thick serial scans focussed on the mPFC were acquired using a fast spin echo pulse sequence with repetition time = 4500ms, effective echo time = 13 ms, field-of-view = 3 cm, matrix size = 256 × 256, slice thickness = 300 μm, number of averages = 2, axial (transverse) image orientation and scan time = 6 min. Following the MRI, mice were placed back into their home cage on a heating pad and monitored for recovery from anesthesia.

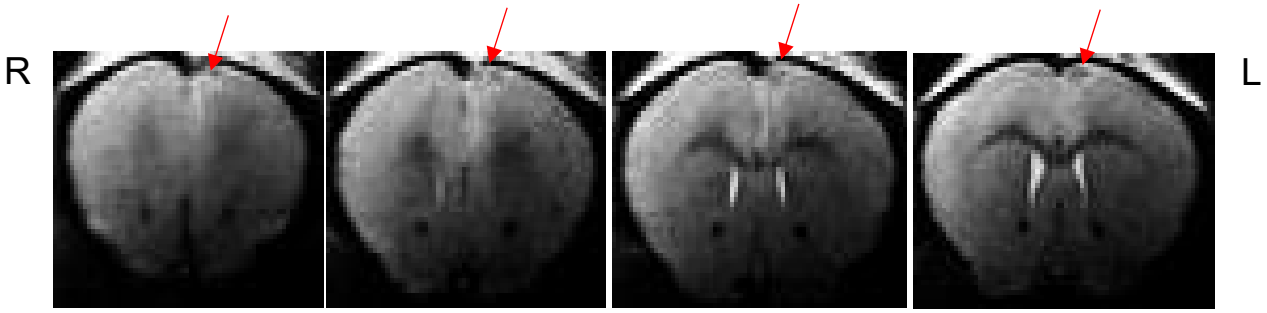

Figure 1. MRI images of ET-1 lesion site. Representative 7-Tesla MRI image done on an anaesthetized female HET mouse at 4 days post-stroke. 300-µm MRI sections in which the lesion site is visualized and limited to the left mPFC. Arrows highlight stroke site.

4.7 Treatment

Mice were treated with either Fluoxetine (80 mg/mL) prepared from powder and dissolved in system water, or system water alone as a vehicle control. Fluoxetine was delivered via drinking water to prevent excess stress by other administration methods (ie. oral gavage or IP injection). Fluoxetine was prepared fresh every 3-4 days and delivered to the mice in 50 mL light-protected amber tubes. Vehicle water was similarly delivered in 50mL clear tubes and also replaced every 3-4 days.

4.8 Tissue collection and processing

At the time of sacrifice, mice were injected interperitoneally with Euthanyl (149.5 mg/kg). Once confirmed unresponsive via limb pinching, mice were pericardially infused with ice cold pH 7.4 1X phosphate buffered saline (PBS) for approximately 4 minutes/25mL or until liquid ran clear. Mice were then infused with pH 7.4 4% paraformaldehyde (PFA) in PBS for 4 mins/25mL or until the body was fully rigid.

Following perfusion, brains were placed in a tube of pH 7.4 4% PFA for 1-2 hours at 4ºC. Brains were then transferred to a 30% sucrose solution and kept at 4ºC for 3+ days until the brains sank. The brains were then frozen rapidly in dry ice-cooled 2-methylbutane and stored at -80ºC until cut. One day prior to cutting, brains were transferred to -20ºC.

Brains were sectioned using a Thermo Shandon HM 525 NX cryostat set to -20 - -25ºC. 25um coronal sections were cut and thaw-mounted onto Superfrost slides (Fisher Scientfic).

4.9 Immunofluorescence staining

Slides were removed from freezer to thaw 1 hour prior to staining. Slides were washed with 1X PBS (3x5 mins) and then incubated with ~200 µl of blocking solution (10% NDS, Triton 0.1% in 1X PBS) and incubated for one hour at room temperature. Blocking solution was tapped off and slides were incubated at 4ºC overnight with ~200 µl of the primary antibody solution (rabbit anti SERT (1:1000, MilliporeSigma Calbiochem) in Triton 0.1% 1X PBS).

The following day the slides were washed 3x5 mins in 1X PBS and placed back into the slide chamber. ~200 µl of the secondary antibody solution was applied (AlexaFluor donkey anti rabbit 488 (1:1000, Invitrogen) in Triton 0.1% 1X PBS) and slides were incubated in the dark for 1 hour at room temperature. Slides were then washed with 1X PBS, cover slipped with Immu-Mount glue (Epredia) and left to dry.

4.10 Confocal Microscopy

Confocal images (2048x2048 pixels) were acquired using the Zeiss LSM 880 AxioObserver Z1 microscope. Regions of interest (Figure 2) were located using the ocular lens and images were taken at 63x magnification using an oil immersed lens using an Argon laser (480 nm line, and emission band path: 493–604 nm). Images were the compilation of 53 z-stacks with a spacing of 0.3um, taken using the ZenBlack 2.3 software.

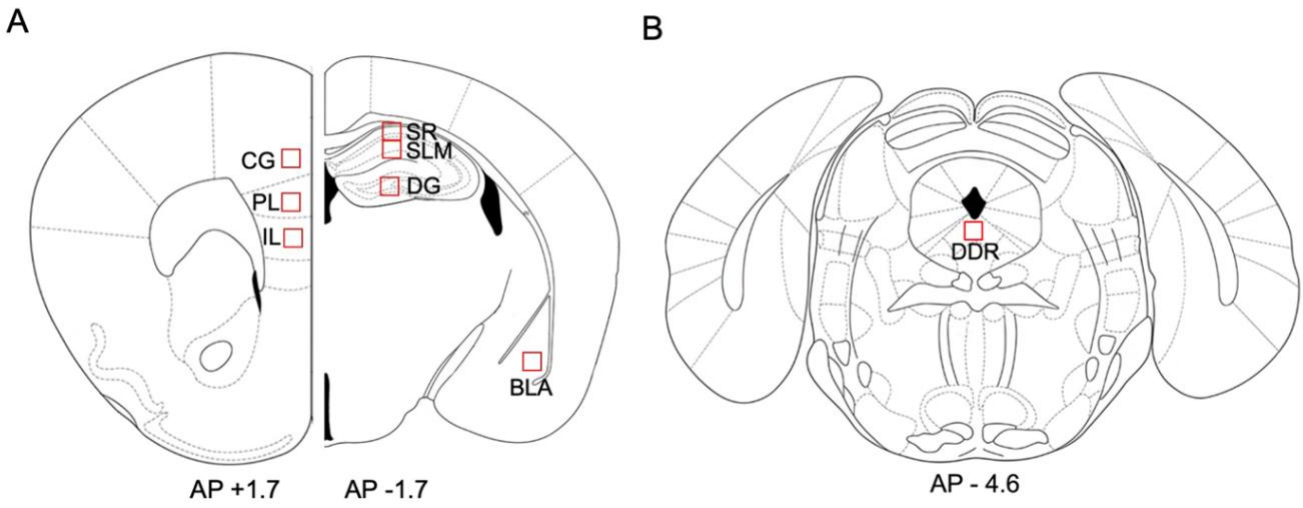

Figure 2. Representative images of brain regions imaged and analyzed. A) Representative image showing two levels of the mouse brain, depicting ROIs in the mPFC, hippocampus and amygdala. B) ROI imaged in the dorsal dorsal raphe. Adapted from Paxinos, George, and Keith B.J. Franklin, 2001. "The mouse brain in stereotaxic coordinates: hard cover edition".

4.11 Quantification using IMARIS

Confocal SERT-stained images were quantified using Imaris x64 10.2. SERT+ fibers were reconstructed using the surfacing tool to generate volume measurement. Minimum axon diameter was set to 0.6 µm, with surface detail set to 0.0732 µm. The final volume output was then divided by the total tissue volume of the image, 89372.8 μm^3, to give the density of SERT+ axons ($\mu m^3/\mu m^3$). Number of varicosities per μm^3 was calculated using the spotting tool.

Detection settings were set to >0.6 μm to ensure each spot was present in at least two z stacks (0.3 μm apart) to limit artifact. Number of spots was divided by the total tissue volume to give varicosity density, represented as number of varicosities per μm^3 of tissue.

4.12 Statistical Analysis

All statistical analyses were completed using GraphPad Prism 9.5.1 (GraphPad Software, La Jolla, CA, USA; www.graphpad.com). All data is expressed as mean ± SEM with the threshold of significance set at $p \leq 0.05$. All data was tested for normality using the Shapiro-Wilk test. Behavioural results and naïve innervation results were analyzed using one-way ANOVA with Tukey's multiple comparison test for normally distributed data, or Kruskal Wallis test with Dunn's multiple comparison test for data that was not normally distributed. Stroke innervation data was analyzed using two-way ANOVAs with Tukey's multiple comparisons tests for primary analysis and using paired t-test or Wilcoxon test in supplementary. A Brown-Forsyth test was used to assess the equality of variances, and a Welch's ANOVA with Dunnett's T3 multiple comparisons test was used in cases that failed the equal variance assumption. Each behaviour data point represents one mouse. Each data point on the SERT+ axonal and varicosity density graphs represent one quantified image of the given ROI. Naïve innervation data was pooled for both left (ipsilesional) and right (contralesional) brain region images, meaning two data points were plotted per brain, per region (one from each hemisphere). Images with unsuccessful staining and values deemed to be significant outliers were excluded from the analyses.

5. Results

5.1 Naïve AC2 5-HT innervation profiles

Naïve AC2 WT, HET and KO mice were analyzed, in the absence of stroke or behavioural testing, to quantify 5-HT innervation at baseline in mice lacking pcdhαc2. Previous studies have quantified hippocampal bunching and have shown qualitative differences across the brain in protocadherin alpha c2/alpha knockout mice, but none have quantified other brain regions.

5.1.1 Medial prefrontal cortex

In the medial prefrontal cortex (mPFC), significant differences between naïve wildtype (WT), heterozygous knockout (HET), and full knockout (KO) AC2 mice were seen for both SERT+ axonal and varicosity density.

In the cingulate cortex (CG), both HET and KO mice showed significantly less SERT+ axonal density (Figure 3A) and SERT+ varicosity density (Figure 3D) compared to WT control mice. HET mice also differed significantly from KO mice in axonal density, representing an intermediate innervation profile between WT and KO (Figure 3A). The density of SERT+ varicosities in AC2 HET mice did not differ significantly from KO but showed a trend increase.

In the prelimbic cortex (PL), the same trends largely remained. KO had significantly less SERT+ axonal density (Figure 3B) and density of SERT+ varicosities (Figure 3E) compared WT mice. HET mice also had significantly reduced SERT+ varicosity density compared to WT mice and significantly increased varicosity density compared to KO mice, again, representing an

intermediate state. However, HET and WT mice did not differ in SERT+ axonal density, with only a slight trend decrease in HET mice (Figure 3B). This suggests the prelimbic cortex may be less affected by the partial loss of pcdhαc2.

The infralimbic cortex (IL) showed no significant differences between any of the groups (Figure 3C, F), suggesting it is properly innervated regardless of pcdhαc2 partial or full knockout.

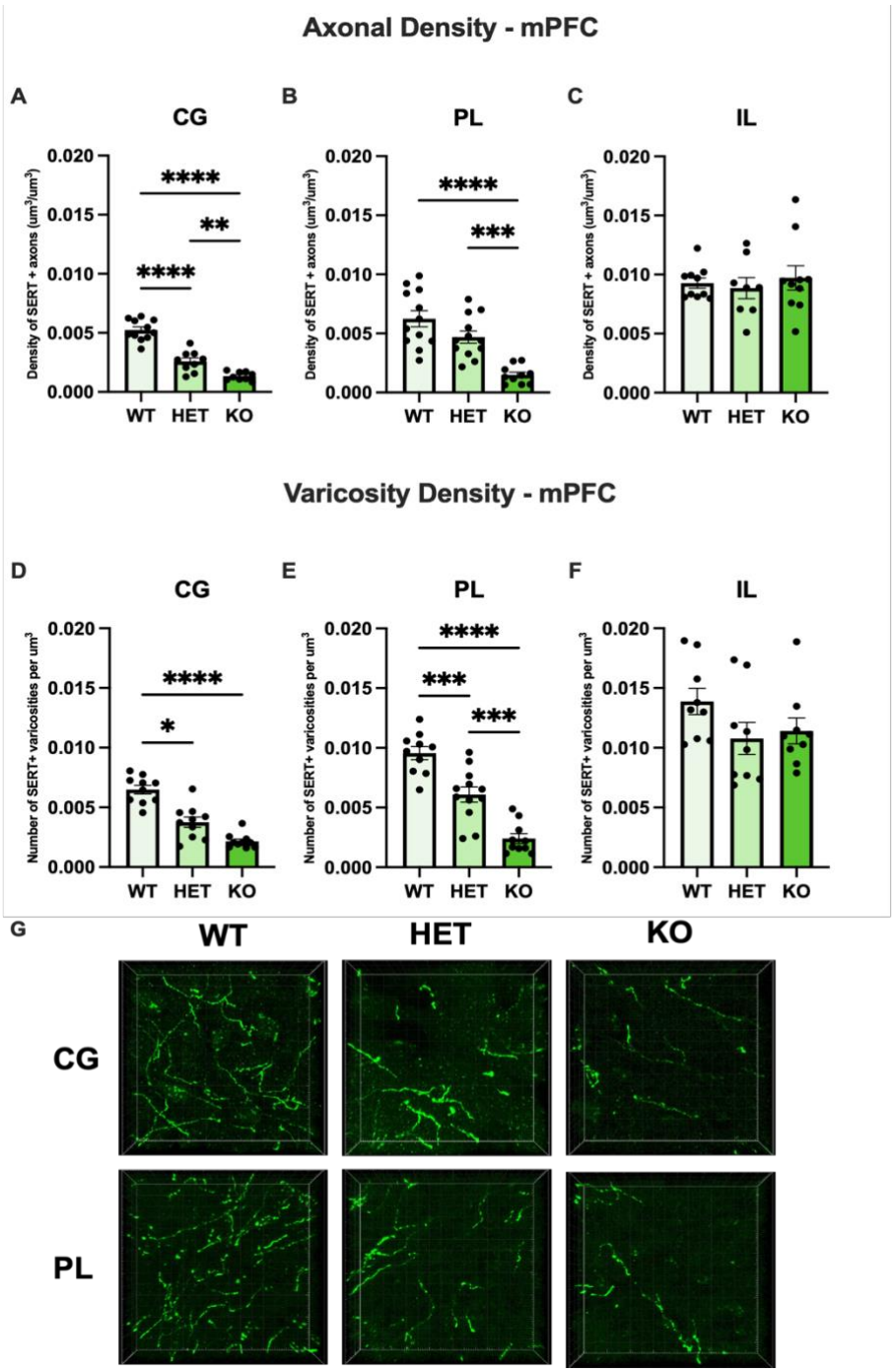

Figure 3. SERT+ axonal and varicosity density in medial prefrontal cortical subregions. A-C shows axonal density in the A) cingulate cortex (CG), B) prelimbic cortex (PL) and C) infralimbic cortex (IL), D-F shows number of varicosities per μm^3 in the D) cingulate cortex (CG), E) prelimbic cortex (PL) and F) infralimbic cortex (IL). G) Representative 63X confocal images of SERT immunostaining in the CG and PL. One-way ANOVAs with Tukey's multiple comparisons tests (A, B, C, E, F) and Kruskal Wallis test with Dunn's multiple comparisons test (D) were performed. Mean ± SEM. *$p < 0.05$, **$p<0.01$, ***$p< 0.001$, ****$p < 0.0001$.

5.1.2 Hippocampus

Three hippocampal regions were analyzed, the stratum radiatum (SR), stratum lacunosum moleculare (SLM) and the dentate gyrus (DG) (Figure 2A). The SR, also known as the suprapyramidal region, contains inputs from the basolateral amygdala, septum, CA3 to CA1 Schaffer collaterals and commissural fibers. The SLM is located just below the SR and receives inputs from the entorhinal cortex and thalamus. The DG, composed primarily of granule cells, receives its major input from the entorhinal cortex via the perforant pathway and projecting via mossy fibers to the CA3 (David & Pierre, 2006). These three regions were analyzed individually due to previously observed differences in SERT+ innervation in similar knockout models (Katori et al., 2009, 2017; Chen et al., 2017).

In the SR, HET and KO mice differed significantly from WT in both SERT+ axonal and varicosity density (Figure 4B, E). HET mice did not differ significantly from KO mice in SERT+ axonal or varicosity density. This may indicate that the innervation of the SR is partially disrupted even when lacking only one copy of pcdhαc2.

In the SLM, KO mice showed a 2-fold increase in both SERT+ axonal density and density of SERT+ varicosities (Figure 4C, F). HET mice differed significantly from WT and KO in axonal density (Figure 4C), but only from KO in varicosity density (Figure 4F). This suggests a single copy of pcdhαc2 may be partially protective and prevent the extreme phenotype observed in KO mice.

In the DG, SERT+ innervation was 10-fold lower than the SR and SLM across groups. Only KO mice differed significantly from WT mice, possessing nearly no innervation or varicosities in this region (Figure 4D, G). HET mice did not differ significantly from HET or KO mice, presenting an intermediate innervation profile.

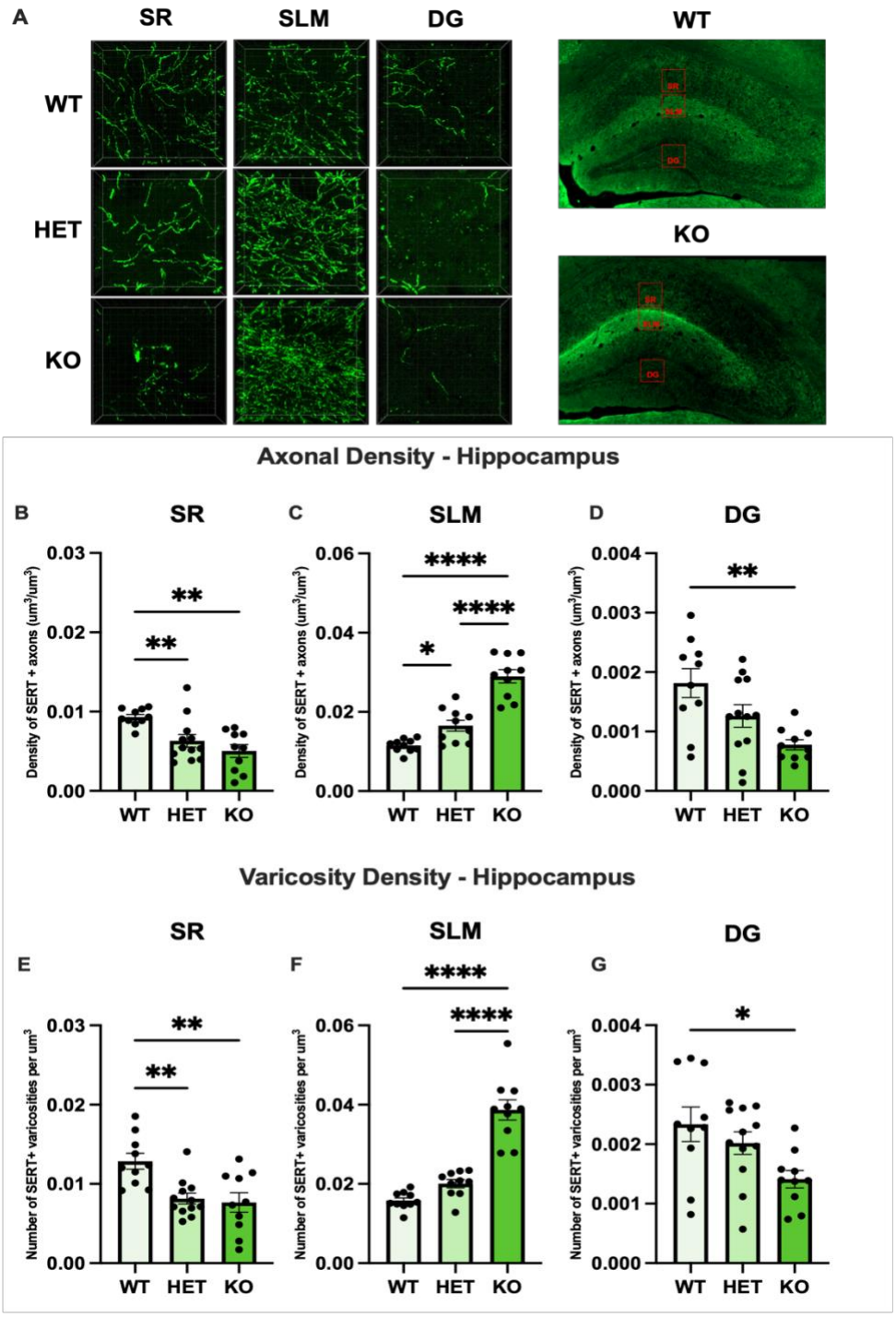

Figure 4. SERT+ axonal and varicosity density in hippocampal subregions.
A) Representative 63X confocal images of SERT immunostaining, and 20x tiled fluorescent microscopy images of WT and KO hippocampi with red boxes indicating ROIs. Axonal density in the B) stratum radiatum (SR), C) stratum lacunosum moleculare (SLM) and D) dentate gyrus (DG), and Number of varicosities per μm^3 in the E) SR, F) SLM and G) DG. Scales vary by region. Kruskal Wallis test with Dunn's multiple comparisons test (A), Welch's ANOVA with Dunnett's T3 multiple comparisons test (C, D, G), and one-way ANOVA with Tukey's multiple comparisons tests (E, F) were performed. Mean ± SEM. *p < 0.05, **p<0.01, ****p < 0.0001.

5.1.3 Basolateral amygdala

No significant differences in SERT+ axonal or varicosity density were observed between groups in the basolateral amygdala (BLA). HET and KO mice showed slight trend increases (Figure 5); however, KO mice show strong variation in axonal and varicosity density, potentially due to the heterogenous innervation profile of these mice.

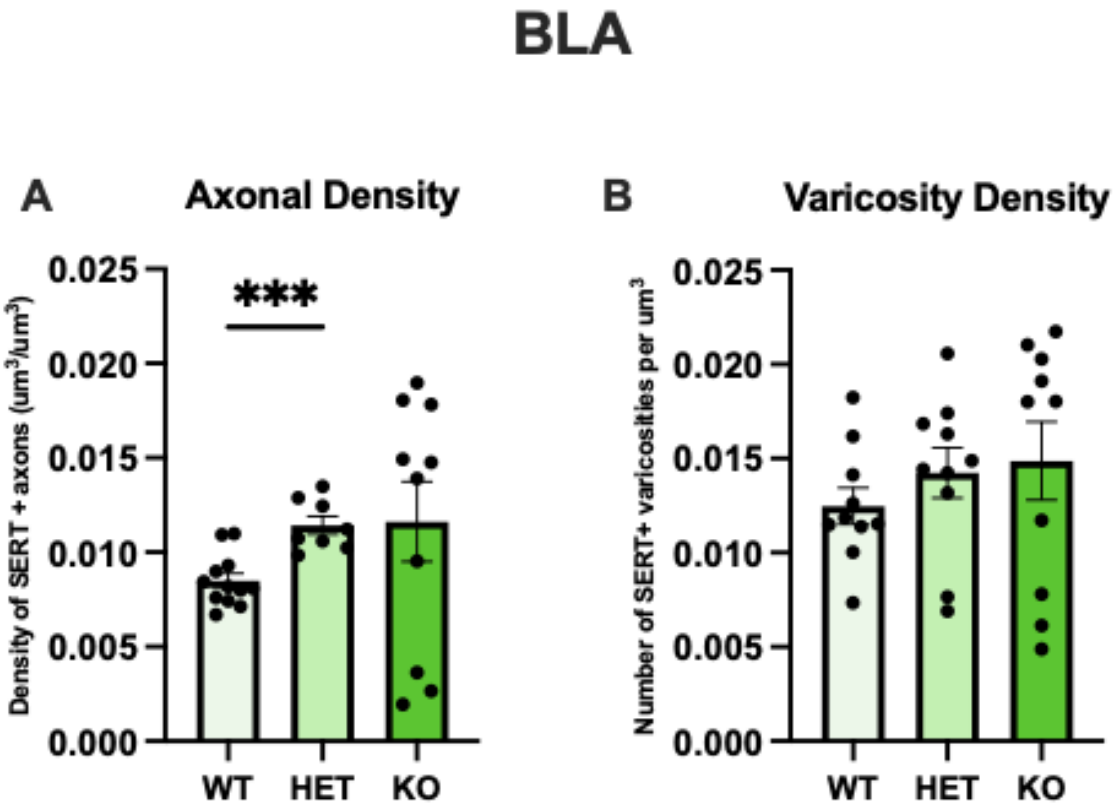

Figure 5. SERT+ axonal and varicosity density in the basolateral amygdala of naïve mice. A) Welch's ANOVA with Dunnett's T3 multiple comparisons test, and B) One-way ANOVAs with Tukey's multiple comparisons tests were performed. Mean ± SEM. ***p< 0.001.

5.1.4 Dorsal dorsal raphe

No significant differences were observed in SERT+ axonal or varicosity density between any groups in the dorsal dorsal raphe (DDR) (Figure 6).

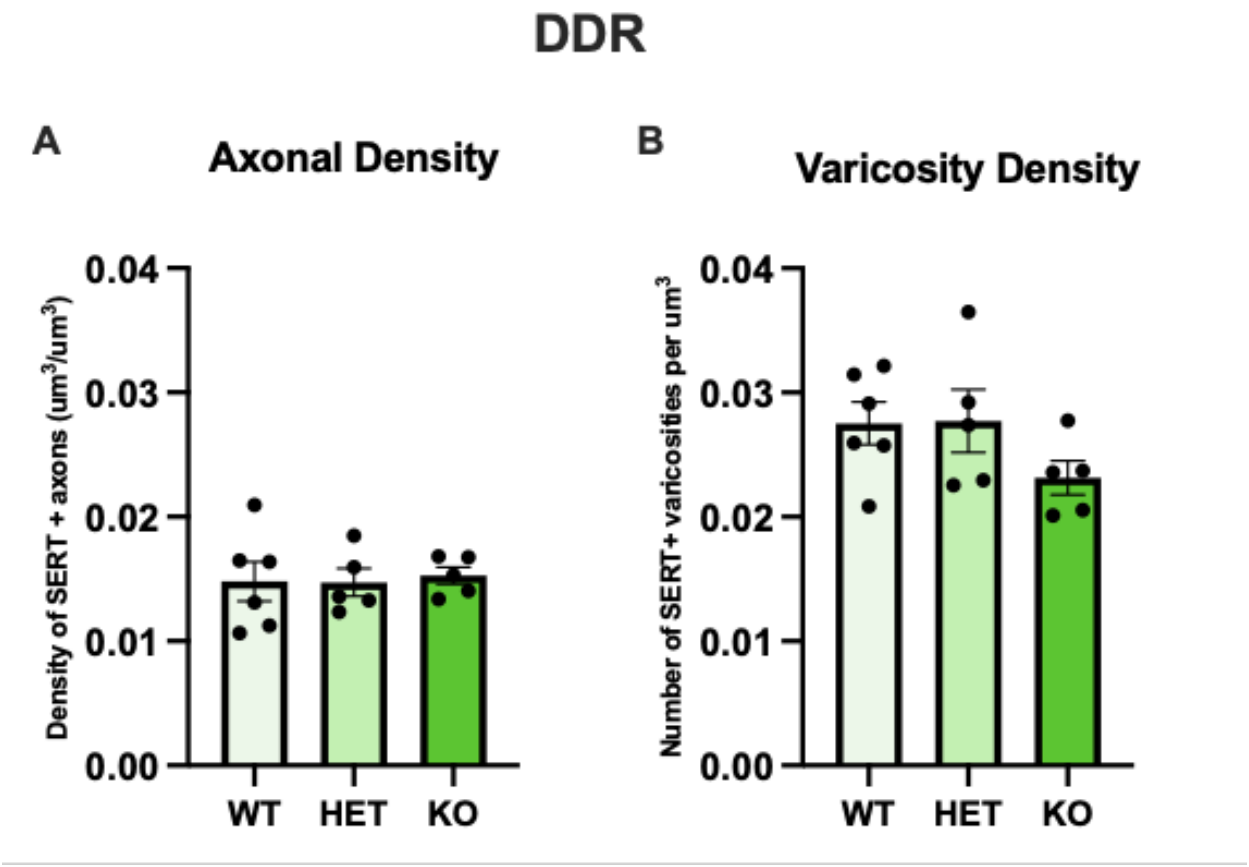

Figure 6. SERT+ axonal and varicosity density in the dorsal dorsal raphe of naïve mice. One-way ANOVAs with Tukey's multiple comparisons tests were performed. Mean ± SEM.

In summary, deficiencies in pcdhαc2 in naïve mice were associated with abnormal serotonergic innervation patterns compared to wildtype mice. AC2 knockout mice showed significantly decreased SERT+ axonal and varicosity density in the CG, PL, SR and DG, and heterozygous mice showed intermediately decreased SERT+ axonal and varicosity density in these regions. In

contrast, full knockout and heterozygous mice showed significantly increased SERT+ axonal and varicosity density in the SLM. No significant differences were observed in the BLA or DDR of these mice; however, the BLA of full knockout mice a had quite heterogenous innervation profile between mice.

5.2 Behavioural Results

Behavioural testing was conducted to assess the anxiety-like and depressive-like phenotypes of mice post-stroke, using the elevated plus maze (EPM) and forced swim test (FST) respectively. This was done in both wildtype (WT) and heterozygous AC2 knockout mice (HET) to test the effect of a partial loss in pcdhαc2 on behavioural recovery. An EPM was conducted pre-stroke, at 1-week post-stroke to check the stroke-induced phenotype, and at 6-weeks post-stroke following 5 weeks of chronic vehicle or FLX treatment. An FST was conducted 2 days after the EPM at each time point (Figure 7A)

5.2.1. Elevated Plus Maze

The elevated plus maze test (EPM) was used to assess the anxiety-like phenotype of AC2 WT and HET mice before and after surgery, with or without fluoxetine (FLX) treatment. Heterozygous knockout mice spent significantly less time in the open arm than they did pre-stroke, in all post-stroke conditions (Figure 7C). This suggests an anxiety-like phenotype at all post-stroke timepoints, regardless of FLX treatment. Wildtype mice also spent significantly less time in the open arm when untreated at 1-week and 6-weeks post stroke, but unexpectedly showed no recovery in this test even when treated with FLX (Figure 7B). This is consistent with their decrease in total distanced moved, representing increased freezing (Figure S15).

5.2.2 Forced Swim Test

The forced swim test (FST) was used to assess the depressive-like phenotype of WT and HET mice before and after surgery, with or without fluoxetine (FLX) treatment. In the FST, heterozygous knockout mice had significantly increased inactivity duration compared to pre-stroke at both untreated timepoints, 1-week and 6-weeks post-stroke. Heterozygous knockout mice treated with FLX no longer significantly differed from the pre-stroke inactivity duration; however, they also did not significantly differ from the untreated post-stroke groups, suggesting the possibility of a partial, though incomplete, recovery (Figure 7E). Wildtype mice also had significantly increased inactivity time compared to baseline at both untreated timepoints, 1-week and 6-weeks post-stroke. When treated with FLX, wildtype mice showed a significant reduction in inactivity duration compared to 1-week post-stroke and vehicle 6-weeks post-stroke mice (Figure 7D). This indicates a significant improvement in the stroke-induced depression-like phenotype in FLX treated AC2 WT mice, but an incomplete response in heterozygous AC2 knockout mice.

Overall, all mice exhibited a persistent anxiety like-phenotype post-stroke, and a significant depression-like phenotype at 1-week post-stroke and 6-weeks post-stroke in vehicle treated mice. When treated with FLX, wildtype mice showed a recovery of their depression-like phenotype back to baseline, while heterozygous mice showed a partial recovery.

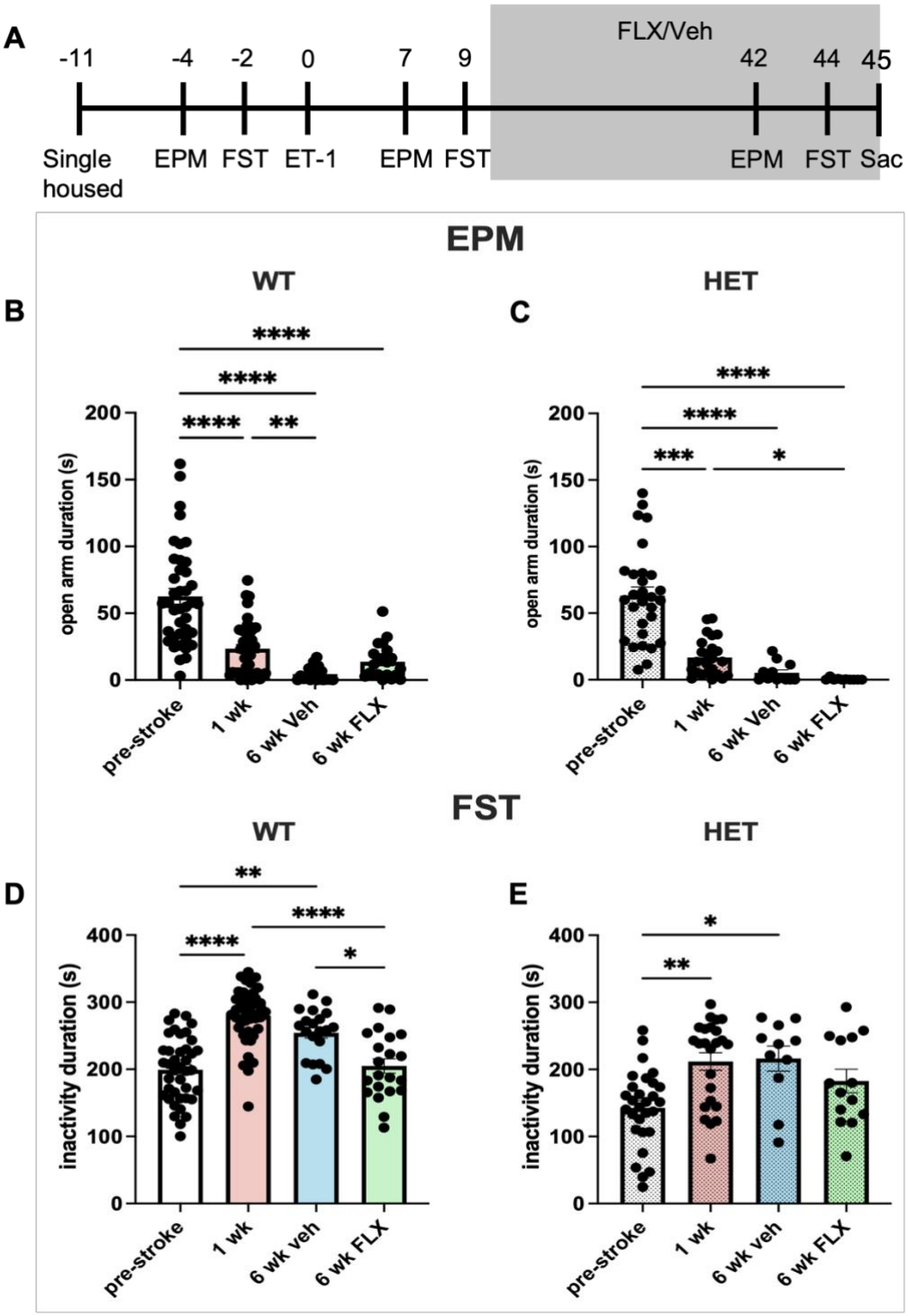

Figure 7. Behavioural test results for AC2 wildtype and heterozygous knockout mice.
A) Experimental timeline expressed in days post-stroke. Grey shaded area represents 5-week chronic treatment window, B) Elevated plus maze test (EPM) open arm duration of WT mice, C) EPM open arm duration of HET mice, D) Forced swim test (FST) immobility duration of WT mice, E) FST immobility duration of HET mice. Data analyzed using Kruskal Wallis test with Dunn's multiple comparison test. Data expressed as mean ± SEM. *p < 0.05, **p<0.01, ****p < 0.0001.

5.3 Post-stroke innervation changes

At 6 weeks post-stroke, WT and HET mice were analyzed for post-stroke changes in 5-HT innervation, to understand the effect of pcdhαc2 knockout and FLX/vehicle treatment on reinnervation.

5.3.1 Medial prefrontal cortex

The left (ipsilesional) cingulate cortex (CG) of the medial prefrontal cortex (mPFC) was the primary area affected by this stroke model. As such, the left CG of vehicle treated WT mice showed significantly less SERT+ axonal density and fewer SERT+ varicosities when compared to the right (contralesional) CG in these mice (Figure 8A, C). This trend was present in heterozygous mice but lacked significance in the 2-way ANOVA analysis (Figure 8B, D). When analyzed via paired t-test to account for inter-animal variability, heterozygous mice showed a significant decrease in SERT+ axonal density (Figure S1C). In WT mice treated with FLX, there was no longer a significant difference in SERT+ axonal or varicosity density between the left and right hemispheres, suggesting proper re-innervation/recovery (Figure 8A, C). In heterozygous mice treated with FLX, the trend decrease in the left CG remained for SERT+ axonal density (Figure 8B), showing significance when analyzed via paired t-test (Fig S1D); however, the varicosity density showed no difference compared to the right CG.

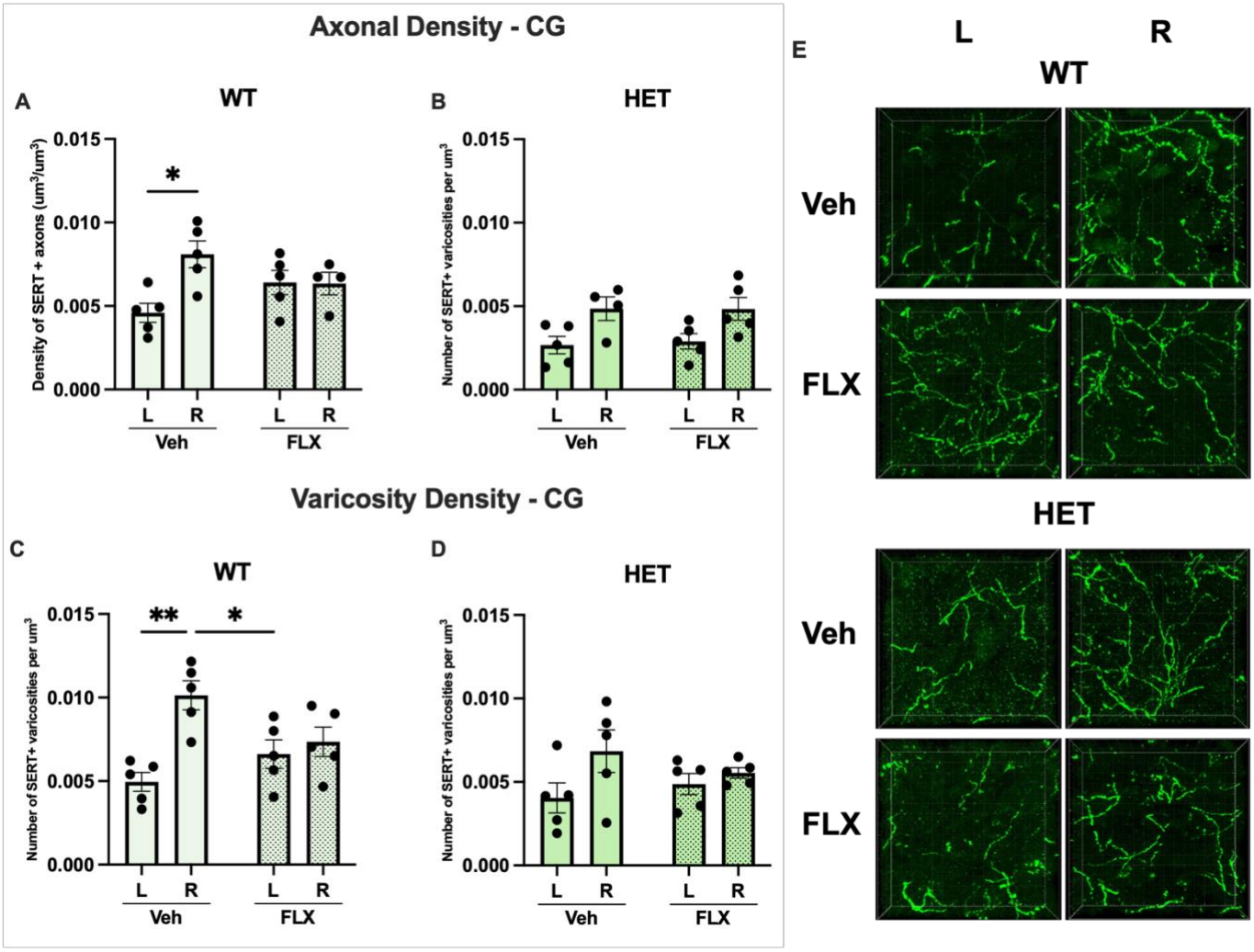

Figure 8. SERT+ axonal and varicosity density in the cingulate cortex (CG) of stroke mice. Ipsilesional (L) vs contralesional (R) sides of the brains are compared. Top row shows axonal density for A) wildtype mice given vehicle or FLX treatment, B) heterozygous knockout mice given vehicle or FLX treatment, bottom row shows varicosity density for C) wildtype mice given vehicle or FLX treatment, D) heterozygous mice given vehicle or FLX treatment. E) Representative 63X confocal images of SERT immunostaining. Two-way ANOVAs with Tukey's multiple comparisons tests, with mean ± SEM. *$p < 0.05$, **$p<0.01$.

The left prelimbic cortex (PL) of vehicle treated WT mice showed trend decreases in axonal density compared to the right PL, and a significantly lower density of SERT+ varicosities compared to the L PL of FLX treated mice (Figure 9A, C). A similar trend existed for heterozygous mice, although it was discrete. When analyzed via paired t-test, the L PL of WT vehicle treated mice had significantly lower axonal density and fewer varicosities than the right PL (Figure S3A, S4A), likely due to the tests ability to match the brain regions from the same animal, thus controlling for inter-mouse variability in innervation levels. The paired t-tests for HET vehicle treated mice showed a strong trend of reduced axonal density ($p= 0.0611$) (Figure S3C) and varicosity density ($p= 0.0576$) (Figure S4C) in the left vs right PL. Following FLX treatment, both wildtype and heterozygous knockout mice no longer had a significant or trend decrease in the innervation of the L PL, suggesting the ability of FLX to promote the reinnervation of this region.

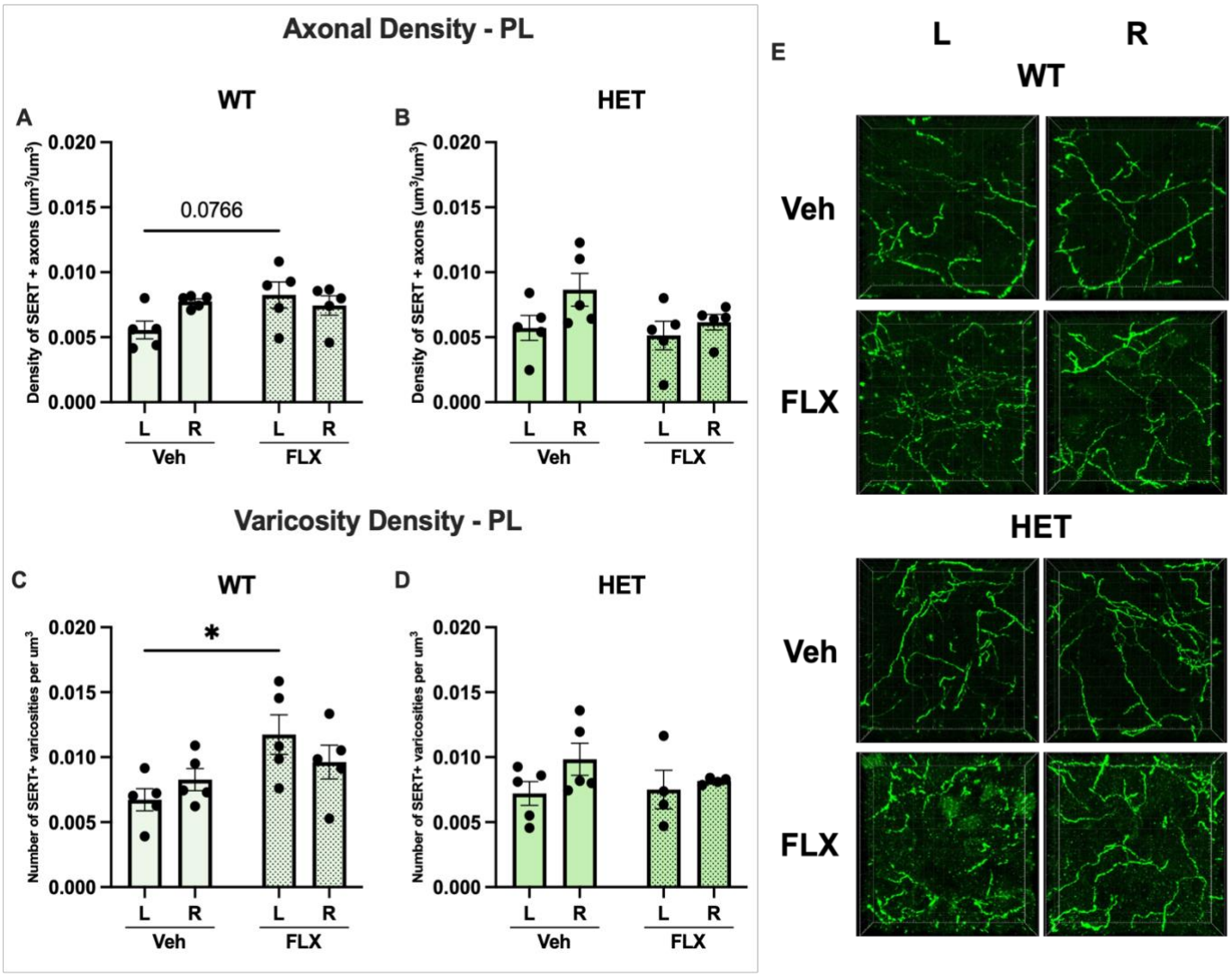

Figure 9. SERT+ axonal and varicosity density in the prelimbic cortex (PL) of stroke mice. Ipsilesional (L) vs contralesional (R) sides of the brains are compared. Top row shows axonal density for A) wildtype mice given vehicle or FLX treatment, B) heterozygous knockout mice given vehicle or FLX treatment, bottom row shows varicosity density for C) wildtype mice given vehicle or FLX treatment, D) heterozygous mice given vehicle or FLX treatment. E) Representative 63X confocal images of SERT immunostaining. Two-way ANOVAs with Tukey's multiple comparisons tests, with mean ± SEM. *$p < 0.05$.

The infralimbic cortex (IL) showed no significant differences in SERT+ axonal or varicosity density between any of the experimental groups. When analyzed with a paired t-test, heterozygous mice did show a significant difference in SERT+ axonal density between the L and R IL in vehicle treated mice which was recovered by FLX treatment (Fig S5C, D). This stoke model only minimally impacts the IL, as it is the most ventral region and is not directly targeted via ET-1 injection.

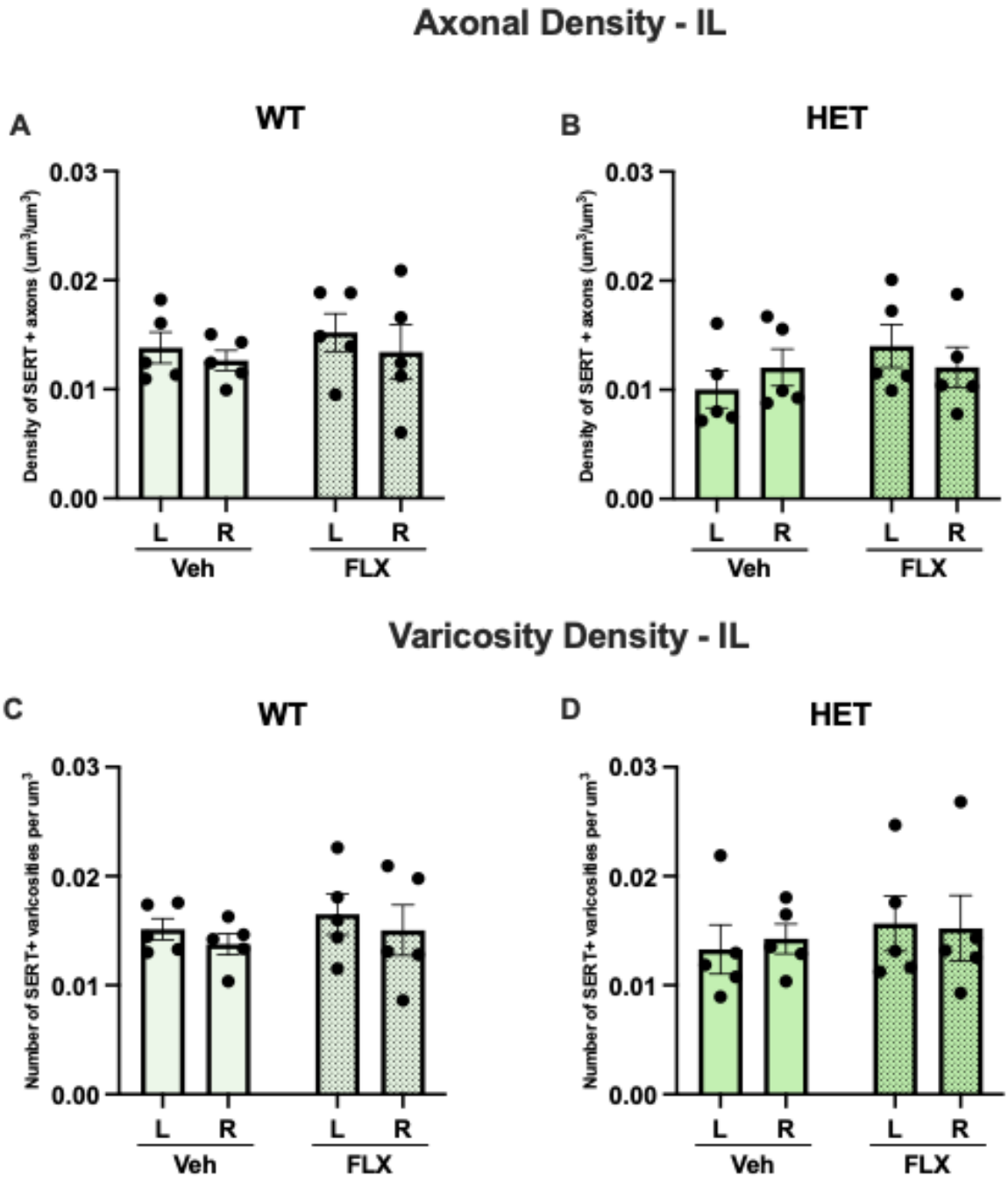

Figure 10. SERT+ axonal and varicosity density in the infralimbic cortex (IL) of stroke mice. Ipsilesional (L) vs contralesional (R) sides of the brains are compared. Top row shows axonal density for A) wildtype mice given vehicle or FLX treatment, B) heterozygous knockout mice given vehicle or FLX treatment, bottom row shows varicosity density for C) wildtype mice given vehicle or FLX treatment, D) heterozygous mice given vehicle or FLX treatment. Two-way ANOVAs with Tukey's multiple comparisons tests, with mean ± SEM.

5.3.2 Hippocampus

When analyzed via two-way ANOVA, there were no significant differences in the innervation of the SR between any experimental groups (Figure 11); however, when analyzed via paired t-test, the L SR of vehicle treated HET mice showed significantly less SERT+ axonal and varicosity density compared to the R SR (Fig S7C, S8C). In HET mice treated with FLX there was no significant difference between the L and R SR (Fig S7D. S8D).

There were no significant differences in SERT+ axonal or varicosity density in the SLM or DG of stroke mice (Figure 12, 13).

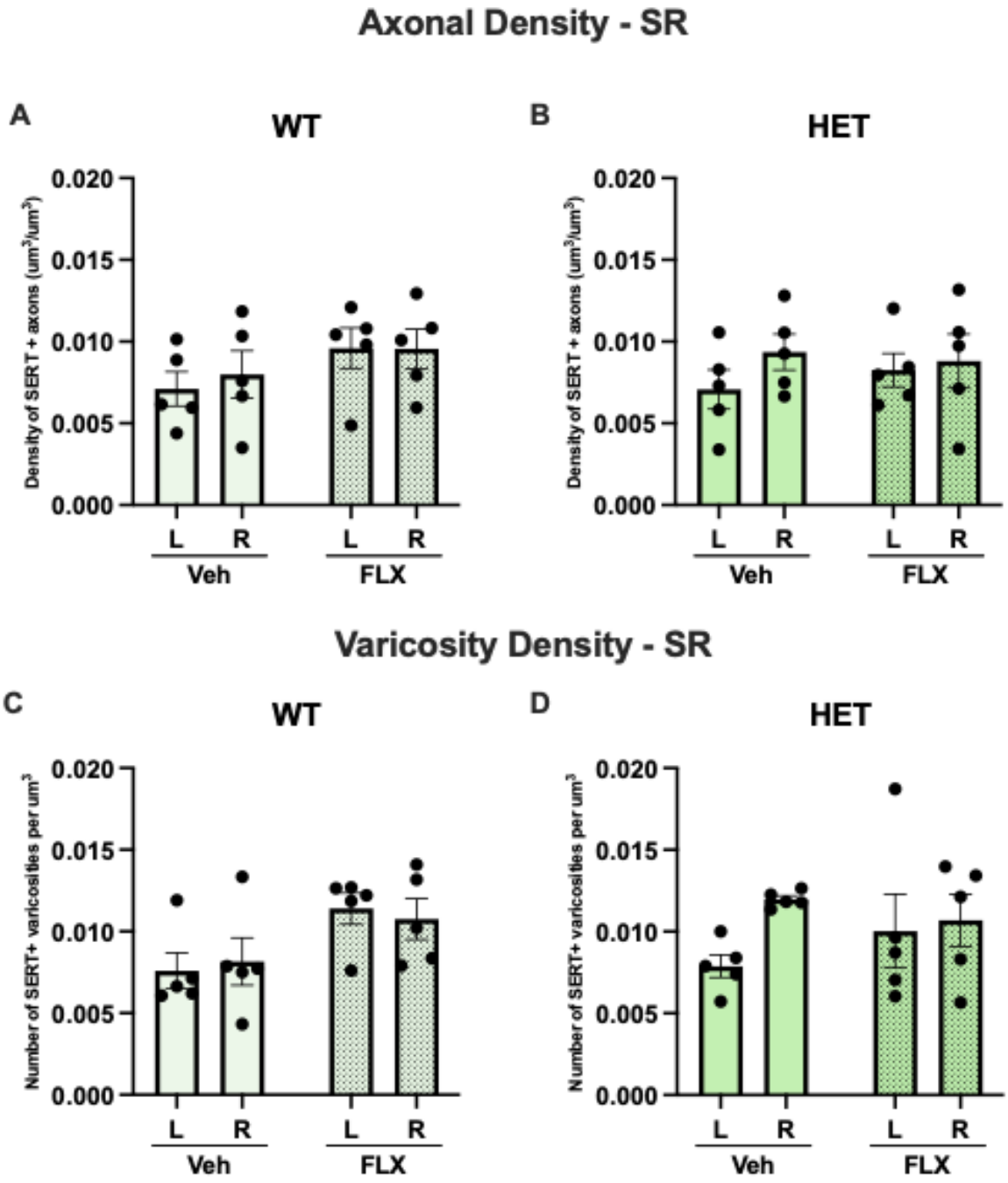

Figure 11. SERT+ axonal and varicosity density in the stratum radiatum (SR) of stroke mice. Ipsilesional (L) vs contralesional (R) sides of the brains are compared. Top row shows axonal density for A) wildtype mice given vehicle or FLX treatment, B) heterozygous knockout mice given vehicle or FLX treatment, bottom row shows varicosity density for C) wildtype mice given vehicle or FLX treatment, D) heterozygous mice given vehicle or FLX treatment. Two-way ANOVAs with Tukey's multiple comparisons tests, with mean ± SEM.

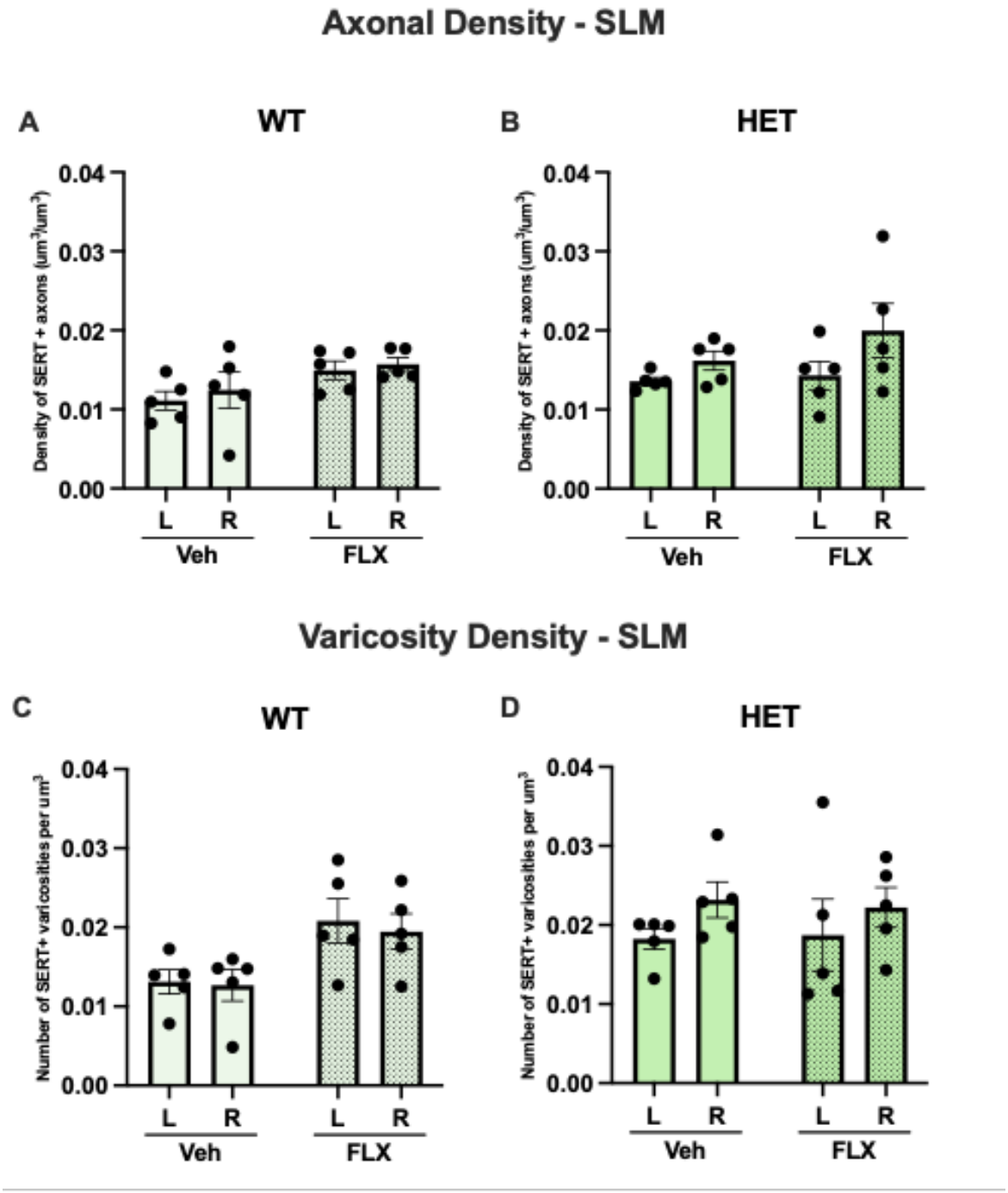

Figure 12. SERT+ axonal and varicosity density in the stratum lacunosum moleculare (SLM) of stroke mice. Ipsilesional (L) vs contralesional (R) sides of the brains are compared. Top row shows axonal density for A) wildtype mice given vehicle or FLX treatment, B) heterozygous knockout mice given vehicle or FLX treatment, bottom row shows varicosity density for C) wildtype mice given vehicle or FLX treatment, D) heterozygous mice given vehicle or FLX treatment. Two-way ANOVAs with Tukey's multiple comparisons tests, with mean ± SEM.

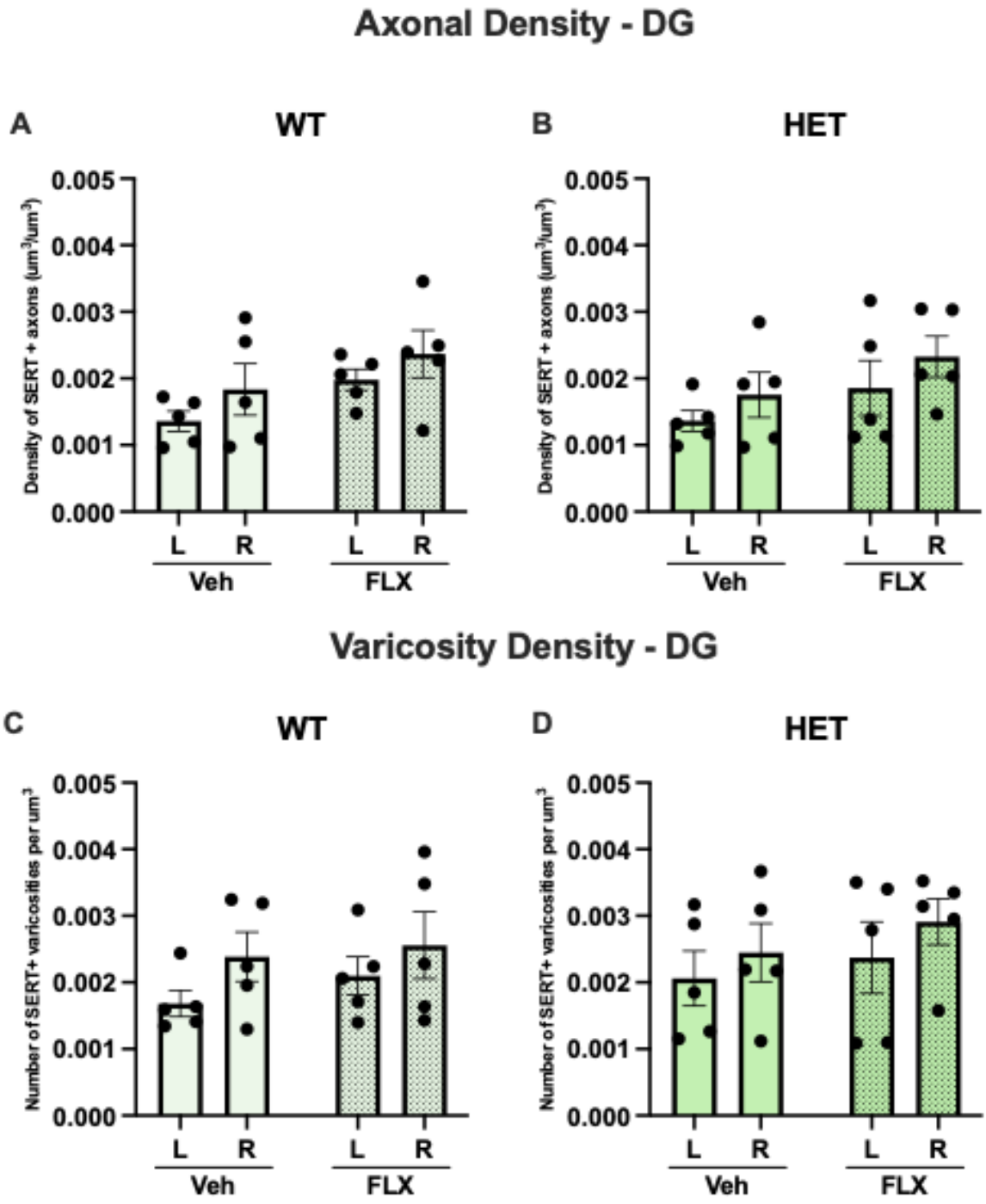

Figure 13. SERT+ axonal and varicosity density in the dentate gyrus (DG) of stroke mice. Ipsilesional (L) vs contralesional (R) sides of the brains are compared. Top row shows axonal density for A) wildtype mice given vehicle or FLX treatment, B) heterozygous knockout mice given vehicle or FLX treatment, bottom row shows varicosity density for C) wildtype mice given vehicle or FLX treatment, D) heterozygous mice given vehicle or FLX treatment. Two-way ANOVAs with Tukey's multiple comparisons tests, with mean ± SEM.

5.3.3 Basolateral amygdala

In the basolateral amygdala (BLA), WT vehicle treated mice showed a nonsignificant decrease in SERT+ axonal and varicosity density on the left side (Figure 14A, C). This difference was significant both for SERT+ axonal and varicosity density when analyzed via paired t-test (Figure S13A, S14A). When treated with chronic FLX, the left BLA recovered its innervation to be on par, or even slightly above that of the right BLA.

In HET mice, vehicle treated mice had a significant reduction in L BLA axonal and varicosity density compared to the R BLA (Figure 14B, D). When treated with FLX, this difference was no longer significant, but the L BLA did not recover to the same extent as in WT mice, with a trend decrease still present.

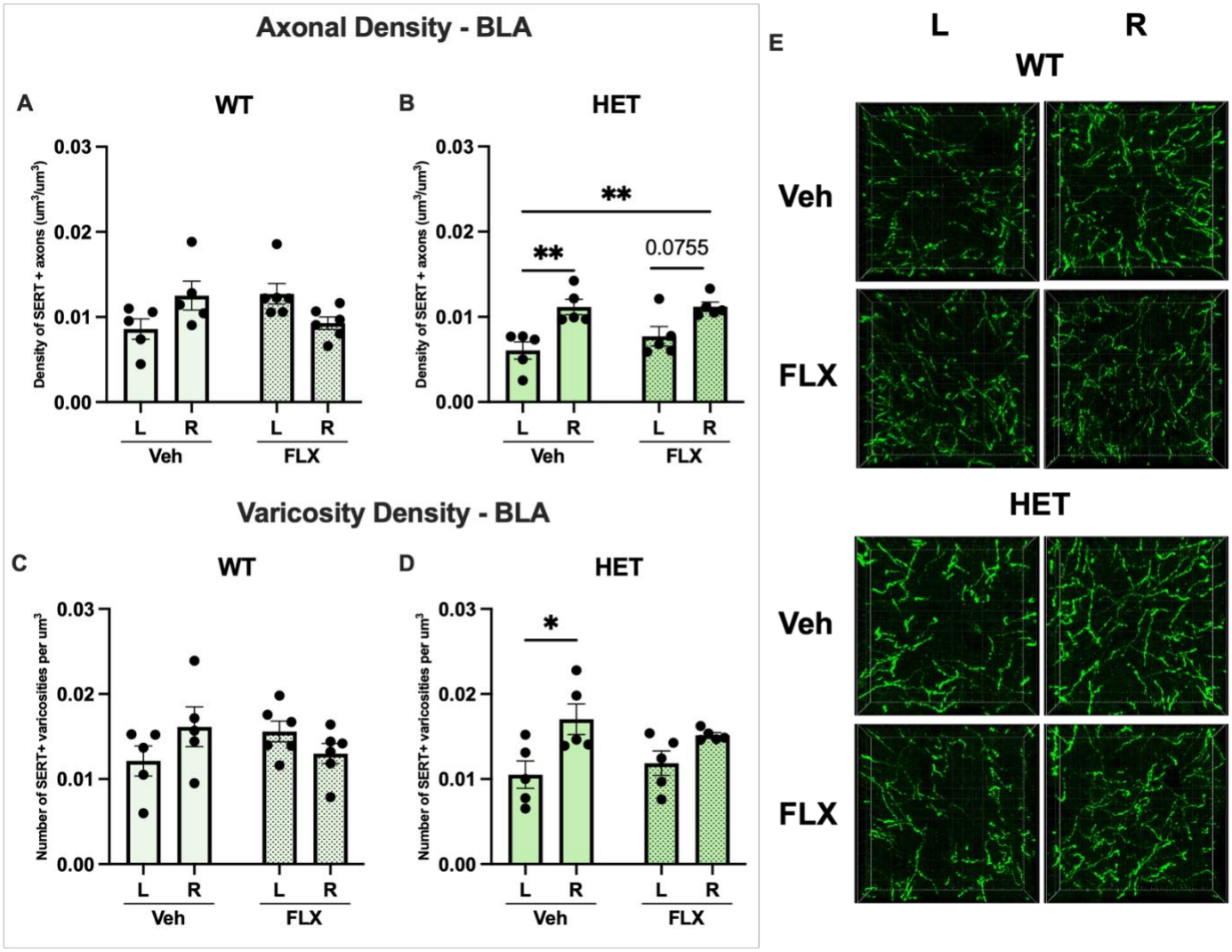

Figure 14. SERT+ axonal and varicosity density in the basolateral amygdala (BLA) of stroke mice. Ipsilesional (L) vs contralesional (R) sides of the brains are compared. Top row shows axonal density for A) wildtype mice given vehicle or FLX treatment, B) heterozygous knockout mice given vehicle or FLX treatment, bottom row shows varicosity density for C) wildtype mice given vehicle or FLX treatment, D) heterozygous mice given vehicle or FLX treatment. E) Representative 63X confocal images of SERT immunostaining. Two-way ANOVAs with Tukey's multiple comparisons tests, with mean ± SEM. *$p < 0.05$, **$p<0.01$.

5.3.4. Dorsal dorsal raphe

In the dorsal dorsal raphe (DDR), there were no significant differences in density of SERT+ axons or varicosities between any experimental groups (Figure 15). In both WT and HET mice treated with FLX, there was a trend increase in SERT+ varicosity density in the DDR. This trend appeared larger in the heterozygous mice, although the data points were highly variable, and the trend remained non-significant. These brains were not analyzed via paired t-test, as only one image was taken in the DDR, so there was no pairing to be done between these mice.

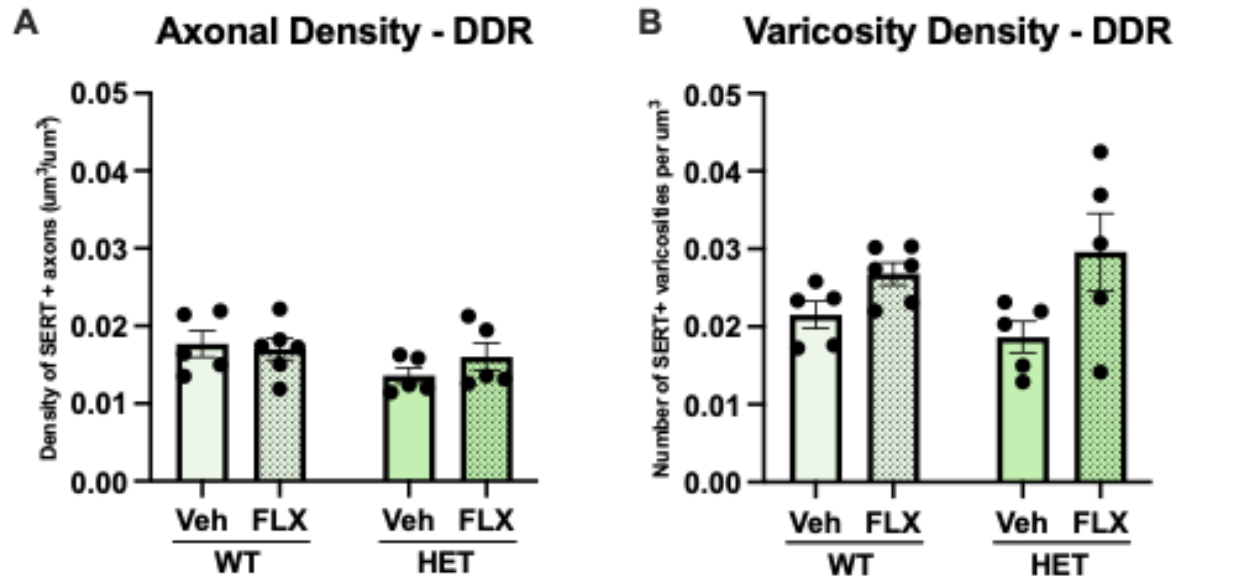

Figure 15. SERT+ axonal and varicosity density in the dorsal dorsal raphe (DDR) of stroke mice. A) SERT+ axonal density B) number of SERT+ varicosities per μm^3. Two-way ANOVAs with Tukey's multiple comparisons tests are shown, with mean ± SEM.

In summary, wildtype mice displayed a significant decrease in innervation of the L CG when vehicle treated post-stroke, and a recovery of innervation in FLX treated mice. A similar trend was shown in the PL but lacked statistical significance. Heterozygous mice showed trends of

decreased innervation in the left CG and PL regardless of FLX treatment. In the left BLA, heterozygous mice had significantly reduced SERT+ axonal and varicosity density, with an impaired recovery in FLX treated mice. WT mice showed a trend decrease in SERT+ axonal and varicosity density in the left BLA post-stroke which was reversed in FLX treated mice. No significant differences were observed for any group in the IL, any hippocampal regions or the DDR. Overall, AC2 WT and HET mice demonstrated region-specific deficits in left-side SERT+ innervation post-stroke, especially in the mPFC and BLA. The response to FLX treatment was impaired in AC2 HET mice compared to AC2 WT mice.

6. Discussion

Post stroke depression is a devastating comorbidity of stroke, impacting 30-50% of stroke survivors (Ayerbe et al., 2013; Hackett & Pickles, 2014; Medeiros et al., 2020). To date, SSRIs and psychotherapy are the primary treatments for this complex disease, but little is understood about the underlying mechanisms of recovery. Past work has shown that the serotonin system is capable of recovery following brain injury, including stroke, and this is amplified when supplemented with FLX treatment (Jin et al., 2016, Zahrai et al., 2020). With this knowledge, and the previous identification of pcdhαc2 as the primary protocadherin in the serotonin system (Chen et al., 2017), this study sought to investigate the role of pcdhαc2 in PSD recovery using a knockout mouse model. Analysis of naïve mice in my study showed significant differences in serotonergic innervation in a variety of brains regions in mice lacking both one or both copies of *pcdhαc2*, with more marked changed in AC2 KO mice. This investigation also revealed that mice with a partial reduction in pcdhαc2 display incomplete behavioural recovery post-stroke, regardless of FLX treatment. Additionally, these mice display incomplete recovery of SERT+

innervation post-stroke when treated with FLX, compared to WT mice, particularly at the stroke site (CG, PL) and basolateral amygdala. Taken together these results suggest that pcdhαc2 is essential for proper serotonergic innervation and for recovery post-stroke.

6.1 SERT+ innervation differences in pcdhαc2 deficient naïve mice

Previous studies have reported axonal tangling and bunching in pcdhα and pcdhαc2 knockout mice. Chen et al. (2017) presented a qualitative analysis of the affected brain areas, and Katori et al. (2017) quantified these changes in the hippocampus. The present study quantified the serotonergic innervation a variety of brain regions to establish a baseline phenotype for pcdhαc2 HET and KO mice.

The cingulate and prelimbic cortices of the medial prefrontal cortex (mPFC) had significantly altered SERT+ innervation profiles in mice deficient in one or both copies of *pcdhαc2*. In the CG, SERT+ axonal and varicosity density were reduced in both heterozygous knockout mice and full knockout mice, compared to wildtype mice. This is consistent with previous work reporting reduced SERT+ innervation throughout the CG in pcdhα constant exon region (CR) mutant mice (Katori et al. 2009). This is also consistent with the findings of Chen et al. (2017), who qualitatively observed bunching along the midline in the CG, primarily cortical layer 1, with sparse innervation of more lateral layers. The ROI of our mPFC images were taken in layers 2/3 which supports the finding of reduced innervation. If the photo were to be taken in layer 1 or 2, the findings may be reversed, capturing the increased bunching observed by Chen et al. (2017). The PL followed largely the same trend as the CG, with KO mice exhibiting significantly decreased axonal and varicosity density, with HET mice showing intermediate decreases. The

decrease in innervation of the PL in mice deficient in pcdhαc2 is consistent with the findings from the CG, as well as the images published by Chen et al. in 2017, which suggest that like the CG, 5-HT fibers bunch along the midline in the PL, with very little projection to more lateral areas, where our images were taken.

The infralimbic cortex exhibited no differences in innervation regardless of phenotype. This is consistent with the lack of previous reports on differences in this region. It may be that the infralimbic, a relatively small subregion of the medial prefrontal cortex, is innervated more completely as the developing axons ascend the medial forebrain bundle. Being a small region, it is possible that terminal field arborization impairments are less apparent. It is also possible that other protocadherin isoforms, such as protocadherin αc1, compensated for the loss of pcdhαc2 in some regions. Although single cell sequencing has shown limited expression of alternate isoforms in wildtype serotonin cells, no analysis has been conducted in knockout mice (Chen et al., 2017).

Early studies of serotonin outgrowth suggest that 5-HT axons extend first into the marginal zone of the cortex, which later arises into layer 1 of the cortex. Axons then project from the more superficial layers to deeper layers. This pattern of development, along with my findings, suggests that 5-HT axonal guidance is not disrupted in early stages when lacking pcdhαc2, but rather in later stages of target innervation. This is supported Katori et al. (2009), who found distribution of serotonergic fibers to be largely the same across brain regions in WT and pcdhα-CR mutant mice at P0 and P7, but by P21 notable differences were observed. This once again suggests that it is

the terminal field arborization, but not the primary outgrowth, or serotonin axons that is dependent on pcdhαc2.

Beyond the cortex, the hippocampus has been shown to have severe disturbances in 5-HT innervation in a variety of protocadherin alpha knockout models (Katori et al. 2009, 2017; Chen et al., 2017). In this study, KO mice, and HET mice to a lesser extent, showed significantly decreased SERT+ axonal and varicosity density in the SR and DG of the hippocampus. In contrast, these mice had a significant increase in SERT+ axonal and varicosity density in the SLM, suggestive of a clumping of hippocampal axons away from the SR and DG into the SLM. These findings are highly consistent with previous studies. Katori et al. (2017) calculated SERT+ density in the stratum oriens (SO), SR, SLM and DG and found a significant increase in the SLM and decrease in the DG in their serotonin specific ac2 knockout mice. In their whole brain ac2 knockout mice, they also saw significant increase in density of SERT+ fibers in the SLM, and significant decrease in the DG for their heterozygous and full knockout mice. The SO of full knockout mice also had significantly lower SERT+ fiber density compared to heterozygous knockouts. Katori et al. (2017) also used an AAV to label and trace a subset of 5-HT projections and found that 5-HT axons in protocadherin alpha c2 knockout mice were more suppressed in crossing the SLM/SR boundary than wildtype mice. Chen et al. (2017) also investigated protocadherin alpha knockout mice and described increased SERT+ fiber density in the SLM and decreased density in the DG. Taken together, this supports my hippocampal results, which displayed significantly increased SERT+ fiber density in the SLM of heterozygous and full knockout mice, and significantly decreased density in the DG. My data also showed a significant decrease in the SERT+ fiber density of the SR, which is not represented in the data by Katori et

al. (2017) or Chen et al. (2017) but appears consistent with the representative images published in Chen et al. (2017). My study was the first to use fiber reconstruction software (IMARIS) to qualify the SERT+ axonal and varicosity density in pcdhαc2 knockout mice, which could explain its ability to reveal such differences.

My findings, as well as previous findings in similar knockout mice, suggest once again that terminal field arborization, rather than primary 5-HT innervation is inhibited by a lack of pcdhαc2. Analysis of developing brains by Katori et al. (2009) and Chen et al. (2017) further support this claim based on their findings of relatively normal hippocampal innervation up until P7, at which point the KO mice begin to differ more from WT mice, up to P21 when the extreme bunching along the SLM is observed. This is also even further supported by the finding that overall density of hippocampal 5-HT innervation is not changed between WT and pcdhα-CR mutant mice, rather only the organization of these axons is changed (Katori et al., 2009). All together this suggests a loss of homophilic repulsion because of pcdhαc2 knockout results in an imbalance of cell extrinsic and intrinsic forces, resulting in improper tiling and subsequently abnormal arborization.

The BLA showed a significant increase in SERT+ innervation in HET mice compares to WT, but not in KO mice. While the difference was not statistically significant, KO mice showed distinct heterogeneity in their innervation profiles. Previous studies have not quantified SERT+ axonal or varicosity density in pcdhαc2 knockout mice, but Chen et al. (2017) saw qualitative differences in their pcdhα constitutive and conditional knockout mice. The BLA of their KO mice appears to have increased tangling and bunching, although it was not quantified. They also mention a

randomness in the tangling observed, primarily in the ventral pallidum, which may also extend to the BLA based on my results. The BLA, being a region with more diffuse projections than the highly organized hippocampus, may experience increased randomness in tangling when lacking pcdhαc2. Changes in the SERT+ innervation of this region could contribute to a baseline depressive-like phenotype as observed in a previous pcdhα knockout model, as the BLA is an important region for mood regulation (Chen et al., 2017).

No significant differences were observed in SERT+ axonal or varicosity density in the DDR. This is consistent with previous studies that found no change in the number of 5-HT cells or primary projections in knockout mice (Katori et al., 2009, Chen et al., 2017). Cell differentiation and early outgrowth appear to be primarily driven by non-protocadherin guidance cues such as: BDNF, S100B, WNTs, Slit 1/2, Robo 1/2, Lmx1B, Pet-1, and ephrins (Vahid-Ansari & Albert, 2021; Deneris & Gaspar, 2018).

6.2 Recovery of PSD behavioural phenotype

In the elevated plus maze test, heterozygous knockout mice were first tested and found to have a complete lack of response to FLX at 6 weeks. Due to breeding limitations, wildtype mice were bred and tested at a later date. When tested, wildtype mice did not recover as expected following FLX treatment, with the anxiety-like phenotype persisting. Previous work with this stroke model has shown recovery at 6 weeks when treated with chronic FLX (Vahid-Ansari & Albert, 2018). This unexpected lack of recovery by the wildtype group could potentially be associated with an additional external stressor. At the time of breeding and testing, construction had begun adjacent to the mouse housing facility. Vibrations were regularly felt by researchers and staff in the

facility. Previous studies have found that mice are highly sensitive to noise and vibrations, and that construction noise can lead to breeding difficulties such as decreased birth rates and increase still births (Rasmussen et al., 2009). At a greater extreme, mice who had experienced an earthquake also displayed increased anxiety and fear conditioning (Yanai et al., 2012). It is possible that the persistent noise and vibrations caused by the construction, present from birth for this group of wildtype mice, could explain their lack of recovery in this test of anxiety-like behaviour.

In the FST, both wildtype and heterozygous knockout AC2 mice had an increased inactivity duration at 1-week-post-stroke and at 6-weeks post-stroke timepoints when treated with vehicle. When treated with chronic FLX, wildtype mice showed reduced inactivity duration, comparable to pre-stroke control levels. This is consistent with the recovery observed in this test using this stroke model in C57BL/6 male mice (Vahid-Ansari & Albert, 2018). Unlike wildtype mice, the increased inactivity duration seen in heterozygous knockout mice did not recover to pre-stroke control levels when treated with chronic FLX. The 6-week FLX timepoint did not differ significantly from the 1-week post-stroke or 6-week post stroke vehicle treated groups. However, the 6-week FLX treated group is also the only post-stroke group that does not differ significantly from the pre-stroke control. This suggests that heterozygous knockout mice, possessing one copy of pcdhαc2, show a partial behavioural recovery in the FST when treated with FLX. Chen et al., (2017) found a significant increase in immobility time in their pcdhα knockout mice compared to WT mice. HET mice were chosen for this study to mitigate the baseline phenotype, but the impaired behavioural recovery post-stroke could be due to the partial knockout of pcdhαc2. The

lack of behavioural recovery in both tests is also consistent with the incomplete recovery of 5-HT innervation in the mPFC and BLA in HET mice.

6.3 SERT+ innervation changes in PSD mice

Unilateral stroke to the left mPFC resulted in a reduction of SERT+ axonal and varicosity density at stroke-specific brain regions. In wildtype mice, these reductions were reversed when treated with chronic FLX. I hypothesized that pcdhαc2 deficient mice would exhibit deficits in serotonergic innervation post stroke, with or without fluoxetine treatment. This hypothesis was based on the indispensability of pcdhαc2 for proper wiring in development (Katori et al., 2009, 2017; Chen et al., 2017). Analysis revealed that HET mice largely lacked proper SERT+ recovery post-stroke, with variability in the degree of recovery by region.

In the left prefrontal cortex, at the site of the stroke, WT mice showed significant decreases compared to the right mPFC, while HET mice showed strong trend decreases in the SERT+ axonal and varicosity density in the left CG, and more minor decreases in the left PL. In the CG, FLX treated mice showed no innervation difference between the L and R CG or PL, suggesting that FLX was able to reverse this loss of innervation post-stroke. In HET mice however, chronic FLX treatment was unable to fully reverse the left-right difference in SERT+ axonal density, with a strong trend still present in the CG and PL. This difference in axonal density between the L and R CG of FLX treated HET mice reached statistical significance when analyzed in a paired manner to account for individual variance, via paired t-test. Interestingly, the density of SERT+ varicosities in the CG and PL of heterozygous mice, which trended lower on the left side following stroke with vehicle treatment, leveled out in the FLX treated group. This could suggest

the ability of FLX to enhance recovery of varicosities, but not the re-innervation of SERT+ fibers in the AC2 HET mice. This could indicate a compensatory mechanism employed by these partial knockout mice, to recovery 5-HT release capacity in the absence of an ability to re-innervate. Future work would be needed to probe the functionality of these varicosities.

When analyzed via two-way ANOVA, there are no significant differences in the innervation of any hippocampal subregions between any experimental groups. This is consistent with the lack of stroke effect on the hippocampus previously observed in this model using C57BL/6 and Pet-ChR2 mice (Zahrai et al., 2020). However, when analyzed via paired t-test, the L SR of vehicle treated AC2 HET mice show significantly reduced SERT+ axonal and varicosity density compared to the R SR. This finding could suggest that heterozygous mice, who in the naïve analysis were shown to possess a baseline reduction in SR innervation compared to WT, may reveal a stroke effect on the hippocampus more prominently than WT mice which have proper baseline innervation in this region. In AC2 HET mice treated with FLX there was no longer a significant difference between the L and R SR which also suggests possible recovery. Although the 5-HT innervation of the cortex and hippocampus is thought to arise from distinct cell populations, there is evidence of mPFC projecting 5-HT neurons having collaterals extending into the hippocampus (Gagnon & Parent, 2014). A loss in these collaterals may explain the observed decrease.

The other notable brain area impacted post-stroke was the BLA. When analyzed via two-way ANOVA, only HET mice displayed a statistically significant reduction in SERT+ axonal and varicosity density in the left vs. right BLA of vehicle treated mice; however, WT mice showed

the same trend, and this trend was statistically significant when analyzed via paired t-test. Following chronic FLX treatment, the trend in WT mice was reversed. This post-stroke reduction and subsequent FLX-induced recovery is consistent with past work in this stroke model where the BLA was prominently affected by the stroke and FLX treatment compared to most other brain regions (Zahrai et al., 2020). Although 5-HT projections to the mPFC and BLA largely originate from distinct cells, a small number have been recorded to project back to the same cells (Fernandez et al., 2016). The observed reduction in innervation of the L BLA following lesion to the L mPFC in this model suggests a connection between the two.

7. Conclusion

In conclusion, this study revealed that pcdhαc2 is indispensable for proper 5-HT innervation and PSD recovery. Naïve pcdhαc2 HET and KO mice show significant differences in 5-HT innervation compared to WT, with significant decreases in innervation of the CG, PL, SR and DG, and a significant increase in innervation of the SLM. This furthers previous findings and provides a baseline innervation profile for future work.

When given a stroke at the left mPFC, WT and HET mice display significant anxiety and depressive-like phenotypes that persist up to 6 weeks untreated. Only WT mice experienced FLX-induced behavioural recovery in the FST, while HET mice experienced incomplete recovery. This finding implicates pcdαac2 in behavioural response to FLX post-stroke.

Finally, mice given a stroke exhibited reduced SERT+ axonal and varicosity density in the left CG, PL and BLA. WT mice treated with FLX recovered their innervation back to right

hemispheric levels; however, AC2 HET mice displayed incomplete recovery even when treated with FLX. This is in line with the impaired behavioural recovery of these mice, and further implicated pcdhαc2 in post-stroke recovery. Taken together these results suggest that pcdhαc2 is indispensable for proper baseline serotonergic innervation, behavioural recovery and re-innervation recovery post-stroke.

8. Future Directions

Various future studies could build upon and further validate the findings from this work.

Future work should investigate the potential cognitive deficits of these pcdhαc2 knockout mice. Using tests such to assess the learning and memory differences in mice lacking pcdhαc2 and build upon the findings of cognitive impairment in pcdhα conditional knockout mice by Chen et al. (2017) could link the innervation differences in the hippocampus with functional outcomes.

Future work could also investigate the connectivity changes of serotonergic fibers in pcdhαc2 knockout mice. Given the changes in fiber distribution and density, region specific activity and connectivity changes may be expected. Investigating the number of synaptic connections in these regions of interest, compared to wildtype mice, could highlight the functional changes underpinning some baseline cognitive and depressive phenotypes seen in a previous study (Chen et al., 2017). Investigating the impact of our stroke model on these connectivity changes could add to this future work. Previous work in our lab has shown changes in excitatory and inhibitory synaptic connections to serotonergic neurons post-stroke (Zahrai et al., 2020). If any pre-existing deficits in synaptic connections existed in pcdhαc2 knockout mice, the stroke may exacerbate

these effects. Based on my results of incomplete FLX induced post-stroke recovery of SERT+ axonal and varicosity density in these mice, any connectivity related effects may also insufficiently recover.

Another interesting future direction that could be considered is in-vivo imaging of recovering axons post-stroke. A previous study has used this imaging technique to trace regrowth following other injury models, but not stroke (Jin et al., 2016). In-vivo imaging post-stroke in HET or KO mice could reveal if damaged axons regrow at all in the absence of pcdhαc2, if they regrow locally at the site of die-back, and if tangling is increased if the axons attempt to reinnervate. My data provides region-wide re-innervation information but lacks the specificity that could be achieved by following individual axons.

Additionally, to validate the above data, and address a limitation of the study, future work should consider imaging/analysis changes. To avoid heterogeneity in the sample confounding the results, as I observed in analysis of the BLA of naïve mice, larger scale images or various averaged images should be considered. Another consideration could be singling out areas of bunching and adjacent areas of sparseness, to achieve a more homogeneous data set.

Lastly, future work should seek to amplify pcdhαc2 post-stroke to investigate its potential as a promoter of regrowth. This could be achieved through a variety of inducible genetic mouse models, or viral delivery, to either first induce or further upregulate pcdhαc2 post-stroke. Investigating the potential of pcdhαc2 as a promoter of stroke-recovery is a promising future direction of this study.

Supplemental Figures

Below I have included paired t-tests comparing L vs R sides of the brain in stroke mice to account for variability between mice. This approach allowed for comparison of the stroke side (left) brain regions, to the intact contralateral regions (right) in each mouse. This revealed deficiencies in SERT+ axons and/or varicosities on the stroke side in WT mice (CG, PL, BLA) that were recovered by FLX, whereas in HET mice these recoveries were incomplete.

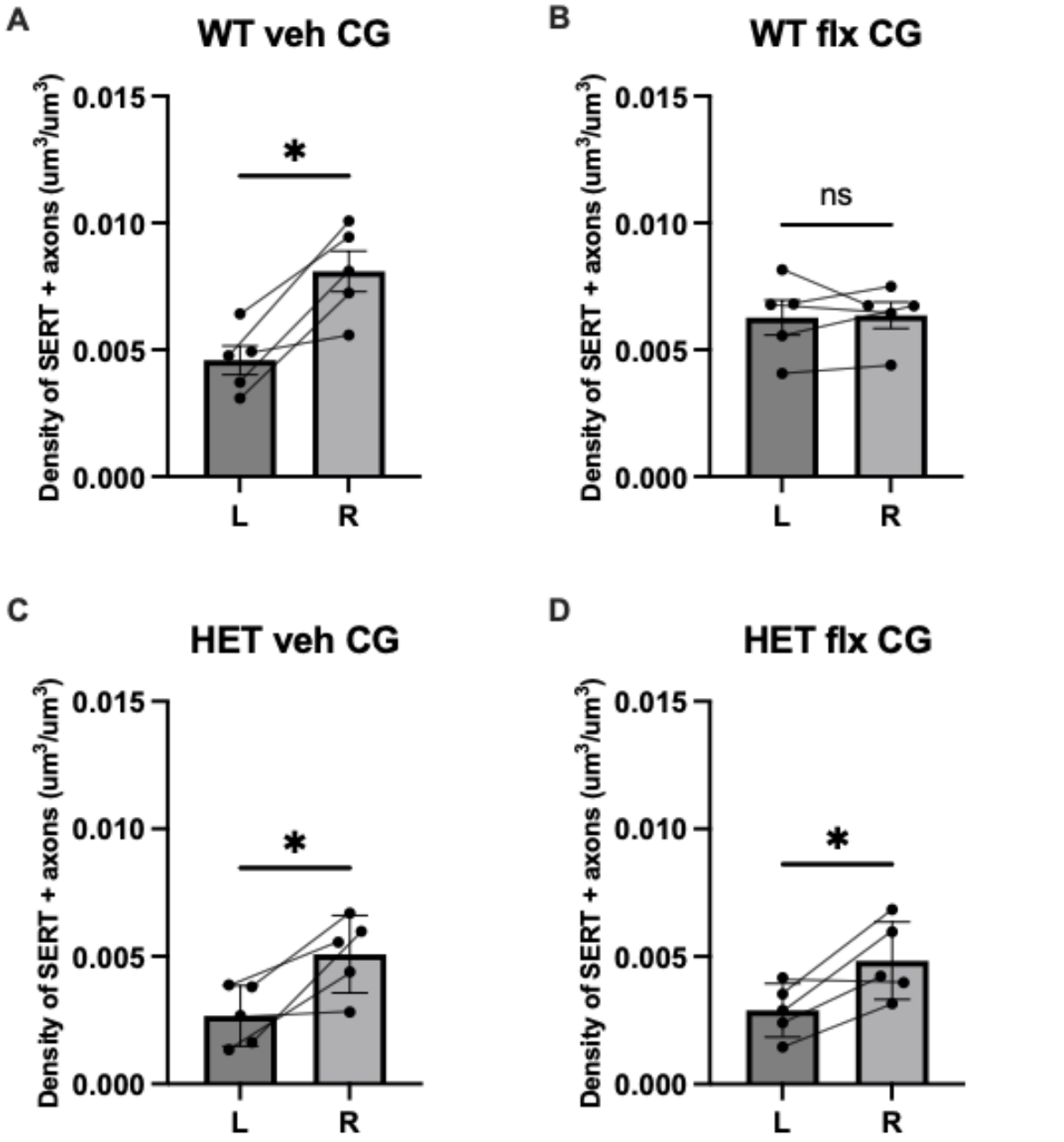

Figure S1. SERT+ axonal density of the cingulate cortex (CG) of stroke mice. Left vs right sides of the brains are compared in the 4 groups: A) wildtype mice given vehicle treatment, B) wildtype mice given FLX treatment, C) heterozygous mice given vehicle treatment and D) heterozygous mice given FLX treatment. Paired t-tests, with mean ± SEM. *$p < 0.05$.

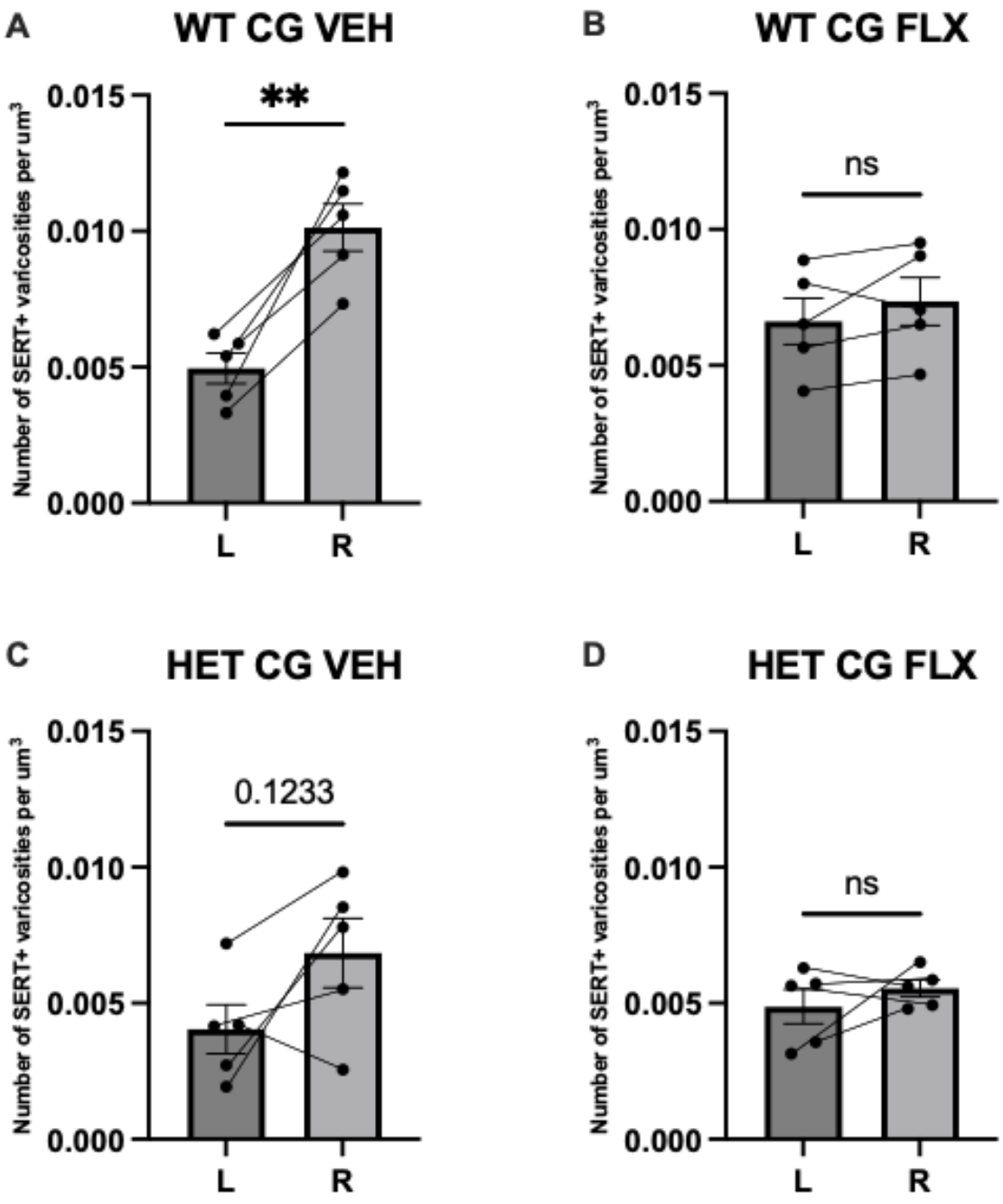

Figure S2. Density of SERT+ varicosities per μm^3 in the cingulate cortex (CG) of stroke mice. Left vs right sides of the brains are compared in the 4 groups: A) wildtype mice given vehicle treatment, B) wildtype mice given FLX treatment, C) heterozygous mice given vehicle treatment and D) heterozygous mice given FLX treatment. Paired t-tests, with mean ± SEM. **p<0.01.

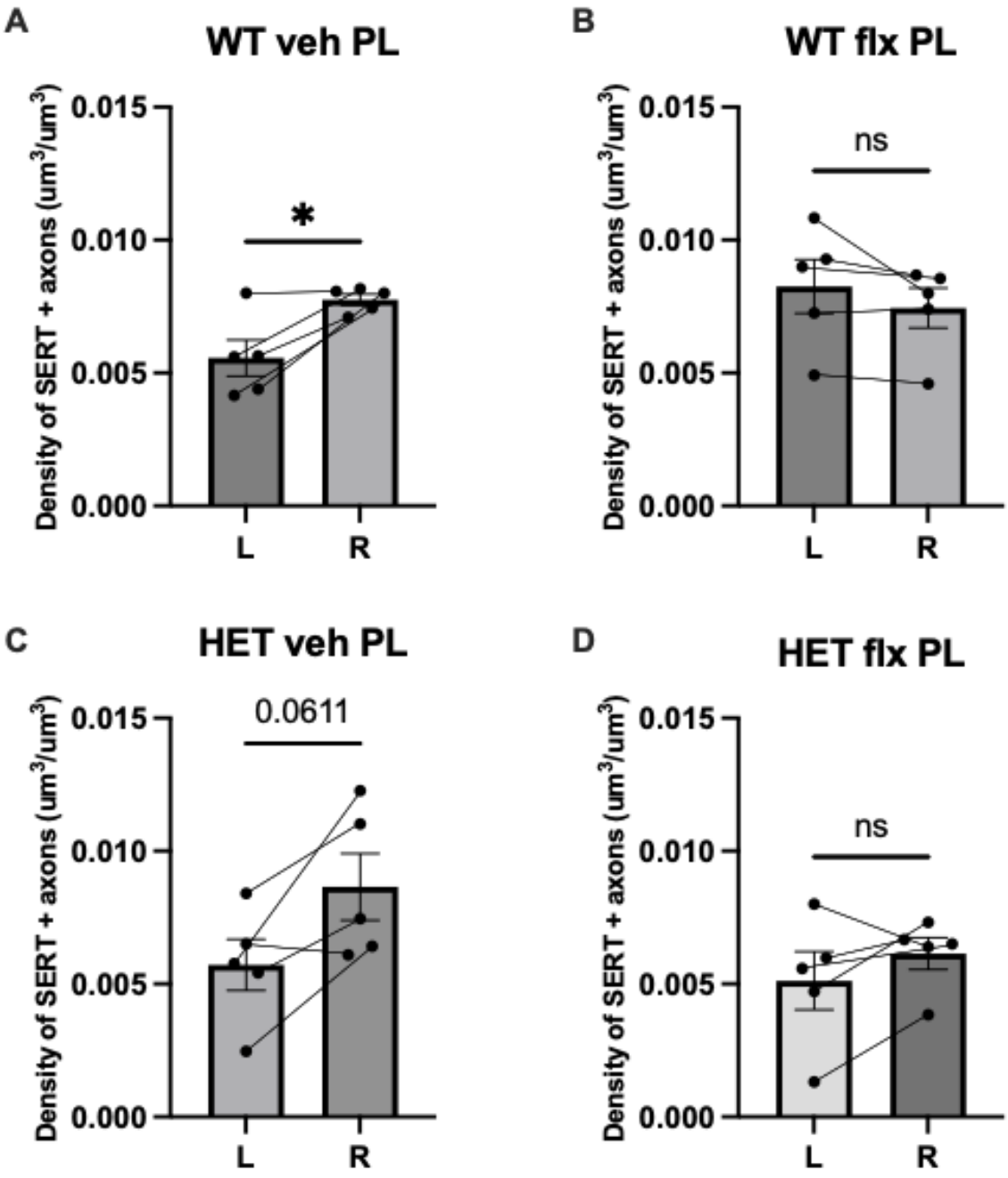

Figure S3. SERT+ axonal density of the prelimbic cortex (PL) of stroke mice. Left vs right sides of the brains are compared in the 4 groups: A) wildtype mice given vehicle treatment, B) wildtype mice given FLX treatment, C) heterozygous mice given vehicle treatment and D) heterozygous mice given FLX treatment. Paired t-tests, with mean ± SEM. *$p < 0.05$.

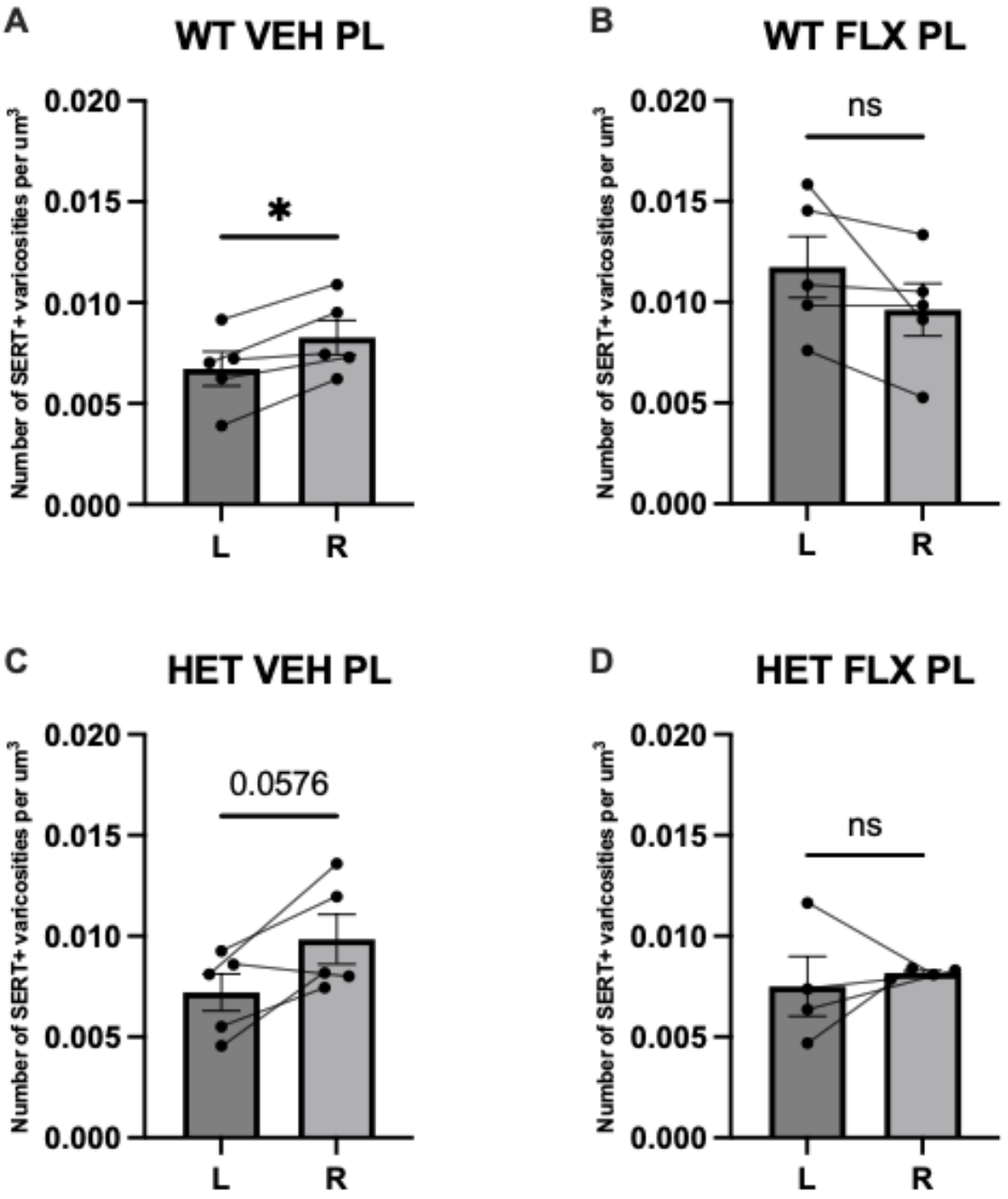

Figure S4. Density of SERT+ varicosities per μm^3 in the prelimbic cortex (PL) of stroke mice. Left vs right sides of the brains are compared in the 4 groups: A) wildtype mice given vehicle treatment, B) wildtype mice given FLX treatment, C) heterozygous mice given vehicle treatment and D) heterozygous mice given FLX treatment. Paired t-tests, with the mean ± SEM. *$p < 0.05$.

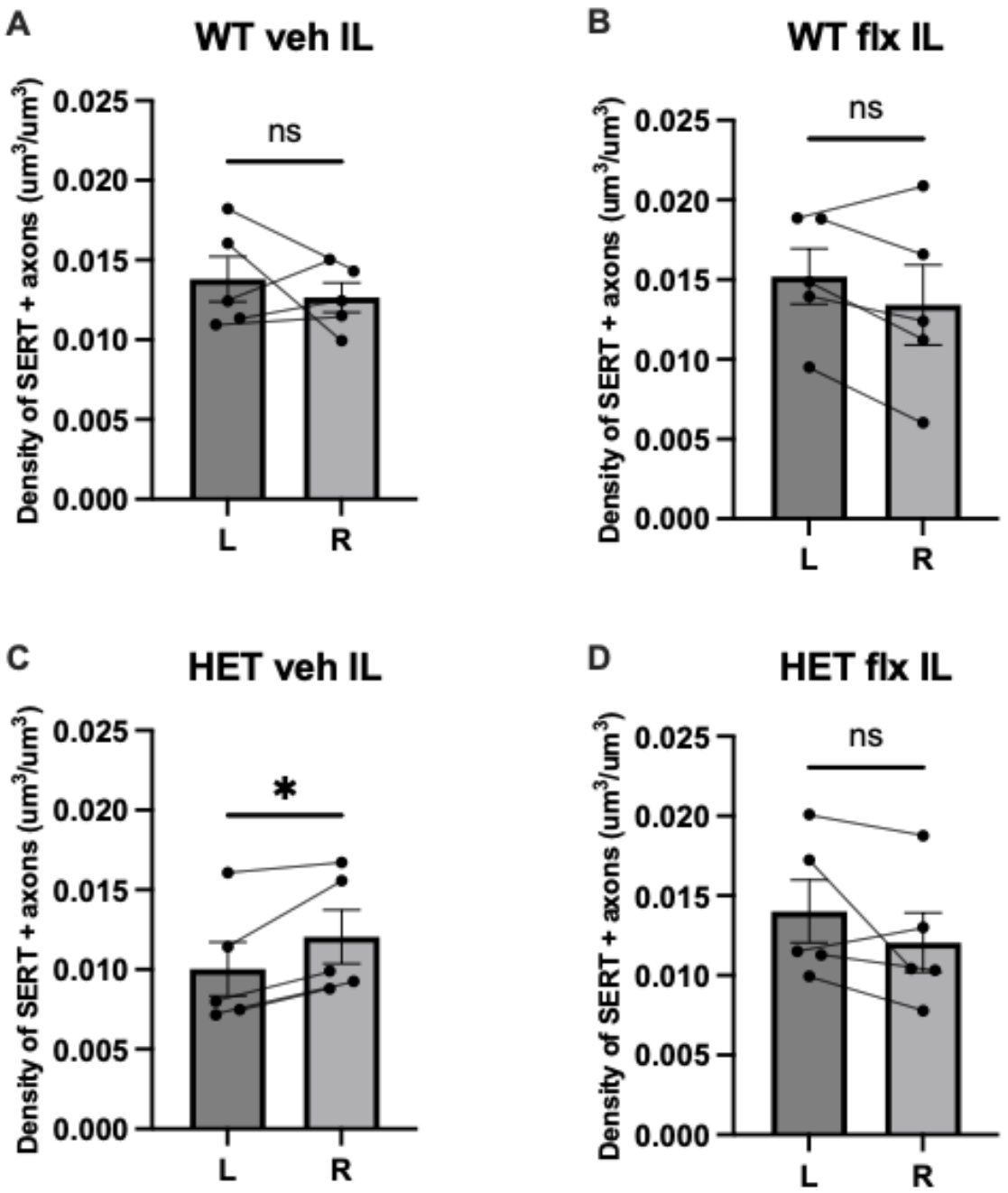

Figure S5. SERT+ axonal density of the infralimbic cortex (IL) of stroke mice. Left vs right sides of the brains are compared in the 4 groups: A) wildtype mice given vehicle treatment, B) wildtype mice given FLX treatment, C) heterozygous mice given vehicle treatment and D) heterozygous mice given FLX treatment. Paired t-tests, with the mean ± SEM. *$p < 0.05$.

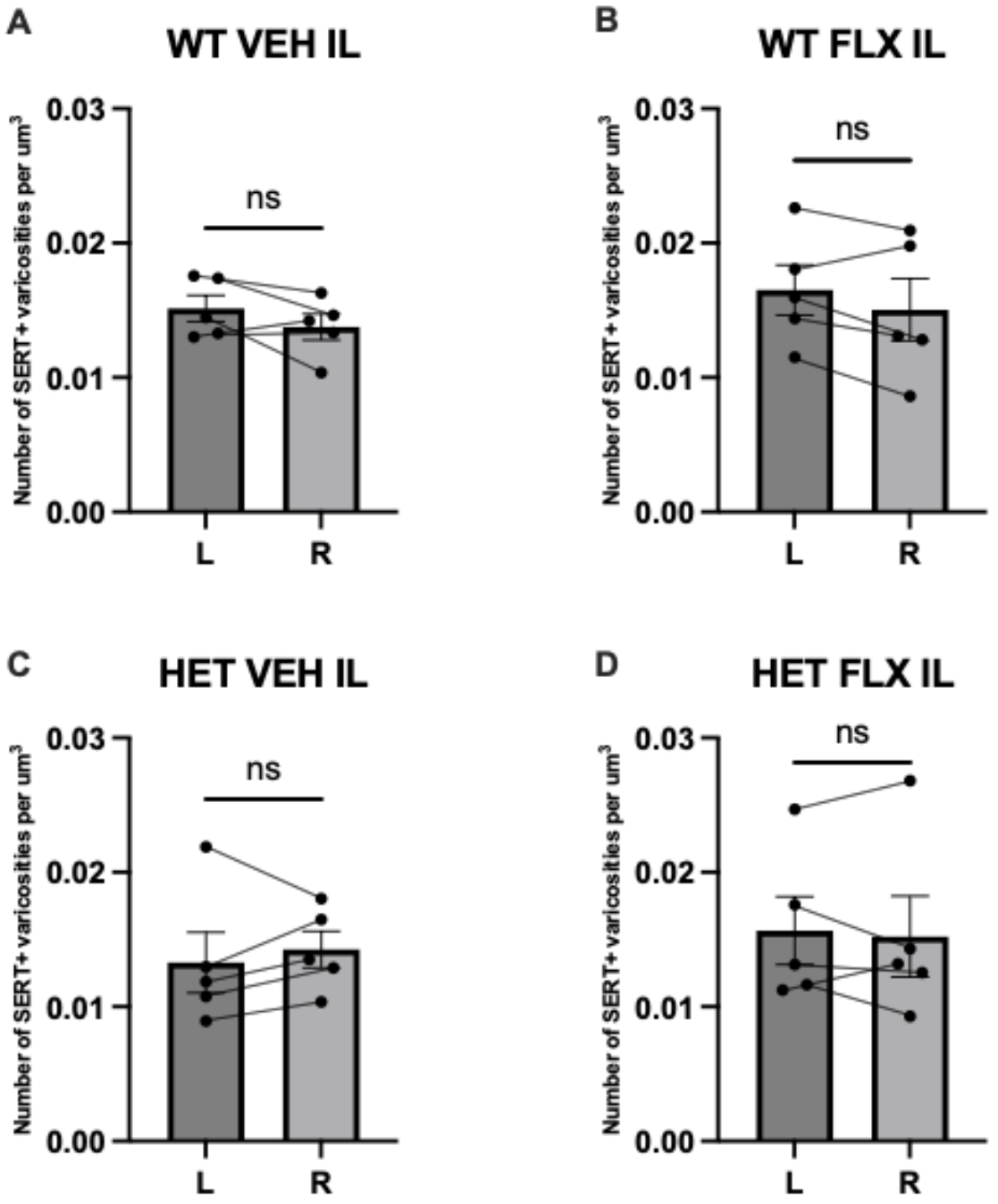

Figure S6. Density of SERT+ varicosities per μm^3 in the infralimbic cortex (IL) of stroke mice. Left vs right sides of the brains are compared in the 4 groups: A) wildtype mice given vehicle treatment, B) wildtype mice given FLX treatment, C) heterozygous mice given vehicle treatment and D) heterozygous mice given FLX treatment. Paired t-tests, with mean ± SEM.

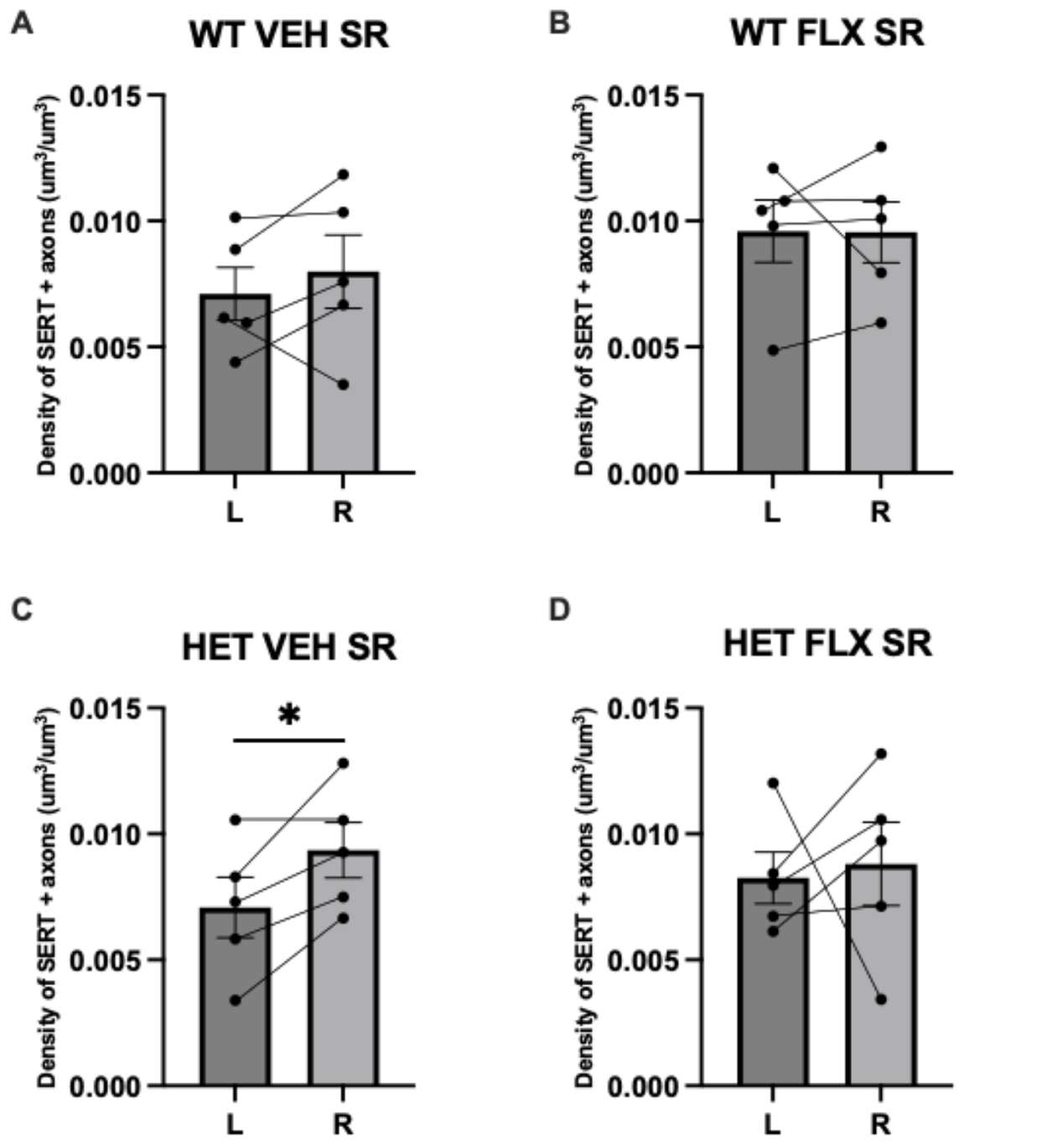

Figure S7. SERT+ axonal density of the stratum radiatum (SR) of stroke mice. Left vs right sides of the brains are compared in the 4 groups: A) wildtype mice given vehicle treatment, B) wildtype mice given FLX treatment, C) heterozygous mice given vehicle treatment and D) heterozygous mice given FLX treatment. Paired t-tests, with the mean ± SEM. *$p < 0.05$.

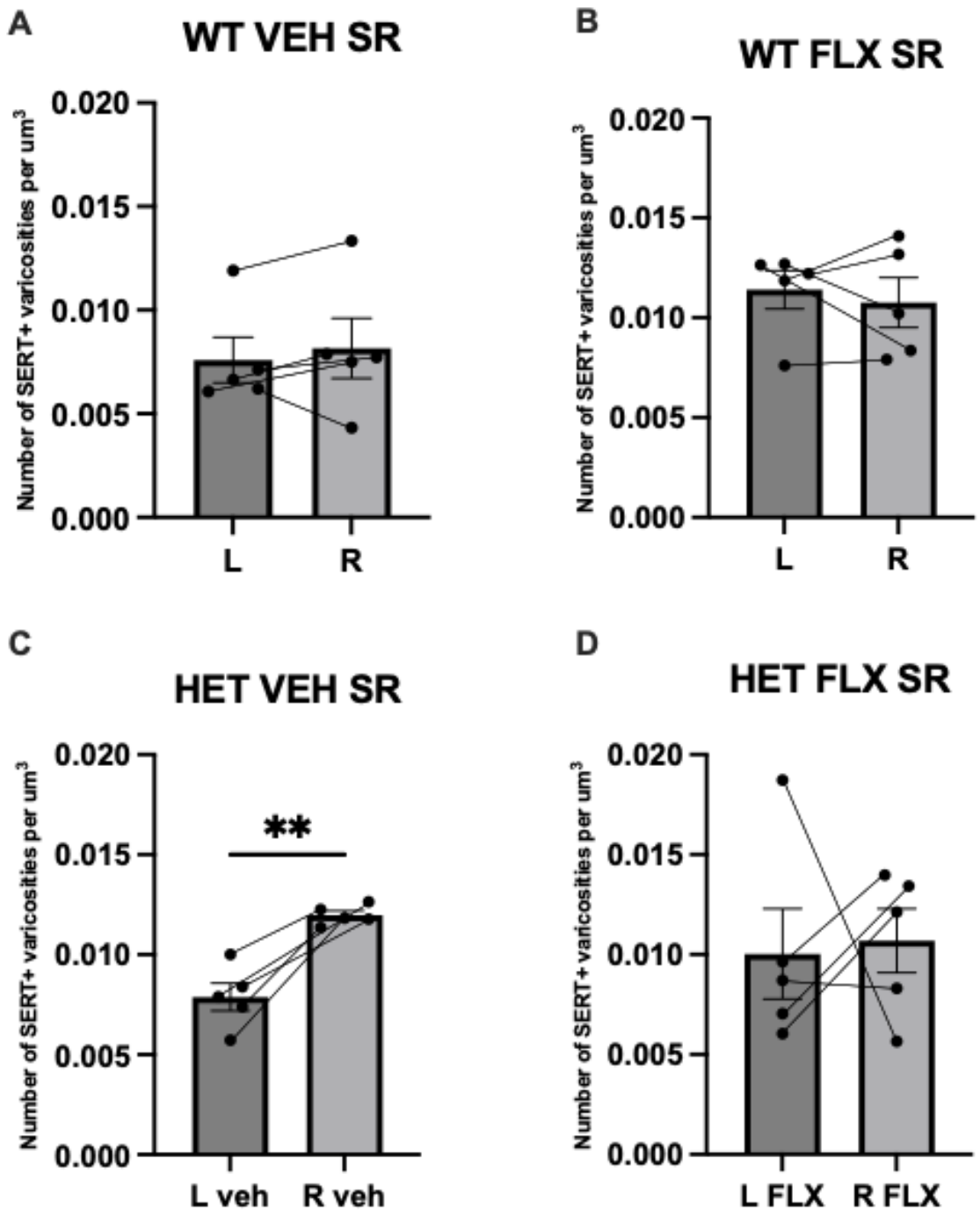

Figure S8. Density of SERT+ varicosities per μm^3 in the stratum radiatum (SR) of stroke mice. Left vs right sides of the brains are compared in the 4 groups: A) wildtype mice given vehicle treatment, B) wildtype mice given FLX treatment, C) heterozygous mice given vehicle treatment and D) heterozygous mice given FLX treatment. Wilcoxon tests (A,B) and paired t-tests (C, D), with mean ± SEM. **p<0.01.

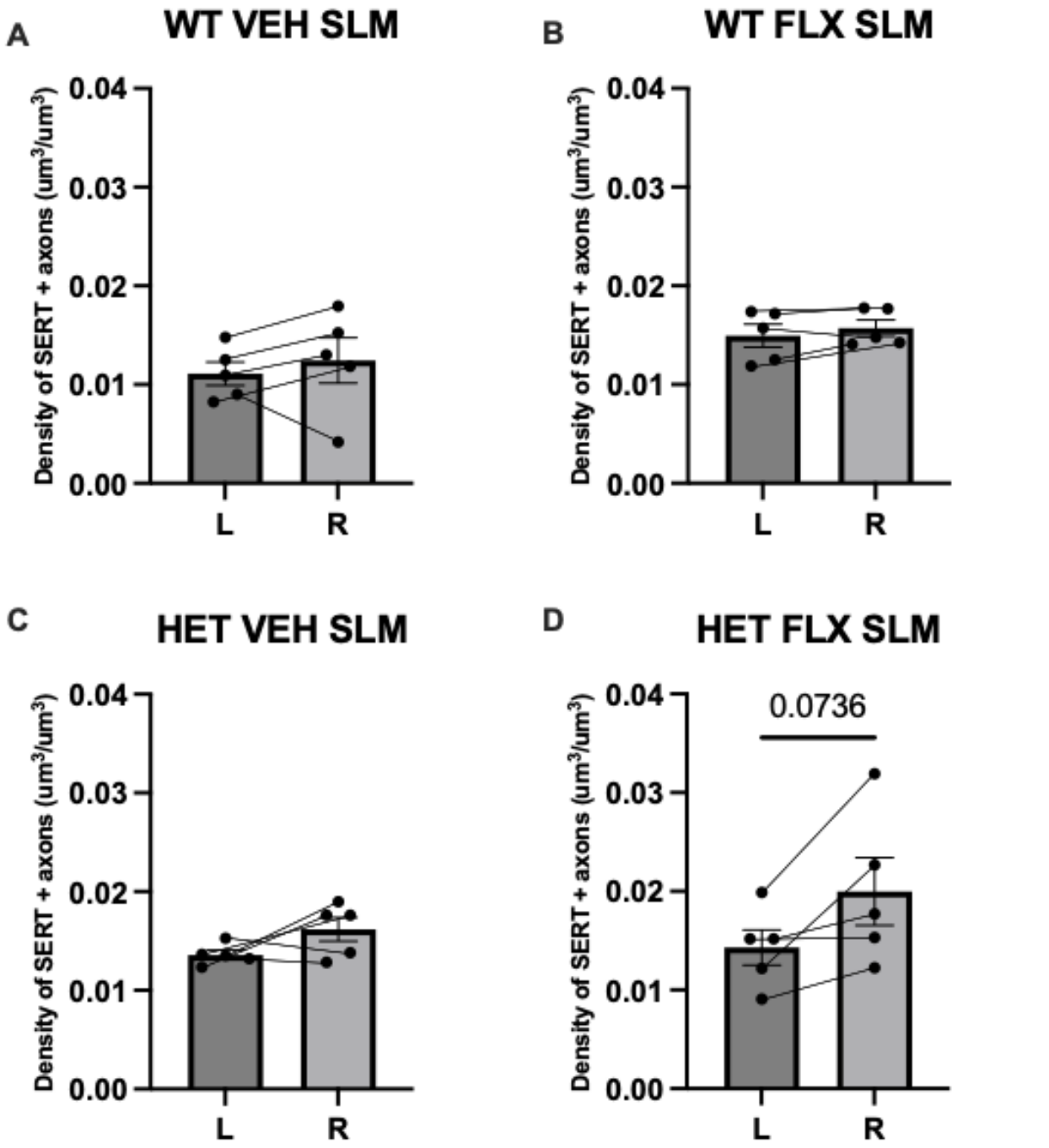

Figure S9. SERT + axonal density of the stratum lacunosum moleculare (SLM) of stroke mice. Left vs right sides of the brains are compared in the 4 groups: A) wildtype mice given vehicle treatment, B) wildtype mice given FLX treatment, C) heterozygous mice given vehicle treatment and D) heterozygous mice given FLX treatment. Paired t-tests, with the mean ± SEM.

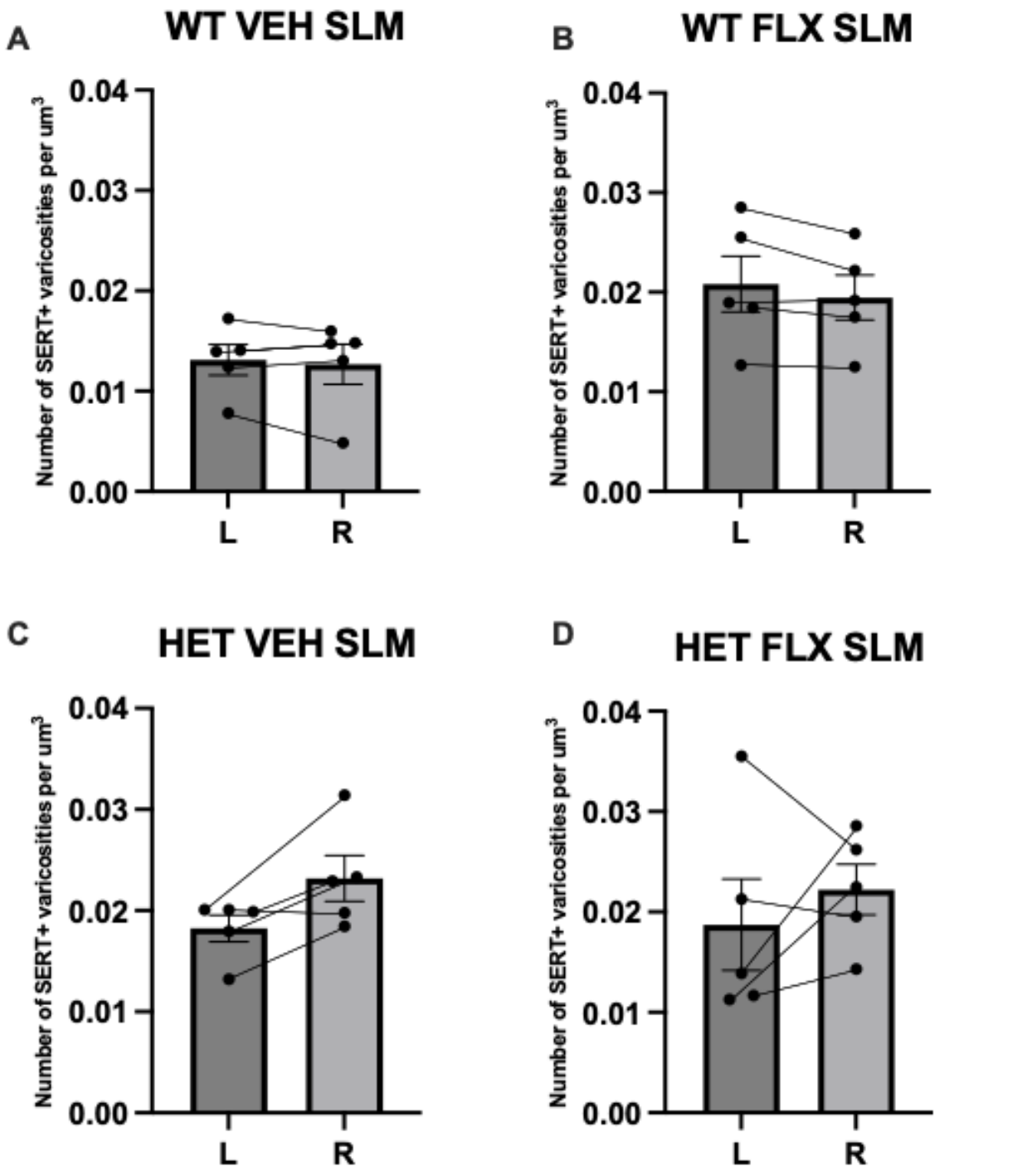

Figure S10. Density of SERT+ varicosities per µm^3 in the stratum lacunosum moleculare (SLM) of stroke mice. Left vs right sides of the brains are compared in the 4 groups: A) wildtype mice given vehicle treatment, B) wildtype mice given FLX treatment, C) heterozygous mice given vehicle treatment and D) heterozygous mice given FLX treatment. Wilcoxon tests (A, C) and paired t-tests (B, D), with mean ± SEM.

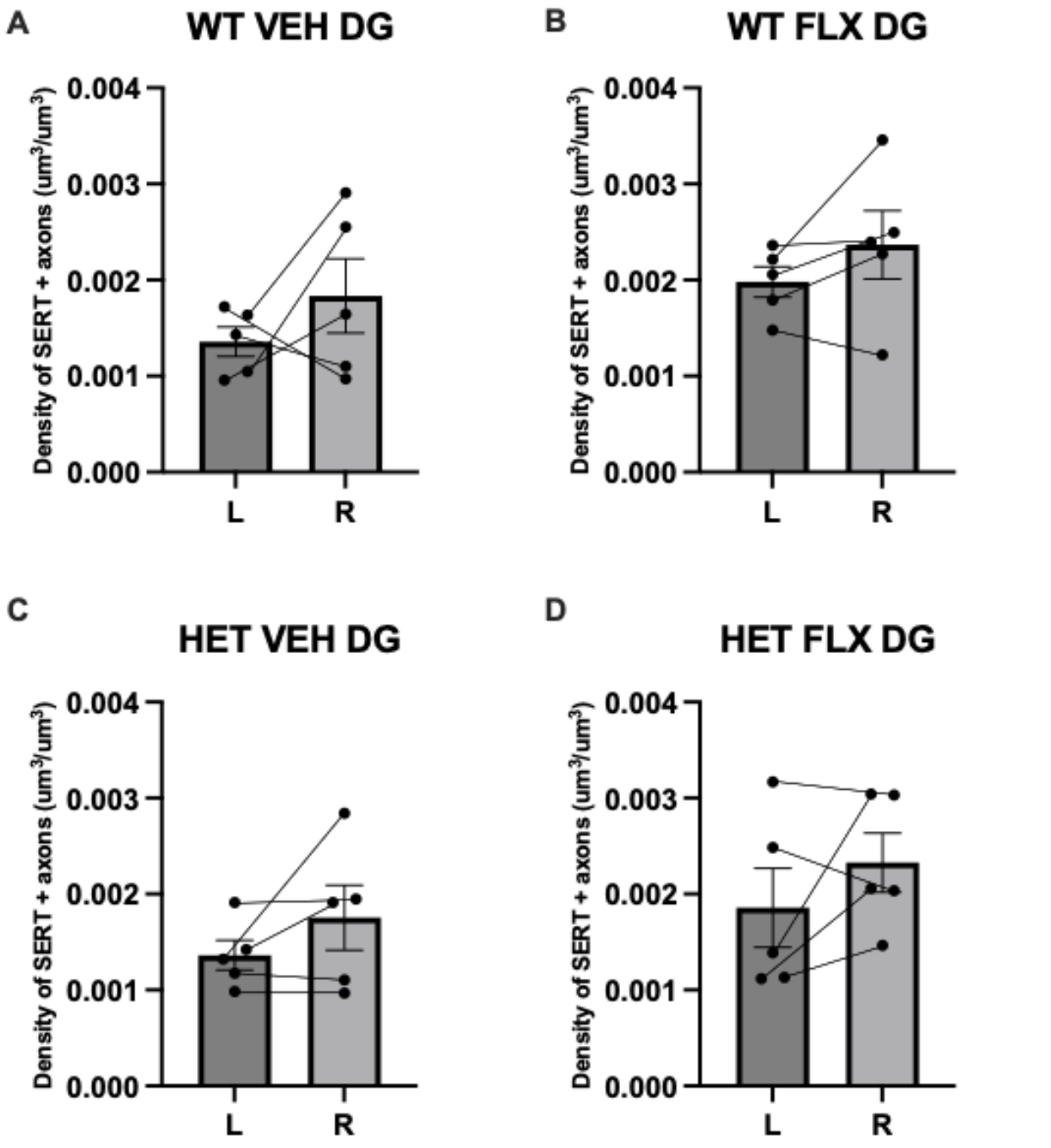

Figure S11. SERT + axonal density of the dentate gyrus (DG) of stroke mice. Left vs right sides of the brains are compared in the 4 groups: A) wildtype mice given vehicle treatment, B) wildtype mice given FLX treatment, C) heterozygous mice given vehicle treatment and D) heterozygous mice given FLX treatment. Paired t-tests, with mean ± SEM.

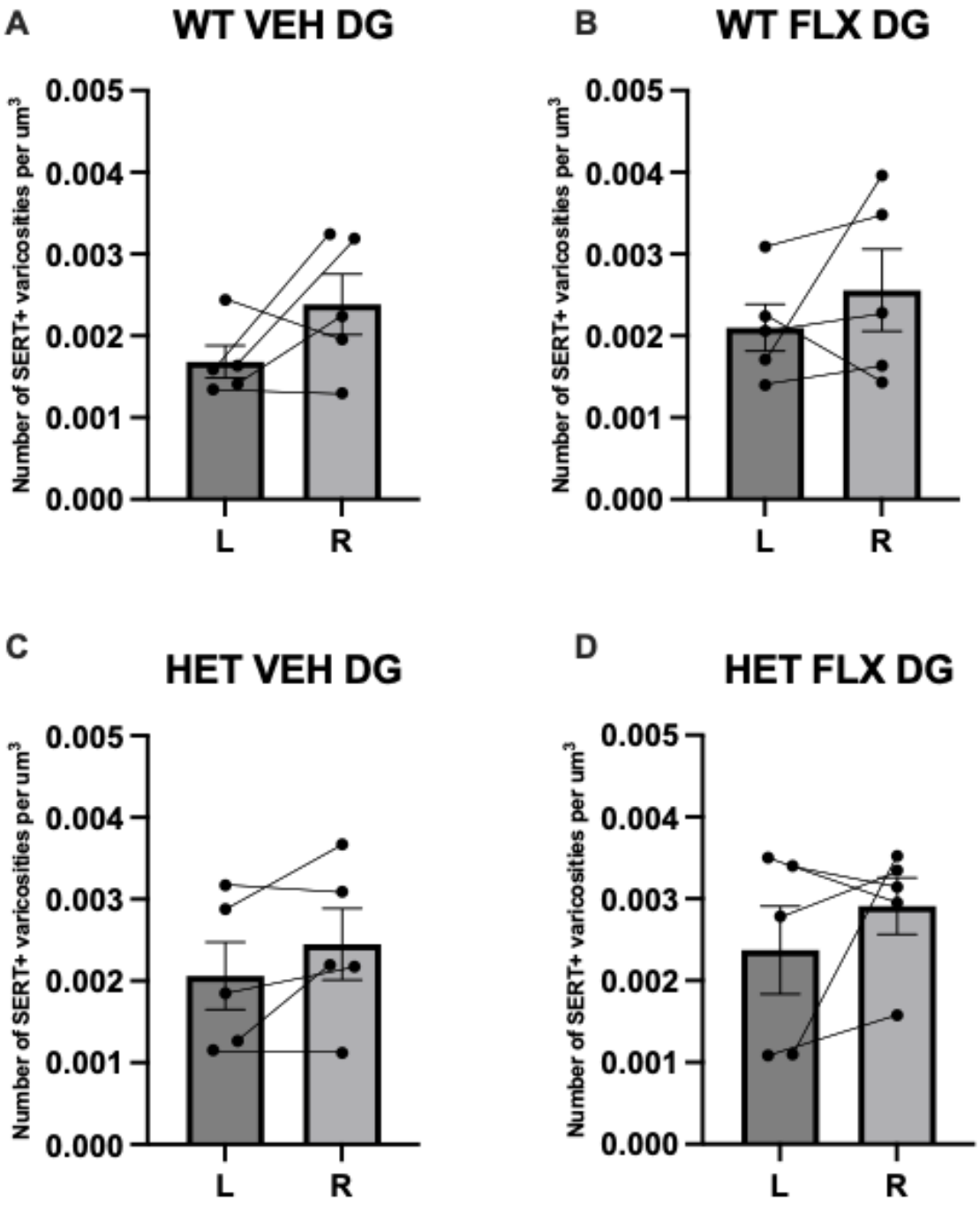

Figure S12. Density of SERT+ varicosities per µm^3 in the dentate gyrus (DG) of stroke mice. Left vs right sides of the brains are compared in the 4 groups: A) wildtype mice given vehicle treatment, B) wildtype mice given FLX treatment, C) heterozygous mice given vehicle treatment and D) heterozygous mice given FLX treatment. Paired t-tests, with mean ± SEM.

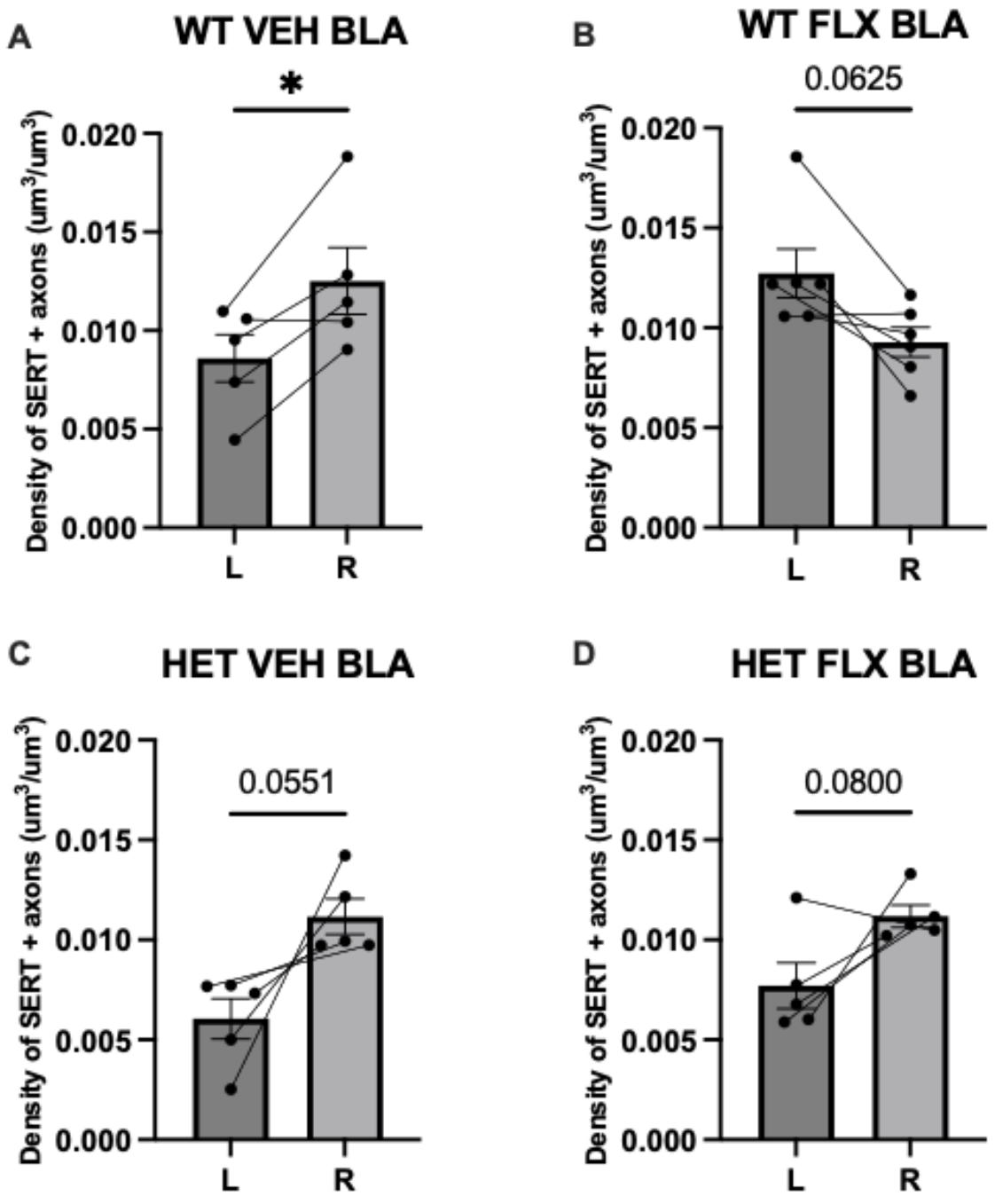

Figure S13. SERT + axonal density in the basolateral amygdala (BLA) of stroke mice. Left vs right sides of the brains are compared in the 4 groups: A) wildtype mice given vehicle treatment, B) wildtype mice given FLX treatment, C) heterozygous mice given vehicle treatment and D) heterozygous mice given FLX treatment. Paired t-tests (A, C, D) and Wilcoxon test (B), with mean ± SEM. *$p < 0.05$.

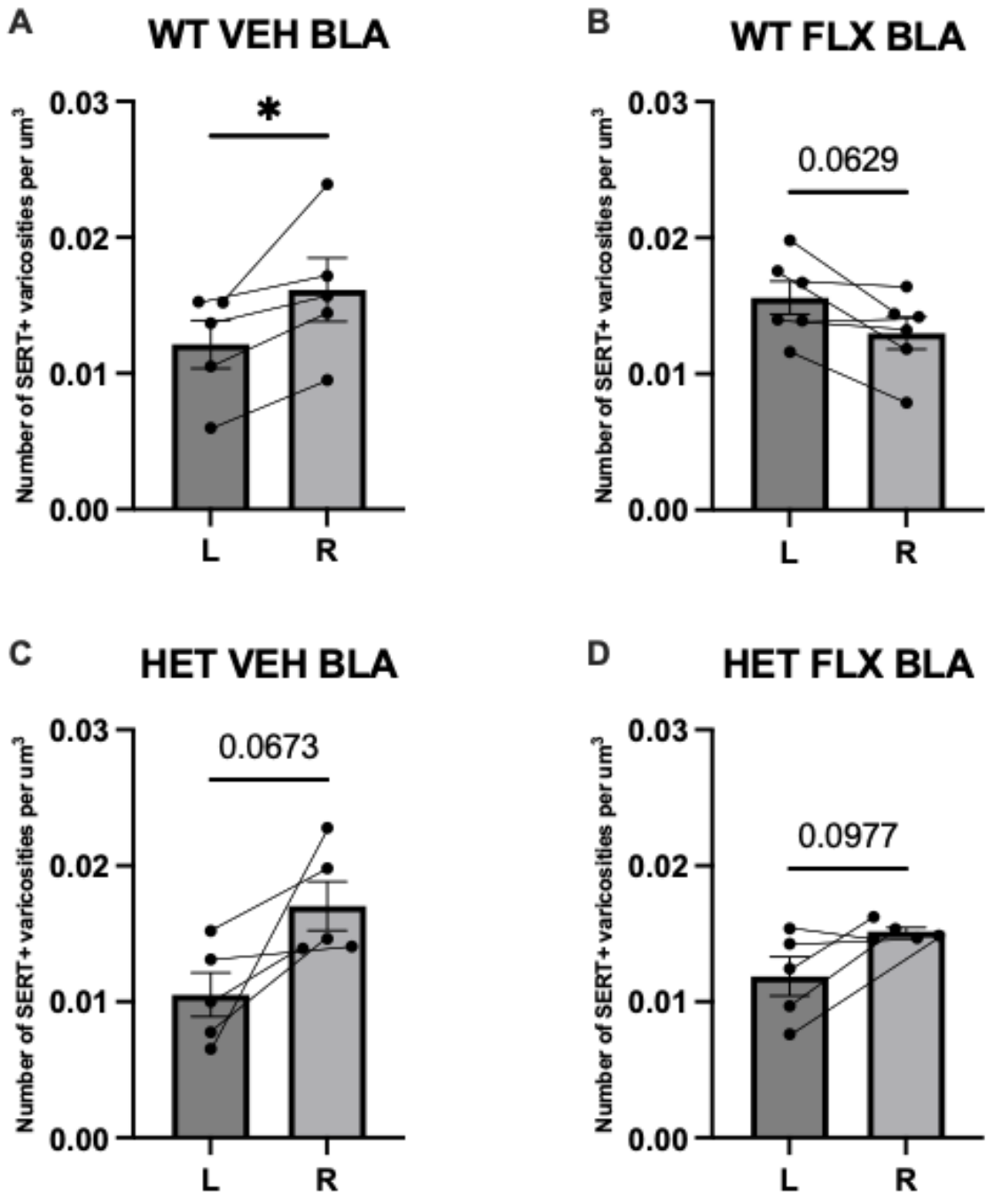

Figure S14. Density of SERT+ varicosities per µm³ in the basolateral amygdala (BLA) of stroke mice. Left vs right sides of the brains are compared in the 4 groups: A) wildtype mice given vehicle treatment, B) wildtype mice given FLX treatment, C) heterozygous mice given vehicle treatment and D) heterozygous mice given FLX treatment. Paired t-tests, with mean ± SEM. *$p < 0.05$.

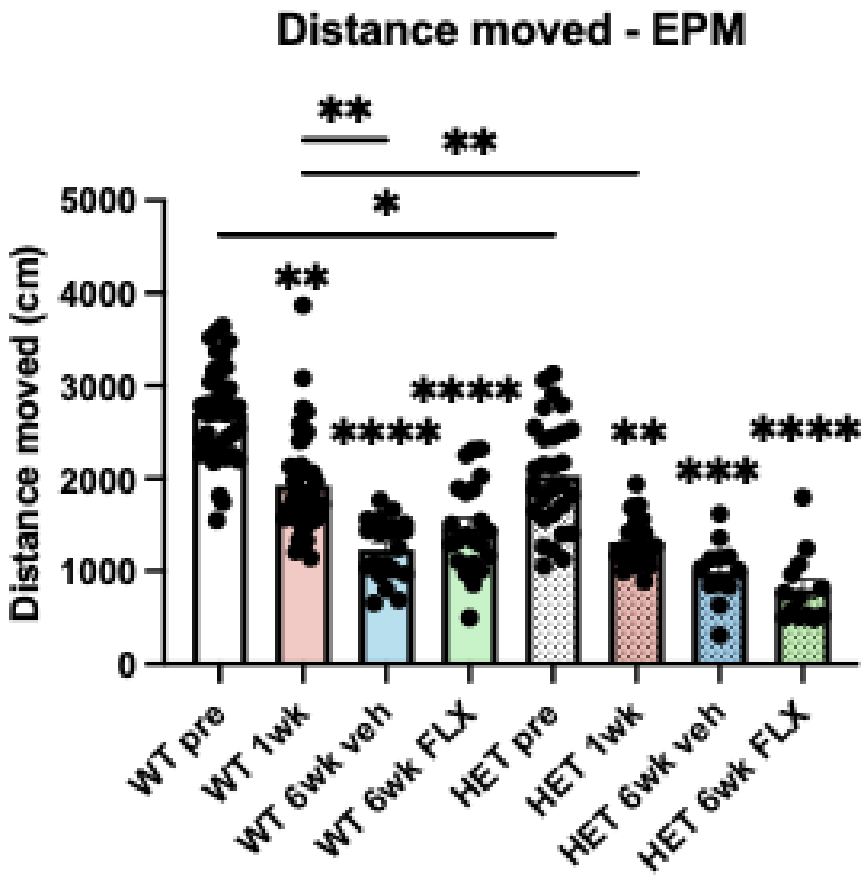

Figure S15. Distance moved in the elevated plus maze test. Distance moved measured in cm, recorded from the centre point of the body. Wildtype (WT), heterozygous AC2 knockout (HET), pre-stroke control (pre), 1-week post-stroke (1wk), 6-weeks post-stroke vehicle (veh) and fluoxetine (FLX) treated mice are shown. Data analyzed using Kruskal Wallis test with Dunn's multiple comparison test. Significance floating above bars represents comparison to respective control groups (WT pre, HET pre), and additional significant bars are as shown. Data expressed as mean ± SEM. *$p < 0.05$, **$p<0.01$, ****$p < 0.0001$.

References

Abelaira, H. M., Réus, G. Z., Petronilho, F., Barichello, T., & Quevedo, J. (2014). Neuroimmunomodulation in Depression: A Review of Inflammatory Cytokines Involved in this Process. *Neurochemical Research*, *39*(9), 1634–1639. https://doi.org/10.1007/s11064-014-1372-5

Aitken, A. R., & Törk, I. (1988). Early development of serotonin-containing neurons and pathways as seen in wholemount preparations of the fetal rat brain. *Journal of Comparative Neurology*, *274*(1), 32–47. https://doi.org/10.1002/cne.902740105

Albert, P. R., Benkelfat, C., & Descarries, L. (2012). The neurobiology of depression—Revisiting the serotonin hypothesis. I. Cellular and molecular mechanisms. *Philosophical Transactions of the Royal Society B: Biological Sciences*, *367*(1601), 2378–2381. https://doi.org/10.1098/rstb.2012.0190

Albert, P. R., & Lemonde, S. (2004). 5-HT1A receptors, gene repression, and depression: Guilt by association. *The Neuroscientist: A Review Journal Bringing Neurobiology, Neurology and Psychiatry*, *10*(6), 575–593. https://doi.org/10.1177/1073858404267382

Allida, S., Cox, K. L., Hsieh, C., Lang, H., House, A., & Hackett, M. L. (2020). Pharmacological, psychological, and non-invasive brain stimulation interventions for treating depression after stroke. *The Cochrane Database of Systematic Reviews*, *2020*(1), CD003437. https://doi.org/10.1002/14651858.CD003437.pub4

American Psychiatric Association. (2013). *Diagnostic and statistical manual of mental disorders: DSM-5* (Fifth edition.). American Psychiatric Association.

Andersen, K. K., Olsen, T. S., Dehlendorff, C., & Kammersgaard, L. P. (2009). Hemorrhagic and Ischemic Strokes Compared. *Stroke*, *40*(6), 2068–2072. https://doi.org/10.1161/STROKEAHA.108.540112

Anitha, A., Thanseem, I., Nakamura, K., Yamada, K., Iwayama, Y., Toyota, T., Iwata, Y., Suzuki, K., Sugiyama, T., Tsujii, M., Yoshikawa, T., & Mori, N. (2013). Protocadherin α (PCDHA) as a novel susceptibility gene for autism. *Journal of Psychiatry & Neuroscience: JPN*, *38*(3), 192–198. https://doi.org/10.1503/jpn.120058

Anrather, J., & Iadecola, C. (2016). Inflammation and Stroke: An Overview. *Neurotherapeutics*, *13*(4), 661–670. https://doi.org/10.1007/s13311-016-0483-x

Aström, M., Adolfsson, R., & Asplund, K. (1993). Major depression in stroke patients. A 3-year longitudinal study. *Stroke*, *24*(7), 976–982. https://doi.org/10.1161/01.str.24.7.976

Ayerbe, L., Ayis, S., Wolfe, C. D. A., & Rudd, A. G. (2013). Natural history, predictors and outcomes of depression after stroke: Systematic review and meta-analysis. *The British Journal of*

Psychiatry: The Journal of Mental Science, *202*(1), 14–21. https://doi.org/10.1192/bjp.bp.111.107664

Azmitia, E. C., Dolan, K., & Whitaker-Azmitia, P. M. (1990). S-100B but not NGF, EGF, insulin or calmodulin is a CNS serotonergic growth factor. *Brain Research*, *516*(2), 354–356. https://doi.org/10.1016/0006-8993(90)90942-5

Babkair, L. A., Chyun, D., Dickson, V. V., & Almekhlafi, M. A. (2022). The Effect of Psychosocial Factors and Functional Independence on Poststroke Depressive Symptoms: A Cross-Sectional Study. *Journal of Nursing Research*, *30*(1), e189. https://doi.org/10.1097/JNR.0000000000000464

Bagri, A., Marín, O., Plump, A. S., Mak, J., Pleasure, S. J., Rubenstein, J. L. R., & Tessier-Lavigne, M. (2002). Slit proteins prevent midline crossing and determine the dorsoventral position of major axonal pathways in the mammalian forebrain. *Neuron*, *33*(2), 233–248. https://doi.org/10.1016/s0896-6273(02)00561-5

Barker-Collo, S. L. (2007). Depression and anxiety 3 months post stroke: Prevalence and correlates. *Archives of Clinical Neuropsychology*, *22*(4), 519–531. https://doi.org/10.1016/j.acn.2007.03.002

Barnes, N. M., Ahern, G. P., Becamel, C., Bockaert, J., Camilleri, M., Chaumont-Dubel, S., Claeysen, S., Cunningham, K. A., Fone, K. C., Gershon, M., Di Giovanni, G., Goodfellow, N. M., Halberstadt, A. L., Hartley, R. M., Hassaine, G., Herrick-Davis, K., Hovius, R., Lacivita, E., Lambe, E. K., … Hoyer, D. (2021). International Union of Basic and Clinical Pharmacology. CX. Classification of Receptors for 5-hydroxytryptamine; Pharmacology and Function. *Pharmacological Reviews*, *73*(1), 310–520. https://doi.org/10.1124/pr.118.015552

Baumgarten, H. G., Klemm, H. P., Sievers, J., & Schlossberger, H. G. (1982). Dihydroxytryptamines as tools to study the neurobiology of serotonin. *Brain Research Bulletin*, *9*(1), 131–150. https://doi.org/10.1016/0361-9230(82)90128-9

Baumgarten, H. G., & Lachenmayer, L. (1972). 5,7-Dihydroxytryptamine: Improvement in chemical lesioning of indoleamine neurons in the mammalian brain. *Zeitschrift Für Zellforschung Und Mikroskopische Anatomie*, *135*(3), 399–414. https://doi.org/10.1007/BF00307184

Berk, M., Köhler-Forsberg, O., Turner, M., Penninx, B. W. J. H., Wrobel, A., Firth, J., Loughman, A., Reavley, N. J., McGrath, J. J., Momen, N. C., Plana-Ripoll, O., O'Neil, A., Siskind, D., Williams, L. J., Carvalho, A. F., Schmaal, L., Walker, A. J., Dean, O., Walder, K., … Marx, W. (2023). Comorbidity between major depressive disorder and physical diseases: A comprehensive review of epidemiology, mechanisms and management. *World Psychiatry*, *22*(3), 366–387. https://doi.org/10.1002/wps.21110

Björklund, A., Nobin, A., & Stenevi, U. (1973). Regeneration of central serotonin neurons after axonal degeneration induced by 5, 6-dihydroxytrptamine. *Brain Research*, *50*(1), 214–220. https://doi.org/10.1016/0006-8993(73)90611-2

Boehme, A. K., Esenwa, C., & Elkind, M. S. V. (2017). Stroke Risk Factors, Genetics, and Prevention. *Circulation Research*, *120*(3), 472–495. https://doi.org/10.1161/CIRCRESAHA.116.308398

Bos, M. J., Koudstaal, P. J., Hofman, A., & Breteler, M. M. B. (2007). Decreased glomerular filtration rate is a risk factor for hemorrhagic but not for ischemic stroke: The Rotterdam Study. *Stroke*, *38*(12), 3127–3132. https://doi.org/10.1161/STROKEAHA.107.489807

Bremshey, S., Groß, J., Renken, K., & Masseck, O. A. (2024). The role of serotonin in depression—A historical roundup and future directions. *Journal of Neurochemistry*, *168*(9), 1751–1779. https://doi.org/10.1111/jnc.16097

Broomfield, N. M., Laidlaw, K., Hickabottom, E., Murray, M. F., Pendrey, R., Whittick, J. E., & Gillespie, D. C. (2011). Post-stroke depression: The case for augmented, individually tailored cognitive behavioural therapy. *Clinical Psychology & Psychotherapy*, *18*(3), 202–217. https://doi.org/10.1002/cpp.711

Brunoni, A. R., Baeken, C., Machado-Vieira, R., Gattaz, W. F., & Vanderhasselt, M.-A. (2014). BDNF blood levels after electroconvulsive therapy in patients with mood disorders: A systematic review and meta-analysis. *The World Journal of Biological Psychiatry: The Official Journal of the World Federation of Societies of Biological Psychiatry*, *15*(5), 411–418. https://doi.org/10.3109/15622975.2014.892633

Carmichael, S. T. (2005). Rodent Models of Focal Stroke: Size, Mechanism, and Purpose. *NeuroRx*, *2*(3), 396–409.

Chang, H., Hoshina, N., Zhang, C., Ma, Y., Cao, H., Wang, Y., Wu, D., Bergen, S. E., Landén, M., Hultman, C. M., Preisig, M., Kutalik, Z., Castelao, E., Grigoroiu-Serbanescu, M., Forstner, A. J., Strohmaier, J., Hecker, J., Schulze, T. G., Müller-Myhsok, B., … Li, M. (2018). The protocadherin 17 gene affects cognition, personality, amygdala structure and function, synapse development and risk of major mood disorders. *Molecular Psychiatry*, *23*(2), 400–412. https://doi.org/10.1038/mp.2016.231

Chen, W. V., & Maniatis, T. (2013). Clustered protocadherins. *Development (Cambridge, England)*, *140*(16), 3297. https://doi.org/10.1242/dev.090621

Chen, W. V., Nwakeze, C. L., Denny, C. A., O'Keeffe, S., Rieger, M. A., Mountoufaris, G., Kirner, A., Dougherty, J. D., Hen, R., Wu, Q., & Maniatis, T. (2017). Pcdhαc2 is required for axonal tiling and assembly of serotonergic circuitries in mice. *Science (New York, N.Y.)*, *356*(6336), 406–411. https://doi.org/10.1126/science.aal3231

Chiu, D., Peterson, L., Elkind, M. S. V., Rosand, J., Gerber, L. M., & Silverstein, M. D. (2010). Comparison of Outcomes after Intracerebral Hemorrhage and Ischemic Stroke. *Journal of Stroke and Cerebrovascular Diseases*, *19*(3), 225–229. https://doi.org/10.1016/j.jstrokecerebrovasdis.2009.06.002

Chollet, F., Tardy, J., Albucher, J.-F., Thalamas, C., Berard, E., Lamy, C., Bejot, Y., Deltour, S., Jaillard, A., Niclot, P., Guillon, B., Moulin, T., Marque, P., Pariente, J., Arnaud, C., & Loubinoux, I. (2011). Fluoxetine for motor recovery after acute ischaemic stroke (FLAME): A randomised placebo-controlled trial. *The Lancet Neurology*, *10*(2), 123–130. https://doi.org/10.1016/S1474-4422(10)70314-8

Cipriani, A., Furukawa, T. A., Salanti, G., Chaimani, A., Atkinson, L. Z., Ogawa, Y., Leucht, S., Ruhe, H. G., Turner, E. H., Higgins, J. P. T., Egger, M., Takeshima, N., Hayasaka, Y., Imai, H., Shinohara, K., Tajika, A., Ioannidis, J. P. A., & Geddes, J. R. (2018). Comparative efficacy and acceptability of 21 antidepressant drugs for the acute treatment of adults with major depressive disorder: A systematic review and network meta-analysis. *Lancet (London, England)*, *391*(10128), 1357–1366. https://doi.org/10.1016/S0140-6736(17)32802-7

Cipriani, A., Zhou, X., Giovane, C. D., Hetrick, S. E., Qin, B., Whittington, C., Coghill, D., Zhang, Y., Hazell, P., Leucht, S., Cuijpers, P., Pu, J., Cohen, D., Ravindran, A. V., Liu, Y., Michael, K. D., Yang, L., Liu, L., & Xie, P. (2016). Comparative efficacy and tolerability of antidepressants for major depressive disorder in children and adolescents: A network meta-analysis. *The Lancet*, *388*(10047), 881–890. https://doi.org/10.1016/S0140-6736(16)30385-3

Crowe, C., Coen, R. F., Kidd, N., Hevey, D., Cooney, J., & Harbison, J. (2016). A qualitative study of the experience of psychological distress post-stroke. *Journal of Health Psychology*, *21*(11), 2572–2579. https://doi.org/10.1177/1359105315581067

Cruz, S. A., Qin, Z., Ricke, K. M., Stewart, A. F. R., & Chen, H.-H. (2020). Neuronal protein-tyrosine phosphatase 1B hinders sensory-motor functional recovery and causes affective disorders in two different focal ischemic stroke models. *Neural Regeneration Research*, *16*(1), 129–136. https://doi.org/10.4103/1673-5374.286970

Cuijpers, P., Driessen, E., Hollon, S. D., van Oppen, P., Barth, J., & Andersson, G. (2012). The efficacy of non-directive supportive therapy for adult depression: A meta-analysis. *Clinical Psychology Review*, *32*(4), 280–291. https://doi.org/10.1016/j.cpr.2012.01.003

Cuijpers, P., Karyotaki, E., Ciharova, M., Miguel, C., Noma, H., & Furukawa, T. A. (2021). The effects of psychotherapies for depression on response, remission, reliable change, and deterioration: A meta-analysis. *Acta Psychiatrica Scandinavica*, *144*(3), 288–299. https://doi.org/10.1111/acps.13335

Cuijpers, P., Noma, H., Karyotaki, E., Vinkers, C. H., Cipriani, A., & Furukawa, T. A. (2020). A network meta-analysis of the effects of psychotherapies, pharmacotherapies and their

combination in the treatment of adult depression. *World Psychiatry*, *19*(1), 92–107. https://doi.org/10.1002/wps.20701

Dahlström, A., & Fuxe, K. (1964). Localization of monoamines in the lower brain stem. *Experientia*, *20*(7), 398–399. https://doi.org/10.1007/BF02147990

David, A., & Pierre, L. (2006). Hippocampal Neuroanatomy. In P. Andersen, R. Morris, D. Amaral, T. Bliss, & J. O'Keefe (Eds.), *The Hippocampus Book* (pp. 37–114). Oxford University Press. https://doi.org/10.1093/acprof:oso/9780195100273.003.0003

Deneris, E., & Gaspar, P. (2018). Serotonin neuron development: Shaping molecular and structural identities. *WIREs Developmental Biology*, *7*(1), e301. https://doi.org/10.1002/wdev.301

Deng, L., Sun, X., Qiu, S., Xiong, Y., Li, Y., Wang, L., Wei, Q., Wang, D., & Liu, M. (2017). Interventions for management of post-stroke depression: A Bayesian network meta-analysis of 23 randomized controlled trials. *Scientific Reports*, *7*(1), 16466. https://doi.org/10.1038/s41598-017-16663-0

Dindo, L., Van Liew, J. R., & Arch, J. J. (2017). Acceptance and Commitment Therapy: A Transdiagnostic Behavioral Intervention for Mental Health and Medical Conditions. *Neurotherapeutics*, *14*(3), 546–553. https://doi.org/10.1007/s13311-017-0521-3

Donovan, L. J., Spencer, W. C., Kitt, M. M., Eastman, B. A., Lobur, K. J., Jiao, K., Silver, J., & Deneris, E. S. (2019). Lmx1b is required at multiple stages to build expansive serotonergic axon architectures. *eLife*, *8*, e48788. https://doi.org/10.7554/eLife.48788

Donovan, S. L., Mamounas, L. A., Andrews, A. M., Blue, M. E., & McCasland, J. S. (2002). GAP-43 Is Critical for Normal Development of the Serotonergic Innervation in Forebrain. *The Journal of Neuroscience*, *22*(9), 3543–3552. https://doi.org/10.1523/JNEUROSCI.22-09-03543.2002

Douven, E., Köhler, S., Rodriguez, M. M. F., Staals, J., Verhey, F. R. J., & Aalten, P. (2017). Imaging Markers of Post-Stroke Depression and Apathy: A Systematic Review and Meta-Analysis. *Neuropsychology Review*, *27*(3), 202–219. https://doi.org/10.1007/s11065-017-9356-2

Elendu, C., Amaechi, D. C., Elendu, T. C., Ibhiedu, J. O., Egbunu, E. O., Ndam, A. R., Ogala, F., Ologunde, T., Peterson, J. C., Boluwatife, A. I., Okongko, A. O., Fatoye, J. O., Akpovona, O. L., Onyekweli, S. O., Temitope, A. Y., Achimugu, A. O., & Temilade, A. V. (2023). Stroke and cognitive impairment: Understanding the connection and managing symptoms. *Annals of Medicine and Surgery*, *85*(12), 6057–6066. https://doi.org/10.1097/MS9.0000000000001441

Fawcett, J. W. (2020). The Struggle to Make CNS Axons Regenerate: Why Has It Been so Difficult? *Neurochemical Research*, *45*(1), 144–158. https://doi.org/10.1007/s11064-019-02844-y

Feigin, V. L., Brainin, M., Norrving, B., Martins, S., Sacco, R. L., Hacke, W., Fisher, M., Pandian, J., & Lindsay, P. (2022). World Stroke Organization (WSO): Global Stroke Fact Sheet 2022. *International Journal of Stroke*, *17*(1), 18–29. https://doi.org/10.1177/17474930211065917

Feng, X., Ma, X., Li, J., Zhou, Q., Liu, Y., Song, J., Liu, J., Situ, Q., Wang, L., Zhang, J., & Lin, F. (2024). Inflammatory Pathogenesis of Post-stroke Depression. *Aging and Disease*, *16*(1), 209–238. https://doi.org/10.14336/AD.2024.0203

Fenstermaker, A. G., Prasad, A. A., Bechara, A., Adolfs, Y., Tissir, F., Goffinet, A., Zou, Y., & Pasterkamp, R. J. (2010). Wnt/Planar Cell Polarity Signaling Controls the Anterior–Posterior Organization of Monoaminergic Axons in the Brainstem. *The Journal of Neuroscience*, *30*(47), 16053–16064. https://doi.org/10.1523/JNEUROSCI.4508-10.2010

Fernandez, S. P., Cauli, B., Cabezas, C., Muzerelle, A., Poncer, J.-C., & Gaspar, P. (2016). Multiscale single-cell analysis reveals unique phenotypes of raphe 5-HT neurons projecting to the forebrain. *Brain Structure and Function*, *221*(8), 4007–4025. https://doi.org/10.1007/s00429-015-1142-4

Flaherty, E., & Maniatis, T. (2020). The role of clustered protocadherins in neurodevelopment and neuropsychiatric diseases. *Current Opinion in Genetics & Development*, *65*, 144–150. https://doi.org/10.1016/j.gde.2020.05.041

Fournet, V., Jany, M., Fabre, V., Chali, F., Orsal, D., Schweitzer, A., Andrieux, A., Messanvi, F., Giros, B., Hamon, M., Lanfumey, L., Deloulme, J.-C., & Martres, M.-P. (2010). The deletion of the microtubule-associated STOP protein affects the serotonergic mouse brain network. *Journal of Neurochemistry*, *115*(6), 1579–1594. https://doi.org/10.1111/j.1471-4159.2010.07064.x

Frankfurt, M., & Azmitia, E. (1984). Regeneration of serotonergic fibers in the rat hypothalamus following unilateral 5,7-dihydroxytryptamine injection. *Brain Research*, *298*(2), 273–282. https://doi.org/10.1016/0006-8993(84)91426-4

Freis, E. D. (1954). Mental depression in hypertensive patients treated for long periods with large doses of reserpine. *The New England Journal of Medicine*, *251*(25), 1006–1008. https://doi.org/10.1056/NEJM195412162512504

Fuxe, K., Cintra, A., Andbjer, B., Anggård, E., Goldstein, M., & Agnati, L. F. (1989). Centrally administered endothelin-1 produces lesions in the brain of the male rat. *Acta Physiologica Scandinavica*, *137*(1), 155–156. https://doi.org/10.1111/j.1748-1716.1989.tb08734.x

Gagnon, D., & Parent, M. (2014). Distribution of VGLUT3 in Highly Collateralized Axons from the Rat Dorsal Raphe Nucleus as Revealed by Single-Neuron Reconstructions. *PLOS ONE*, *9*(2), e87709. https://doi.org/10.1371/journal.pone.0087709

Global Burden of Disease Collaborative Network. Global Burden of Disease Study 2021 (GBD 2021). Seattle, United States: Institute for Health Metrics and Evaluation (IHME), 2024.

Goodwin, G. M., Aaronson, S. T., Alvarez, O., Arden, P. C., Baker, A., Bennett, J. C., Bird, C., Blom, R. E., Brennan, C., Brusch, D., Burke, L., Campbell-Coker, K., Carhart-Harris, R., Cattell, J., Daniel, A., DeBattista, C., Dunlop, B. W., Eisen, K., Feifel, D., … Malievskaia, E. (2022). Single-Dose Psilocybin for a Treatment-Resistant Episode of Major Depression. *New England Journal of Medicine*, *387*(18), 1637–1648. https://doi.org/10.1056/NEJMoa2206443

Grajny, K., Pyata, H., Spiegel, K., Lacey, E. H., Xing, S., Brophy, C., & Turkeltaub, P. E. (2016). Depression Symptoms in Chronic Left Hemisphere Stroke Are Related to Dorsolateral Prefrontal Cortex Damage. *The Journal of Neuropsychiatry and Clinical Neurosciences*, *28*(4), 292–298. https://doi.org/10.1176/appi.neuropsych.16010004

Gray, N. A., Milak, M. S., DeLorenzo, C., Ogden, R. T., Huang, Y., Mann, J. J., & Parsey, R. V. (2013). Antidepressant Treatment Reduces Serotonin-1A Autoreceptor Binding in Major Depressive Disorder. *Biological Psychiatry*, *74*(1), 26–31. https://doi.org/10.1016/j.biopsych.2012.11.012

Grueber, W. B., & Sagasti, A. (2010). Self-avoidance and Tiling: Mechanisms of Dendrite and Axon Spacing. *Cold Spring Harbor Perspectives in Biology*, *2*(9), a001750. https://doi.org/10.1101/cshperspect.a001750

Gutiérrez-Rojas, L., Porras-Segovia, A., Dunne, H., Andrade-González, N., & Cervilla, J. A. (2020). Prevalence and correlates of major depressive disorder: A systematic review. *Brazilian Journal of Psychiatry*, *42*(6), 657. https://doi.org/10.1590/1516-4446-2019-0650

Hackett, M. L., & Pickles, K. (2014). Part I: Frequency of Depression after Stroke: An Updated Systematic Review and Meta-Analysis of Observational Studies. *International Journal of Stroke*, *9*(8), 1017–1025. https://doi.org/10.1111/ijs.12357

Hatcher, M. A., & Starr, J. A. (2011). Role of tissue plasminogen activator in acute ischemic stroke. *The Annals of Pharmacotherapy*, *45*(3), 364–371. https://doi.org/10.1345/aph.1P525

Hayley, S., Hakim, A., & Albert, P. (2020). Depression, Dementia and Immune Dysregulation. *Brain*, *144*. https://doi.org/10.1093/brain/awaa405

He, Q., Wang, W., Zhang, Y., Xiong, Y., Tao, C., Ma, L., Ma, J., You, C., & Wang, C. (2024). Global, Regional, and National Burden of Stroke, 1990–2021: A Systematic Analysis for Global Burden of Disease 2021. *Stroke*, *55*(12), 2815–2824. https://doi.org/10.1161/STROKEAHA.124.048033

Health Quality Ontario. (2017). Psychotherapy for Major Depressive Disorder and Generalized Anxiety Disorder: A Health Technology Assessment. *Ontario Health Technology Assessment Series*, *17*(15), 1–167.

Hillhouse, T. M., & Porter, J. H. (2015). A brief history of the development of antidepressant drugs: From monoamines to glutamate. *Experimental and Clinical Psychopharmacology*, *23*(1), 1–21. https://doi.org/10.1037/a0038550

Hirabayashi, T., & Yagi, T. (2014). Protocadherins in Neurological Diseases. In *Cell Adhesion Molecules* (pp. 293–314). Springer, New York, NY. https://doi.org/10.1007/978-1-4614-8090-7_13

Jin, H.-J., Pei, L., Li, Y.-N., Zheng, H., Yang, S., Wan, Y., Mao, L., Xia, Y.-P., He, Q.-W., Li, M., Yue, Z.-Y., & Hu, B. (2017). Alleviative effects of fluoxetine on depressive-like behaviors by epigenetic regulation of BDNF gene transcription in mouse model of post-stroke depression. *Scientific Reports*, *7*(1), 14926. https://doi.org/10.1038/s41598-017-13929-5

Jin, Y., Dougherty, S. E., Wood, K., Sun, L., Cudmore, R. H., Abdalla, A., Kannan, G., Pletnikov, M., Hashemi, P., & Linden, D. J. (2016). Regrowth of Serotonin Axons in the Adult Mouse Brain Following Injury. *Neuron*, *91*(4), 748–762. https://doi.org/10.1016/j.neuron.2016.07.024

Jog, M. A., Anderson, C., Kubicki, A., Boucher, M., Leaver, A., Hellemann, G., Iacoboni, M., Woods, R., & Narr, K. (2023). Transcranial direct current stimulation (tDCS) in depression induces structural plasticity. *Scientific Reports*, *13*(1), 2841. https://doi.org/10.1038/s41598-023-29792-6

Kajstura, T. J., Dougherty, S. E., & Linden, D. J. (2018). Serotonin axons in the neocortex of the adult female mouse regrow after traumatic brain injury. *Journal of Neuroscience Research*, *96*(4), 512–526. https://doi.org/10.1002/jnr.24059

Karrouri, R., Hammani, Z., Benjelloun, R., & Otheman, Y. (2021). Major depressive disorder: Validated treatments and future challenges. *World Journal of Clinical Cases*, *9*(31), 9350–9367. https://doi.org/10.12998/wjcc.v9.i31.9350

Katori, S., Noguchi-Katori, Y., Okayama, A., Kawamura, Y., Luo, W., Sakimura, K., Hirabayashi, T., Iwasato, T., & Yagi, T. (2017). Protocadherin-αC2 is required for diffuse projections of serotonergic axons. *Scientific Reports*, *7*(1), 15908. https://doi.org/10.1038/s41598-017-16120-y

Kawczak, P., Feszak, I., & Bączek, T. (2024). Ketamine, Esketamine, and Arketamine: Their Mechanisms of Action and Applications in the Treatment of Depression and Alleviation of Depressive Symptoms. *Biomedicines*, *12*(10), 2283. https://doi.org/10.3390/biomedicines12102283

Khedr, E. M., Abdelrahman, A. A., Desoky, T., Zaki, A. F., & Gamea, A. (2020). Post-stroke depression: Frequency, risk factors, and impact on quality of life among 103 stroke patients—hospital-based study. *The Egyptian Journal of Neurology, Psychiatry and Neurosurgery*, *56*(1), 66. https://doi.org/10.1186/s41983-020-00199-8

Kim, J.-M., Kang, H.-J., Kim, J.-W., Bae, K.-Y., Kim, S.-W., Kim, J.-T., Park, M.-S., & Cho, K.-H. (2017). Associations of Tumor Necrosis Factor-α and Interleukin-1β Levels and Polymorphisms with Post-Stroke Depression. *The American Journal of Geriatric Psychiatry: Official Journal of the American Association for Geriatric Psychiatry*, *25*(12), 1300–1308. https://doi.org/10.1016/j.jagp.2017.07.012

Kim, S.-Y., Yasuda, S., Tanaka, H., Yamagata, K., & Kim, H. (2011). Non-clustered protocadherin. *Cell Adhesion & Migration*, *5*(2), 97–105. https://doi.org/10.4161/cam.5.2.14374

Kiyasova, V., Fernandez, S. P., Laine, J., Stankovski, L., Muzerelle, A., Doly, S., & Gaspar, P. (2011). A Genetically Defined Morphologically and Functionally Unique Subset of 5-HT Neurons in the Mouse Raphe Nuclei. *The Journal of Neuroscience*, *31*(8), 2756–2768. https://doi.org/10.1523/JNEUROSCI.4080-10.2011

Kiyasova, V., & Gaspar, P. (2011). Development of raphe serotonin neurons from specification to guidance. *European Journal of Neuroscience*, *34*(10), 1553–1562. https://doi.org/10.1111/j.1460-9568.2011.07910.x

Klein, J., Winter, C., Coquery, N., Heinz, A., Morgenstern, R., Kupsch, A., & Juckel, G. (2010). Lesion of the medial prefrontal cortex and the subthalamic nucleus selectively affect depression-like behavior in rats. *Behavioural Brain Research*, *213*(1), 73–81. https://doi.org/10.1016/j.bbr.2010.04.036

Klingbeil, J., Brandt, M.-L., Wawrzyniak, M., Stockert, A., Schneider, H. R., Baum, P., Hoffmann, K.-T., & Saur, D. (2022). Association of Lesion Location and Depressive Symptoms Poststroke. *Stroke*, *53*(11), e467–e471. https://doi.org/10.1161/STROKEAHA.122.039068

Koning, H., Sayers, I., Stewart, C. E., de Jong, D., Ten Hacken, N. H. T., Postma, D. S., van Oosterhout, A. J. M., Nawijn, M. C., & Koppelman, G. H. (2012). Characterization of protocadherin-1 expression in primary bronchial epithelial cells: Association with epithelial cell differentiation. *FASEB Journal: Official Publication of the Federation of American Societies for Experimental Biology*, *26*(1), 439–448. https://doi.org/10.1096/fj.11-185207

Koo, J. W., & Duman, R. S. (2008). IL-1β is an essential mediator of the antineurogenic and anhedonic effects of stress. *Proceedings of the National Academy of Sciences of the United States of America*, *105*(2), 751–756. https://doi.org/10.1073/pnas.0708092105

Kumar, M. B., & Tjepkema, M. (2019). *Suicide among First Nations people, Métis and Inuit (2011-2016): Findings from the Canadian Census Health and Environment Cohort (CanCHEC)*. *99*.

Labat-gest, V., & Tomasi, S. (2013). Photothrombotic Ischemia: A Minimally Invasive and Reproducible Photochemical Cortical Lesion Model for Mouse Stroke Studies. *Journal of Visualized Experiments : JoVE*, *76*, 50370. https://doi.org/10.3791/50370

Laux, G. (2022). Antidepressants: Definition, Classification, Guidelines. In *NeuroPsychopharmacotherapy* (pp. 1101–1108). Springer, Cham. https://doi.org/10.1007/978-3-030-62059-2_24

Lavu, V. K., Mohamed, R. A., Huang, R., Potla, S., Bhalla, S., Al Qabandi, Y., Nandula, S. A., Boddepalli, C. S., Gutlapalli, S. D., & Mohammed, L. (2022). Evaluation and Treatment of Depression in Stroke Patients: A Systematic Review. *Cureus*, *14*(8), e28137. https://doi.org/10.7759/cureus.28137

Lefebvre, J. L., Kostadinov, D., Chen, W. V., Maniatis, T., & Sanes, J. R. (2012). PROTOCADHERINS MEDIATE DENDRITIC SELF-AVOIDANCE IN THE MAMMALIAN NERVOUS SYSTEM. *Nature*, *488*(7412), 517–521. https://doi.org/10.1038/nature11305

Legg, L. A., Tilney, R., Hsieh, C., Wu, S., Lundström, E., Rudberg, A., Kutlubaev, M. A., Dennis, M., Soleimani, B., Barugh, A., Hackett, M. L., Hankey, G. J., & Mead, G. E. (2019). Selective serotonin reuptake inhibitors (SSRIs) for stroke recovery. *The Cochrane Database of Systematic Reviews*, *2019*(11), CD009286. https://doi.org/10.1002/14651858.CD009286.pub3

Leschik, J., Gentile, A., Cicek, C., Péron, S., Tevosian, M., Beer, A., Radyushkin, K., Bludau, A., Ebner, K., Neumann, I., Singewald, N., Berninger, B., Lessmann, V., & Lutz, B. (2022). Brain-derived neurotrophic factor expression in serotonergic neurons improves stress resilience and promotes adult hippocampal neurogenesis. *Progress in Neurobiology*, *217*, 102333. https://doi.org/10.1016/j.pneurobio.2022.102333

Li, J., Yang, L., Lv, R., Kuang, J., Zhou, K., & Xu, M. (2022). Mediating effect of post-stroke depression between activities of daily living and health-related quality of life: Meta-analytic structural equation modeling. *Quality of Life Research*, *32*(2), 331–338. https://doi.org/10.1007/s11136-022-03225-9

Lidov, H. G. W., & Molliver, M. E. (1982). An immunohistochemical study of serotonin neuron development in the rat: Ascending pathways and terminal fields. *Brain Research Bulletin*, *8*(4), 389–430. https://doi.org/10.1016/0361-9230(82)90077-6

Lincoln, N. B., & Flannaghan, T. (2003). Cognitive Behavioral Psychotherapy for Depression Following Stroke. *Stroke*, *34*(1), 111–115. https://doi.org/10.1161/01.STR.0000044167.44670.55

Lincoln, N., Flannaghan, T., Sutcliffe, L., & Rother, L. (1997). Evaluation of cognitive behavioural treatment for depression after stroke: A pilot study. *Clinical Rehabilitation*, *11*(2), 114–122. https://doi.org/10.1177/026921559701100204

Liu, J. P., & Lauder, J. M. (1992). S-100β and insulin-like growth factor-II differentially regulate growth of developing serotonin and dopamine neurons in vitro. *Journal of Neuroscience Research*, *33*(2), 248–256. https://doi.org/10.1002/jnr.490330208

Liu, S., Sheng, J., Li, B., & Zhang, X. (2017). Recent Advances in Non-invasive Brain Stimulation for Major Depressive Disorder. *Frontiers in Human Neuroscience*, *11*. https://doi.org/10.3389/fnhum.2017.00526

López-Bendito, G., Flames, N., Ma, L., Fouquet, C., Di Meglio, T., Chedotal, A., Tessier-Lavigne, M., & Marín, O. (2007). Robo1 and Robo2 Cooperate to Control the Guidance of Major Axonal Tracts in the Mammalian Forebrain. *The Journal of Neuroscience*, *27*(13), 3395–3407. https://doi.org/10.1523/JNEUROSCI.4605-06.2007

Majumder, D. (2024). Ischemic Stroke: Pathophysiology and Evolving Treatment Approaches. *Neuroscience Insights*, *19*, 26331055241292600. https://doi.org/10.1177/26331055241292600

Mamounas, L. A., Altar, C. A., Blue, M. E., Kaplan, D. R., Tessarollo, L., & Lyons, W. E. (2000). BDNF Promotes the Regenerative Sprouting, But Not Survival, of Injured Serotonergic Axons in the Adult Rat Brain. *The Journal of Neuroscience*, *20*(2), 771–782. https://doi.org/10.1523/JNEUROSCI.20-02-00771.2000

Mancini, M., Bassani, S., & Passafaro, M. (2020). Right Place at the Right Time: How Changes in Protocadherins Affect Synaptic Connections Contributing to the Etiology of Neurodevelopmental Disorders. *Cells*, *9*(12). https://doi.org/10.3390/cells9122711

Mane, R., Wu, Z., & Wang, D. (2022). Poststroke motor, cognitive and speech rehabilitation with brain–computer interface: A perspective review. *Stroke and Vascular Neurology*, *7*(6), 541–549. https://doi.org/10.1136/svn-2022-001506

McCann, S. K., Irvine, C., Mead, G. E., Sena, E. S., Currie, G. L., Egan, K. E., Macleod, M. R., & Howells, D. W. (2014). Efficacy of Antidepressants in Animal Models of Ischemic Stroke. *Stroke*, *45*(10), 3055–3063. https://doi.org/10.1161/STROKEAHA.114.006304

Mead, G. E., Hsieh, C., Lee, R., Kutlubaev, M. A., Claxton, A., Hankey, G. J., & Hackett, M. L. (2012). Selective serotonin reuptake inhibitors (SSRIs) for stroke recovery. *The Cochrane Database of Systematic Reviews*, *2012*(11), CD009286. https://doi.org/10.1002/14651858.CD009286.pub2

Meader, N., Moe-Byrne, T., Llewellyn, A., & Mitchell, A. J. (2014). Screening for poststroke major depression: A meta-analysis of diagnostic validity studies. *Journal of Neurology, Neurosurgery & Psychiatry*, *85*(2), 198–206. https://doi.org/10.1136/jnnp-2012-304194

Mechawar, N., & Savitz, J. (2016). Neuropathology of mood disorders: Do we see the stigmata of inflammation? *Translational Psychiatry*, *6*(11), e946. https://doi.org/10.1038/tp.2016.212

Medeiros, G. C., Roy, D., Kontos, N., & Beach, S. R. (2020). Post-stroke depression: A 2020 updated review. *General Hospital Psychiatry*, *66*, 70–80. https://doi.org/10.1016/j.genhosppsych.2020.06.011

Meng, X., Brunet, A., Turecki, G., Liu, A., D'Arcy, C., & Caron, J. (2017). Risk factor modifications and depression incidence: A 4-year longitudinal Canadian cohort of the Montreal Catchment Area Study. *BMJ Open*, *7*(6), e015156. https://doi.org/10.1136/bmjopen-2016-015156

Meyer, J. H., Matveychuk, D., Holt, A., Santhirakumar, A., & Baker, G. B. (2022). Monoamine Oxidase Inhibitors in Depressive Disorders. In *NeuroPsychopharmacotherapy* (pp. 1347–1379). Springer, Cham. https://doi.org/10.1007/978-3-030-62059-2_98

Migliarini, S., Pacini, G., Pelosi, B., Lunardi, G., & Pasqualetti, M. (2013). Lack of brain serotonin affects postnatal development and serotonergic neuronal circuitry formation. *Molecular Psychiatry*, *18*(10), 1106–1118. https://doi.org/10.1038/mp.2012.128

Miller, A. H., & Raison, C. L. (2016). The role of inflammation in depression: From evolutionary imperative to modern treatment target. *Nature Reviews. Immunology*, *16*(1), 22–34. https://doi.org/10.1038/nri.2015.5

Modak, D., & Sotomayor, M. (2019). Identification of an adhesive interface for the non-clustered δ1 protocadherin-1 involved in respiratory diseases. *Communications Biology*, *2*(1), 1–13. https://doi.org/10.1038/s42003-019-0586-0

Molliver, M. E., Berger, U. V., Mamounas, L. A., Molliver, D. C., O'Hearn, E., & Wilson, M. A. (1990). Neurotoxicity of MDMA and Related Compounds: Anatomic Studies. *Annals of the New York Academy of Sciences*, *600*(1), 640–661. https://doi.org/10.1111/j.1749-6632.1990.tb16916.x

Munder, T., Flückiger, C., Leichsenring, F., Abbass, A. A., Hilsenroth, M. J., Luyten, P., Rabung, S., Steinert, C., & Wampold, B. E. (2018). Is psychotherapy effective? A re-analysis of treatments for depression. *Epidemiology and Psychiatric Sciences*, *28*(3), 268–274. https://doi.org/10.1017/S2045796018000355

Narushima, K., Kosier, J. T., & Robinson, R. G. (2003). A Reappraisal of Poststroke Depression, Intra- and Inter-Hemispheric Lesion Location Using Meta-Analysis. *The Journal of Neuropsychiatry and Clinical Neurosciences*, *15*(4), 422–430. https://doi.org/10.1176/jnp.15.4.422

Niu, Y., Sheng, S., Chen, Y., Ding, J., Li, H., Shi, S., Wu, J., & Ye, D. (2022). The Efficacy of Group Acceptance and Commitment Therapy for Preventing Post-Stroke Depression: A Randomized Controlled Trial. *Journal of Stroke and Cerebrovascular Diseases: The Official Journal of National Stroke Association*, *31*(2), 106225. https://doi.org/10.1016/j.jstrokecerebrovasdis.2021.106225

Northcott, S., Moss, B., Harrison, K., & Hilari, K. (2016). A systematic review of the impact of stroke on social support and social networks: Associated factors and patterns of change. *Clinical Rehabilitation*, *30*(8), 811–831. https://doi.org/10.1177/0269215515602136

Nutt, D. J., Peill, J. M., Weiss, B., Godfrey, K., Carhart-Harris, R. L., & Erritzoe, D. (2023). Psilocybin and Other Classic Psychedelics in Depression. In *Emerging Neurobiology of Antidepressant Treatments* (pp. 149–174). Springer, Cham. https://doi.org/10.1007/7854_2023_451

O'Hearn, E., Battaglia, G., De Souza, E. B., Kuhar, M. J., & Molliver, M. E. (1988). Methylenedioxyamphetamine (MDA) and methylenedioxymethamphetamine (MDMA) cause selective ablation of serotonergic axon terminals in forebrain: Immunocytochemical evidence for neurotoxicity. *The Journal of Neuroscience: The Official Journal of the Society for Neuroscience*, *8*(8), 2788–2803. https://doi.org/10.1523/JNEUROSCI.08-08-02788.1988

O'Keefe, L. M., Doran, S. J., Mwilambwe-Tshilobo, L., Conti, L. H., Venna, V. R., & McCullough, L. D. (2014). Social isolation after stroke leads to depressive-like behavior and decreased BDNF levels in mice. *Behavioural Brain Research*, *260*, 162–170. https://doi.org/10.1016/j.bbr.2013.10.047

Paolucci, S., Gandolfo, C., Provinciali, L., Torta, R., & Toso, V. (2006). The Italian multicenter observational study on post–stroke depression (DESTRO). *Journal of Neurology*, *253*(5), 556–562. https://doi.org/10.1007/s00415-006-0058-6

Parsey, R. V., Ogden, R. T., Miller, J. M., Tin, A., Hesselgrave, N., Goldstein, E., Mikhno, A., Milak, M., Zanderigo, F., Sullivan, G. M., Oquendo, M. A., & Mann, J. J. (2010). Higher Serotonin 1A Binding in a Second Major Depression Cohort: Modeling and Reference Region Considerations. *Biological Psychiatry*, *68*(2), 170–178. https://doi.org/10.1016/j.biopsych.2010.03.023

Parsey, R. V., Oquendo, M. A., Ogden, R. T., Olvet, D. M., Simpson, N., Huang, Y.-Y., Van Heertum, R. L., Arango, V., & Mann, J. J. (2006). Altered serotonin 1A binding in major depression: A [carbonyl-C-11]WAY100635 positron emission tomography study. *Biological Psychiatry*, *59*(2), 106–113. https://doi.org/10.1016/j.biopsych.2005.06.016

Pelosof, R., Santos, L. A. D., Farhat, L. C., Gattaz, W. F., Talib, L., & Brunoni, A. R. (2023). BDNF blood levels after electroconvulsive therapy in patients with mood disorders: An updated systematic review and meta-analysis. *The World Journal of Biological Psychiatry: The Official Journal of the World Federation of Societies of Biological Psychiatry*, *24*(1), 24–33. https://doi.org/10.1080/15622975.2022.2058083

Qin, B., Chen, H., Gao, W., Zhao, L. B., Zhao, M. J., Qin, H. X., Chen, W., Chen, L., & Yang, M. X. (2018). Efficacy, acceptability, and tolerability of antidepressant treatments for patients with post-stroke depression: A network meta-analysis. *Brazilian Journal of Medical and Biological Research = Revista Brasileira De Pesquisas Medicas E Biologicas*, *51*(7), e7218. https://doi.org/10.1590/1414-431x20187218

Rajkowska, G., Mahajan, G., Legutko, B., Challagundla, L., Griswold, M., Albert, P. R., Daigle, M., Miguel-Hidalgo, J. J., Austin, M. C., Blakely, R. D., Steffens, D. C., & Stockmeier, C. A. (2017). Length of axons expressing the serotonin transporter in orbitofrontal cortex is lower with age in depression. *Neuroscience*, *359*, 30–39. https://doi.org/10.1016/j.neuroscience.2017.07.006

Rasmussen, S., Glickman, G., Norinsky, R., Quimby, F. W., & Tolwani, R. J. (2009). Construction Noise Decreases Reproductive Efficiency in Mice. *Journal of the American Association for Laboratory Animal Science : JAALAS*, *48*(4), 363–370.

Rasquin, S. M. C., Van De Sande, P., Praamstra, A. J., & Van Heugten, C. M. (2009). Cognitive-behavioural intervention for depression after stroke: Five single case studies on effects and feasibility. *Neuropsychological Rehabilitation*, *19*(2), 208–222. https://doi.org/10.1080/09602010802091159

Roberson-Nay, R., Lapato, D. M., Wolen, A. R., Lancaster, E. E., Webb, B. T., Verhulst, B., Hettema, J. M., & York, T. P. (2020). An epigenome-wide association study of early-onset major depression in monozygotic twins. *Translational Psychiatry*, *10*(1), 1–12. https://doi.org/10.1038/s41398-020-00984-2

Robinson, R. G., Kubos, K. L., Starr, L. B., Rao, K., & Price, T. R. (1984). Mood disorders in stroke patients. Importance of location of lesion. *Brain: A Journal of Neurology*, *107 (Pt 1)*, 81–93. https://doi.org/10.1093/brain/107.1.81

Rumajogee, P., Madeira, A., Vergé, D., Hamon, M., & Miquel, M.-C. (2002). Up-regulation of the neuronal serotoninergic phenotype in vitro: BDNF and cAMP share Trk B-dependent mechanisms. *Journal of Neurochemistry*, *83*(6), 1525–1528. https://doi.org/10.1046/j.1471-4159.2002.01264.x

Rush, A. J., Warden, D., Wisniewski, S. R., Fava, M., Trivedi, M. H., Gaynes, B. N., & Nierenberg, A. A. (2009). STAR*D. *CNS Drugs*, *23*(8), 627–647. https://doi.org/10.2165/00023210-200923080-00001

Saadi, A., Okeng'o, K., Biseko, M. R., Shayo, A. F., Mmbando, T. N., Grundy, S. J., Xu, A., Parker, R. A., Wibecan, L., Iyer, G., Onesmo, P. M., Kapina, B. N., Regenhardt, R. W., & Mateen, F. J. (2018). Post-Stroke Social Networks, Depressive Symptoms, and Disability in Tanzania: A Prospective Study. *International Journal of Stroke : Official Journal of the International Stroke Society*, *13*(8), 840–848. https://doi.org/10.1177/1747493018772788

Salik, I., & Marwaha, R. (2025). Electroconvulsive Therapy. In *StatPearls*. StatPearls Publishing. http://www.ncbi.nlm.nih.gov/books/NBK538266/

Sari, Y. (2004). Serotonin1B receptors: From protein to physiological function and behavior. *Neuroscience and Biobehavioral Reviews*, *28*(6), 565–582. https://doi.org/10.1016/j.neubiorev.2004.08.008

Saver, J. L., Goyal, M., van der Lugt, A., Menon, B. K., Majoie, C. B. L. M., Dippel, D. W., Campbell, B. C., Nogueira, R. G., Demchuk, A. M., Tomasello, A., Cardona, P., Devlin, T. G., Frei, D. F., du Mesnil de Rochemont, R., Berkhemer, O. A., Jovin, T. G., Siddiqui, A. H., van Zwam, W. H., Davis, S. M., … HERMES Collaborators. (2016). Time to Treatment With Endovascular Thrombectomy and Outcomes From Ischemic Stroke: A Meta-analysis. *JAMA*, *316*(12), 1279–1288. https://doi.org/10.1001/jama.2016.13647

Shao, D., Zhao, Z. N., Zhang, Y. Q., Zhou, X. Y., Zhao, L. B., Dong, M., Xu, F. H., Xiang, Y. J., & Luo, H. Y. (2021). Efficacy of repetitive transcranial magnetic stimulation for post-stroke depression: A systematic review and meta-analysis of randomized clinical trials. *Brazilian Journal of Medical and Biological Research*, *54*(3), e10010. https://doi.org/10.1590/1414-431X202010010

Shen, X., Liu, M., Cheng, Y., Jia, C., Pan, X., Gou, Q., Liu, X., Cao, H., & Zhang, L. (2017). Repetitive transcranial magnetic stimulation for the treatment of post-stroke depression: A systematic review and meta-analysis of randomized controlled clinical trials. *Journal of Affective Disorders*, *211*, 65–74. https://doi.org/10.1016/j.jad.2016.12.058

Shiga, T., Suda, K., Yoshida, H., Nakamura, S., Natsume, M., Yoshikawa, M., & Senzaki, K. (2006). Serotonin: A Key Regulator for the Development of Brain and Mind. *KANSEI Engineering International*, *6*(2), 19–24. https://doi.org/10.5057/kei.6.2_19

Sibolt, G., Curtze, S., Melkas, S., Pohjasvaara, T., Kaste, M., Karhunen, P. J., Oksala, N. K. J., Vataja, R., & Erkinjuntti, T. (2013). Post-Stroke Depression and Depression-Executive Dysfunction Syndrome Are Associated with Recurrence of Ischaemic Stroke. *Cerebrovascular Diseases*, *36*(5–6), 336–343. https://doi.org/10.1159/000355145

Simon, G. E., Moise, N., & Mohr, D. C. (2024). Management of Depression in Adults: A Review. *JAMA*, *332*(2), 141–152. https://doi.org/10.1001/jama.2024.5756

Suicide Worldwide In 2019: Global Health Estimates (1st ed). (2021). World Health Organization.

Teng, T., Gaillard, A., Muzerelle, A., & Gaspar, P. (2017). EphrinA5 Signaling Is Required for the Distinctive Targeting of Raphe Serotonin Neurons in the Forebrain. *eNeuro*, *4*(1). https://doi.org/10.1523/ENEURO.0327-16.2017

Teoh, V., Sims, J., & Milgrom, J. (2009). Psychosocial predictors of quality of life in a sample of community-dwelling stroke survivors: A longitudinal study. *Topics in Stroke Rehabilitation*, *16*(2), 157–166. https://doi.org/10.1310/tsr1602-157

Terroni, L., Amaro, E., Iosifescu, D. V., Tinone, G., Sato, J. R., Leite, C. C., Sobreiro, M. F. M., Lucia, M. C. S., Scaff, M., & Fráguas, R. (2011). Stroke lesion in cortical neural circuits and post-stroke incidence of major depressive episode: A 4-month prospective study. *The World*

Journal of Biological Psychiatry, *12*(7), 539–548. https://doi.org/10.3109/15622975.2011.562242

Thaipisuttikul, P., Ittasakul, P., Waleeprakhon, P., Wisajun, P., & Jullagate, S. (2014). Psychiatric comorbidities in patients with major depressive disorder. *Neuropsychiatric Disease and Treatment*, *10*, 2097–2103. https://doi.org/10.2147/NDT.S72026

Thomas, R. (2023). Risk factors of post-stroke depression after acute ischemic stroke—A prospective study from a tertiary care hospital in South India. *Asian Journal of Medical Sciences*, *14*(11), Article 11.

Tickell, A., Ball, S., Bernard, P., Kuyken, W., Marx, R., Pack, S., Strauss, C., Sweeney, T., & Crane, C. (2020). The Effectiveness of Mindfulness-Based Cognitive Therapy (MBCT) in Real-World Healthcare Services. *Mindfulness*, *11*(2), 279–290. https://doi.org/10.1007/s12671-018-1087-9

Titus, A., & Marappa-Ganeshan, R. (2025). Physiology, Endothelin. In *StatPearls*. StatPearls Publishing. http://www.ncbi.nlm.nih.gov/books/NBK551627/

Towfighi, A., Ovbiagele, B., El Husseini, N., Hackett, M. L., Jorge, R. E., Kissela, B. M., Mitchell, P. H., Skolarus, L. E., Whooley, M. A., Williams, L. S., & on behalf of the American Heart Association Stroke Council; Council on Cardiovascular and Stroke Nursing; and Council on Quality of Care and Outcomes Research. (2017). Poststroke Depression: A Scientific Statement for Healthcare Professionals From the American Heart Association/American Stroke Association. *Stroke*, *48*(2), e30–e43. https://doi.org/10.1161/STR.0000000000000113

Underwood, M. D., Kassir, S. A., Bakalian, M. J., Galfalvy, H., Dwork, A. J., Mann, J. J., & Arango, V. (2018). Serotonin receptors and suicide, major depression, alcohol use disorder and reported early life adversity. *Translational Psychiatry*, *8*(1), 279. https://doi.org/10.1038/s41398-018-0309-1

Underwood, M. D., Kassir, S. A., Bakalian, M. J., Galfalvy, H., Mann, J. J., & Arango, V. (2012). Neuron Density and Serotonin Receptor Binding in Prefrontal Cortex in Suicide. *The International Journal of Neuropsychopharmacology / Official Scientific Journal of the Collegium Internationale Neuropsychopharmacologicum (CINP)*, *15*(4), 435–447. https://doi.org/10.1017/S1461145711000691

Unnithan, A. K. A., Das, J. M., & Mehta, P. (2025). Hemorrhagic Stroke. In *StatPearls*. StatPearls Publishing. http://www.ncbi.nlm.nih.gov/books/NBK559173/

Vadodaria, K. C., Ji, Y., Skime, M., Paquola, A. C., Nelson, T., Hall-Flavin, D., Heard, K. J., Fredlender, C., Deng, Y., Elkins, J., Dani, K., Le, A. T., Marchetto, M. C., Weinshilboum, R., & Gage, F. H. (2019). Altered serotonergic circuitry in SSRI-resistant major depressive disorder patient-derived neurons. *Molecular Psychiatry*, *24*(6), 808–818. https://doi.org/10.1038/s41380-019-0377-5

Vahid-Ansari, F., & Albert, P. R. (2018). Chronic Fluoxetine Induces Activity Changes in Recovery From Poststroke Anxiety, Depression, and Cognitive Impairment. *Neurotherapeutics*, *15*(1), 200–215. https://doi.org/10.1007/s13311-017-0590-3

Vahid-Ansari, F., & Albert, P. R. (2021). Rewiring of the Serotonin System in Major Depression. *Frontiers in Psychiatry*, *12*. https://doi.org/10.3389/fpsyt.2021.802581

Vahid-Ansari, F., Lagace, D. C., & Albert, P. R. (2016). Persistent post-stroke depression in mice following unilateral medial prefrontal cortical stroke. *Translational Psychiatry*, *6*(8), e863. https://doi.org/10.1038/tp.2016.124

Vahid-Ansari, F., Zhang, M., Zahrai, A., & Albert, P. R. (2019). Overcoming Resistance to Selective Serotonin Reuptake Inhibitors: Targeting Serotonin, Serotonin-1A Receptors and Adult Neuroplasticity. *Frontiers in Neuroscience*, *13*. https://doi.org/10.3389/fnins.2019.00404

Valiengo, L. C. L., Goulart, A. C., de Oliveira, J. F., Benseñor, I. M., Lotufo, P. A., & Brunoni, A. R. (2017). Transcranial direct current stimulation for the treatment of post-stroke depression: Results from a randomised, sham-controlled, double-blinded trial. *Journal of Neurology, Neurosurgery, and Psychiatry*, *88*(2), 170–175. https://doi.org/10.1136/jnnp-2016-314075

Varin, M., Orpana, H. M., Palladino, E., Pollock, N. J., & Baker, M. M. (2021). Trends in Suicide Mortality in Canada by Sex and Age Group, 1981 to 2017: A Population-Based Time Series Analysis: Tendances de la mortalité par suicide au Canada selon le sexe et le groupe d'âge, 1981 – 2017 : Une analyse de séries chronologiques dans la population. *Canadian Journal of Psychiatry. Revue Canadienne de Psychiatrie*, *66*(2), 170–178. https://doi.org/10.1177/0706743720940565

Vasiliu, O. (2023). Esketamine for treatment-resistant depression: A review of clinical evidence (Review). *Experimental and Therapeutic Medicine*, *25*(3), 111. https://doi.org/10.3892/etm.2023.11810

Vicenzi, S., Foa, L., & Gasperini, R. J. (2020). Serotonin functions as a bidirectional guidance molecule regulating growth cone motility. *Cellular and Molecular Life Sciences: CMLS*, *78*(5), 2247–2262. https://doi.org/10.1007/s00018-020-03628-2

Volz, M., Möbus, J., Letsch, C., & Werheid, K. (2016). The influence of early depressive symptoms, social support and decreasing self-efficacy on depression 6 months post-stroke. *Journal of Affective Disorders*, *206*, 252–255. https://doi.org/10.1016/j.jad.2016.07.041

Wang, S.-B., Wang, Y.-Y., Zhang, Q.-E., Wu, S.-L., Ng, C. H., Ungvari, G. S., Chen, L., Wang, C.-X., Jia, F.-J., & Xiang, Y.-T. (2018). Cognitive behavioral therapy for post-stroke depression: A meta-analysis. *Journal of Affective Disorders*, *235*, 589–596. https://doi.org/10.1016/j.jad.2018.04.011

Wang, Y.-M., Li, N., Yang, L.-L., Song, M., Shi, L., Chen, W.-H., Li, S.-X., Wang, X.-Y., & Lu, L. (2017). Randomized controlled trial of repetitive transcranial magnetic stimulation combined with paroxetine for the treatment of patients with first-episode major depressive disorder. *Psychiatry Research*, *254*, 18–23. https://doi.org/10.1016/j.psychres.2017.04.005

Watson, B. D., Dietrich, W. D., Busto, R., Wachtel, M. S., & Ginsberg, M. D. (1985). Induction of reproducible brain infarction by photochemically initiated thrombosis. *Annals of Neurology*, *17*(5), 497–504. https://doi.org/10.1002/ana.410170513

Weaver, N. A., Lim, J.-S., Schilderinck, J., Biessels, G. J., Kang, Y., Kim, B. J., Kuijf, H. J., Lee, B.-C., Lee, K.-J., Yu, K.-H., Bae, H.-J., & Biesbroek, J. M. (2023). Strategic Infarct Locations for Poststroke Depressive Symptoms: A Lesion- and Disconnection-Symptom Mapping Study. *Biological Psychiatry. Cognitive Neuroscience and Neuroimaging*, *8*(4), 387–396. https://doi.org/10.1016/j.bpsc.2021.09.002

Wei, N., Yong, W., Li, X., Zhou, Y., Deng, M., Zhu, H., & Jin, H. (2015). Post-stroke depression and lesion location: A systematic review. *Journal of Neurology*, *262*(1), 81–90. https://doi.org/10.1007/s00415-014-7534-1

Wijeratne, T., & Sales, C. (2021). Understanding Why Post-Stroke Depression May Be the Norm Rather Than the Exception: The Anatomical and Neuroinflammatory Correlates of Post-Stroke Depression. *Journal of Clinical Medicine*, *10*(8), 1674. https://doi.org/10.3390/jcm10081674

Williams, A. J., Jones, C., Arcelus, J., Townsend, E., Lazaridou, A., & Michail, M. (2021). A systematic review and meta-analysis of victimisation and mental health prevalence among LGBTQ+ young people with experiences of self-harm and suicide. *PLOS ONE*, *16*(1), e0245268. https://doi.org/10.1371/journal.pone.0245268

Wilson, M. A., & Molliver, M. E. (1994). Microglial response to degeneration of serotonergic axon terminals. *Glia*, *11*(1), 18–34. https://doi.org/10.1002/glia.440110105

Windle, V., Szymanska, A., Granter-Button, S., White, C., Buist, R., Peeling, J., & Corbett, D. (2006). An analysis of four different methods of producing focal cerebral ischemia with endothelin-1 in the rat. *Experimental Neurology*, *201*(2), 324–334. https://doi.org/10.1016/j.expneurol.2006.04.012

Wohleb, E. S., Franklin, T., Iwata, M., & Duman, R. S. (2016). Integrating neuroimmune systems in the neurobiology of depression. *Nature Reviews. Neuroscience*, *17*(8), 497–511. https://doi.org/10.1038/nrn.2016.69

Wu, Q., & Jia, Z. (2020). Wiring the Brain by Clustered Protocadherin Neural Codes. *Neuroscience Bulletin*, *37*(1), 117–131. https://doi.org/10.1007/s12264-020-00578-4

Wu, Q., & Maniatis, T. (1999). A Striking Organization of a Large Family of Human Neural Cadherin-like Cell Adhesion Genes. *Cell*, *97*(6), 779–790. https://doi.org/10.1016/S0092-8674(00)80789-8

Xiao, X., Zheng, F., Chang, H., Ma, Y., Yao, Y.-G., Luo, X.-J., & Li, M. (2018). The Gene Encoding Protocadherin 9 (PCDH9), a Novel Risk Factor for Major Depressive Disorder. *Neuropsychopharmacology: Official Publication of the American College of Neuropsychopharmacology*, *43*(5), 1128–1137. https://doi.org/10.1038/npp.2017.241

Xu, X., Zou, D., Shen, L., Liu, Y., Zhou, X., Pu, J., Dong, M., & Wei, Y. (2016). Efficacy and feasibility of antidepressant treatment in patients with post-stroke depression. *Medicine*, *95*(45), e5349. https://doi.org/10.1097/MD.0000000000005349

Yanai, S., Semba, Y., & Endo, S. (2012). Remarkable Changes in Behavior and Physiology of Laboratory Mice after the Massive 2011 Tohoku Earthquake in Japan. *PLoS ONE*, *7*(9), e44475. https://doi.org/10.1371/journal.pone.0044475

Yatham, L. N., Liddle, P. F., Sossi, V., Erez, J., Vafai, N., Lam, R. W., & Blinder, S. (2012). Positron emission tomography study of the effects of tryptophan depletion on brain serotonin(2) receptors in subjects recently remitted from major depression. *Archives of General Psychiatry*, *69*(6), 601–609. https://doi.org/10.1001/archgenpsychiatry.2011.1493

Young, S. N., & Leyton, M. (2002). The role of serotonin in human mood and social interaction: Insight from altered tryptophan levels. *Pharmacology Biochemistry and Behavior*, *71*(4), 857–865. https://doi.org/10.1016/S0091-3057(01)00670-0

Zahrai, A., Vahid-Ansari, F., Daigle, M., & Albert, P. R. (2020). Fluoxetine-induced recovery of serotonin and norepinephrine projections in a mouse model of post-stroke depression. *Translational Psychiatry*, *10*(1), Article 1. https://doi.org/10.1038/s41398-020-01008-9

Zhang, G., Chen, L., Yang, L., Hua, X., Zhou, B., Miao, Z., Li, J., Hu, H., Namaka, M., Kong, J., & Xu, X. (2015). Combined use of spatial restraint stress and middle cerebral artery occlusion is a novel model of post-stroke depression in mice. *Scientific Reports*, *5*(1), 16751. https://doi.org/10.1038/srep16751

Zhang, Y., Yang, Y., Li, H., Feng, Q., Ge, W., & Xu, X. (2024). Investigating the Potential Mechanisms and Therapeutic Targets of Inflammatory Cytokines in Post-stroke Depression. *Molecular Neurobiology*, *61*(1), 132–147. https://doi.org/10.1007/s12035-023-03563-w

Zhou, H., Wei, Y.-J., & Xie, G.-Y. (2024). Research progress on post-stroke depression. *Experimental Neurology*, *373*, 114660. https://doi.org/10.1016/j.expneurol.2023.114660

Zipursky, S. L., & Sanes, J. R. (2010). Chemoaffinity revisited: Dscams, protocadherins, and neural circuit assembly. *Cell*, *143*(3), 343–353. https://doi.org/10.1016/j.cell.2010.10.009